

# **Preparation and Characterization of Silica Aerogel Polymer Composites**

by

Zeynep Ülker

A Thesis Submitted to the  
Graduate School of Sciences and Engineering  
in Partial Fulfillment of the Requirements for  
the Degree of

**Master of Science**  
**in**  
**Chemical and Biological Engineering**

**Koç University**

**August, 2011**

Koç University  
Graduate School of Sciences and Engineering

This is to certify that I have examined this copy of a master's thesis by  
Zeynep Ülker  
and have found that it is complete and satisfactory in all respects,  
and that any and all revisions required by the final  
examining committee have been made.

Committee Members:

---

Can Erkey Ph.D. (Advisor)

---

Seda Kızılel Ph.D

---

Murat Sözer Ph.D

Date:

---

*to my family...*

## ABSTRACT

In this study, new nanotechnology-based high performance insulation systems for energy efficiency, nanostructured composites of silica aerogels with polymers are being developed as core materials for vacuum insulation panels in buildings. Monolithic composites of a wide variety of polymers with silica aerogels were synthesized by modification of the conventional sol-gel method to produce silica aerogels. The polymers used in the study are poly(ethylene block poly ethylene glycol) (PEPEG), poly(vinyl pyrrolidone) (PVP), poly(vinyl acetate) (PVAc) and poly(methyl vinyl ether) (PMVE). Characterization of the composite materials was performed by Fourier Transform Infrared - Attenuated Total Reflectance (FTIR-ATR) spectroscopy, Thermal Gravimetric Analysis (TGA) and by Nitrogen Physisorption using BET. Both transparent and opaque crack-free monolithic composites suitable for testing and use in VIPs were obtained. The presence of polymer in the composites was confirmed by IR spectroscopy and TGA. The composites were mesoporous materials with high surface areas around 800 m<sup>2</sup>/g and average pore sizes around 5 nm. Incorporation of polymers did not significantly change the pore size distribution and the specific surface area of the pure silica aerogels. The effects of the time of polymer addition at various stages of the conventional sol-gel process such as before/after the hydrolysis step and during the aging step, on the properties of the composites were investigated. Opacity was found to be correlated to the phase separation of the polymer from the reaction mixture. The effect of polymer content on the resulting properties was also investigated along with density, porosity and shrinkage calculations.

## ÖZET

Bu çalışmada, binalarda vakumlu yalıtım panelleri olarak kullanılarak enerji verimliliğini artırmak için silica arojel-polimer nanokompozit malzemeleri geliştirilmiştir. Değişik polimerler kullanılarak yapılan monolitik kompozitler geleneksel sol-jel yöntemi kullanılarak sentezlenmiştir. Kullanılan polimerler poli(etilen blok polietilen glikol) (PEPEG), polivinil pirolidon (PVP), polivinil asetat (PVAc) ve poli(vinil metil eter) (PMVE)'dir. Kompozit malzemeler Fourier Transform Infrared Spektrometresi (ATR-FTIR), Termo Gravimetrik Analiz Cihazı ve de Nitrojen Fizisorpsiyon Tekniği (BET) ile analiz edilmiştir. Vakum yalıtım panellerinde test edilmek üzere şeffaf veya opak, monolitik kompozit malzemeler üretilmiştir. Kompozit içerisinde polimerin bulunduğu infrared spektrometresi ya da termo gravimetrik analiz ile doğrulanmıştır. Üretilen malzemelerin ortalama yüzey alanı  $800 \text{ m}^2/\text{g}$ , ortalama gözenek çapı ise 5 nm olarak bulunmuştur. Polimer eklenmesinin spesifik yüzey alanını ve gözenek boyu dağılımını önemli ölçüde değiştirmedeği gözlemlenmiştir. Polimer ekleme zamanı değiştirilerek, bu parametrenin kompozitin özelliklerini nasıl değiştirdiği incelenmiştir. Eklenen polimer miktarının malzemenin yoğunluğunu, gözenek yapısını ve hacimsel olarak çekme miktarını nasıl değiştirdiği de ayrıca gözlemlenmiştir.

## ACKNOWLEDGEMENTS

First and foremost, I would like to thank my advisor Professor Can Erkey whose encouragement, supervision, patience and support from the preliminary to the final level enabled me to complete this thesis. His experience, great knowledge, kindness and friendly attitude towards his students did not only guide me through my master thesis but also inspired me to continue my academic career. It was a great pleasure and honor to be a member of his research group. One simply could not wish a better or friendlier supervisor.

I acknowledge the financial support of the NANOINSULATE Project being funded by the EU Program EeB.NMP.2010-1 for my thesis. I also acknowledge the financial support of the Scientific and Technological Research Council of Turkey (TÜBİTAK) during my whole graduate study

I also would like to thank my colleagues Deniz Şanlı, Oğuz Canıaz, Selmi Bozbağ, Ümmühan Canan, Sezin Nargül and also thank my former colleagues Seda Giray, Nil Ezgi Dinçer and Erdal Uzunlar for their help and support in the research laboratory during my graduate study. I would like to give my special thanks to Deniz Şanlı with her endless help, friendship and support in the laboratory. It was a great chance to work with you.

I would like to give my special thanks to my housemates Melis Yavuz, Esin Çakıroğlu, Bengisu Seferoğlu and my dear friends Damla Aktaş, Şule Namırtı, Gülce Kuntay and Deniz Eyüce who made these two years an enjoyable period of time with their endless support and friendship. Special thanks go again to my housemate of many years: Melis Yavuz. She was a true friend throughout all my studies. It would be impossible to finish this degree without your support and lifelong friendship.

Last but not least, I would like to thank those closest to me, whose presence helped make the completion of my graduate work possible. Endless thanks to my lovely parents

and my lovely sister for their great love, understanding, concern, friendship, encouragement and support throughout my life. I would like to thank them for their absolute confidence in me. This thesis would not have been possible without them, without the knowledge that they would always be present when I need them. Another special thanks to Enis Demir for his love, patience and friendship from the time he is in my life. I always felt his support, encouragement and affection. It is hard to explain my gratitude for all of you. I love you so much.

## Table of Contents

<b>ABSTRACT</b> .....	iv
<b>ÖZET</b> .....	v
<b>ACKNOWLEDGEMENTS</b> .....	vi
<b>LIST OF TABLES</b> .....	xii
<b>LIST OF FIGURES</b> .....	xiii
<b>NOMENCLATURE</b> .....	xvii
<b>Chapter 1: INTRODUCTION</b> .....	1
<b>Chapter 2: LITERATURE REVIEW</b> .....	3
Organic-Inorganic Hybrid Materials: .....	3
2.1 Brief Introduction about Organic-Inorganic Hybrid Materials.....	3
2.2 Types of Inorganic-Polymer Composites .....	5
2.3 Silica Aerogel-Polymer Composites.....	8
2.3.1 Silica Aerogels .....	8
2.3.1.1 Sol-Gel Process:.....	10
2.3.1.1.1 Gel Preparation: .....	10
2.3.1.1.2 Chemical Precursors: .....	11
2.3.1.1.3 Hydrolysis:.....	12
2.3.1.1.4 Condensation: .....	14
2.3.1.1.5 Gelation and Aging:.....	16
2.3.1.1.6 Drying: .....	17
2.3.2 Synthesis of Silica Aerogel Composites:.....	18
2.3.2.1 Co-condensation reactions by the use of organically substituted co-precursors	
.....	19
2.3.2.2 Liquid Phase Modification in the wet nanocomposite stage .....	22
2.3.2.2.1 Diffusion Controlled Polymer Cross-Linking .....	22



2.3.2.2.2 Direct Addition of the Monomer in the Initial Solution for Polymer Cross-Linking.....	28
2.3.2.3 Post-synthesis modification of the final dried product by dissolved organic species.....	29
2.3.2.3.1 Chemical Vapor Deposition Technique (CVD).....	30
2.3.2.4 Addition of molecular, but non-reactive compounds to the precursor solution.....	33
2.3.2.4.1 Addition before the hydrolysis.....	33
2.3.2.4.2 Addition after the hydrolysis.....	34
2.3.2.5 Use of single source precursors in which the organic entity is a part of the network forming species.....	35
2.4 Silica Xerogel-Polymer Composites.....	37
<b>Chapter 3: EXPERIMENTAL METHODS AND CHARACTERIZATION</b>	
TECHNIQUES.....	43
3.1 Pure Silica Aerogel Synthesis.....	43
3.2 Preparation of Silica Aerogel-Polymer Composites.....	45
3.2.1 Silica Aerogel PEPEG Composite Synthesis.....	46
3.2.2 Silica Aerogel Poly(vinylpyrrolidone) Composite Synthesis.....	47
3.2.3 Silica Aerogel Poly(vinyl acetate) Composite Synthesis:.....	47
3.2.4 Silica Aerogel Poly(methyl vinyl ether) Composite Synthesis.....	48
3.3 Characterization of Silica Aerogel Polymer Composites.....	48
3.3.1 Monolithicity, Bulk Shrinkage, Density and Porosity.....	48
3.3.2 Surface Area Measurements by BET.....	49
3.3.3 Infrared Spectroscopy, IR.....	50
3.3.4 Thermal Gravimetric Analysis, TGA.....	51
<b>Chapter 4: RESULTS &amp; DISCUSSION.....</b>	<b>53</b>

4.1 Photographic Images of Silica Aerogel Polymer Composites .....	53
4.1.1 Silica Aerogel-PEPEG Composites .....	53
4.1.2 Silica Aerogel-PVP Composites .....	54
4.1.3 Silica Aerogel-PVAc Composites.....	55
4.1.4 Silica Aerogel-PMVE Composites .....	57
4.2 Physical Characterization Results.....	59
4.2.1 Bulk Density of the Composites .....	59
4.2.2 Volumetric (or Linear) Shrinkage of Composites .....	61
4.2.3 Porosity of Composites .....	63
4.2.4 Pore Volume of Composites .....	63
4.3 ATR-FTIR Spectra Results.....	63
4.3.1 Silica Aerogel-PEPEG Composites .....	64
4.3.1 Silica Aerogel-PVP Composites .....	66
4.3.2 Silica Aerogel-PVAc Composites.....	69
4.3.4 Silica Aerogel-PMVE Composites .....	73
4.4 TGA Results.....	75
4.4.1 Silica Aerogel PEPEG Composites .....	76
4.4.2 Silica Aerogel PVP Composites .....	77
4.4.3 Silica Aerogel PVAc Composites.....	79
4.4.4 Silica Aerogel PMVE Composites.....	82
4.5 BET Results .....	84
4.6 Unified Results and Discussion .....	85
Chapter 5: CONCLUSION .....	88
REFERENCES: .....	91
APPENDIX A:.....	98
APPENDIX B:.....	101

<b>VITA</b> .....	105
-------------------	-----

## LIST OF TABLES

<b>Table 1.1:</b> Properties of SilicaAerogels.....	9
<b>Table 3.1</b> Amounts of reactants used in a typical procedure.....	43

## LIST OF FIGURES

<b>Figure 2-1:</b> Different Types of Organic-Inorganic Polymeric Hybrid Materials.....	7
<b>Figure 2-2:</b> Two step acid base catalysis of silica aerogels.....	12
<b>Figure 2-3:</b> Ternary Phase Diagram of TEOS-Ethanol-Water system at 25°C [2].....	13
<b>Figure 2-4:</b> Dependence of the relative hydrolysis and condensation rates on the pH of the solution [2].....	14
<b>Figure 2-5:</b> Water and Alcohol Condensation Reactions respectively.....	15
<b>Figure 2-6:</b> Gel structure for acid and base catalyzed reactions respectively [3].....	15
<b>Figure 2-7:</b> Amine Modified Silica Surface [4].....	23
<b>Figure 2-8:</b> CVD Deposition and Subsequent Polymerization of Methyl Cyanoacrylate On the Surface of Silica Aerogels [5].....	30
<b>Figure 3-1:</b> Schematic Representation of the Silica Aerogel Synthesis Procedure Using Two-Step Sol-Gel Method.....	44
<b>Figure 3-2:</b> The Schematic Representation of Silica Aerogel Polymer Composites With Different Addition Steps Indicated by Red Arrows.....	45
<b>Figure 4-1:</b> Silica Aerogel-PEPEG Composite (Addition Before the Hydrolysis Step) ....	54
<b>Figure 4-2:</b> Silica Aerogel-PEPEG Composite (Addition Before the Condensation Step)	54
<b>Figure 4-3:</b> Silica Aerogel-PVP Composite (Addition Before the Condensation Step).....	55
<b>Figure 4-4:</b> Silica Aerogel-PVP Composites (Addition During the Aging Step). A) Higher Amount of Polymer Addition B) Lower Amount of Polymer Addition.....	55
<b>Figure 4-5:</b> Silica Aerogel-PVAc Composites (Addition Before the Hydrolysis Step). A) Lower Amount of Polymer Addition, B) Higher Amount of Polymer Addition.....	56
<b>Figure 4-6:</b> Silica Aerogel-PVAc Composites (Addition After the Hydrolysis Step). A) Lower Amount of Polymer Addition, B) Higher Amount of Polymer Addition.....	57

<b>Figure 4-7:</b> Silica Aerogel-PVAc Composites (Addition During the Aging Step). A) Higher Amount of Polymer Addition, B) Lower Amount of Polymer Addition.....	57
<b>Figure 4-8:</b> Silica Aerogel-PMVE Composites (Addition Before the Hydrolysis Step), A) Ethanol as the only solvent B) Acetone as the co-solvent along ethanol .....	58
<b>Figure 4-9:</b> Silica Aerogel-PMVE Composites (Addition Before the Hydrolysis Step), Acetone as the co-solvent along ethanol (Polymer Amount is higher compared with Fig. 4-8).....	58
<b>Figure 4-10:</b> Silica Aerogel-PMVE Composite (Addition During the Aging Step).....	59
<b>Figure 4-11:</b> ATR Spectrum of Silica Aerogel-PEPEG Composites (Addition After the Hydrolysis Step), Increasing Polymer Mass for the Samples P2707 and P1207 respectively .....	65
<b>Figure 4-12:</b> ATR Spectrum of Silica Aerogel-PEPEG Composites (Addition During the Aging Step) .....	66
<b>Figure 4-13:</b> ATR Spectrum of Silica Aerogel-PVP Composites (Addition After the Hydrolysis Step) Increasing Polymer Mass for the Samples PVP2408 and PVP1208 respectively .....	67
<b>Figure 4-14:</b> ATR Spectrum of Silica Aerogel-PVP Composites (Addition During the Aging Step), Increasing Polymer Mass for the Samples PVP2508_1,PVP2508_2 and PVP2508_3 respectively .....	68
<b>Figure 4-15:</b> ATR Spectrum of Silica Aerogel-PVP Composites, (Similar Amount of Polymer Addition) Addition Before the Hydrolysis Step, Addition After the Hydrolysis Step, Addition During the Aging Step for Samples PVP3011_2, PVP3011_1 and PVP2508_1 respectively.....	69
<b>Figure 4-16:</b> ATR Spectrum of Silica Aerogel-PVAc Composites (Similar Amount of Polymer Addition) Addition Before the Hydrolysis Step, Addition After the	

Hydrolysis Step, Addition During the Aging Step for Samples PVAc3011_2, PVAc3011_1 and PVAc1105 respectively .....	70
<b>Figure 4-17:</b> ATR Spectrum of Silica Aerogel-PVAc Composites, (Polymer Addition Before the Hydrolysis Step), Increasing Polymer Mass for the Samples PVAc0601_1, PVAc0411_2, PVAc3011_2 and PVAc1201_1 respectively .....	71
<b>Figure 4-18:</b> ATR Spectrum of Silica Aerogel-PVAc Composites (Polymer Addition After the Hydrolysis Step), Increasing Polymer Mass for the Samples PVAc2510, PVAc0411_1, PVAc0601_3 respectively.....	71
<b>Figure 4-19:</b> ATR Spectrum of Silica Aerogel-PVAc Composites (Polymer Addition During the Aging Step), Increasing Polymer Mass for the Samples PVAc2302_3, PVAc2302_4 respectively. ....	72
<b>Figure 4-20:</b> ATR Spectrum of Silica Aerogel-PVAc Composites, Aging With and Without Solution.....	72
<b>Figure 4-21:</b> ATR Spectrum of Silica Aerogel-PMVE Composites, (Polymer Addition Before the Hydrolysis Step), Increasing Polymer Mass for the Samples PMVE1904_1 and PMVE2004 respectively .....	74
<b>Figure 4-22:</b> ATR Spectrum of Silica Aerogel-PMVE Composites, (Similar Amount of Polymer Addition) Addition Before the Hydrolysis Step, Addition After the Hydrolysis Step, Addition During the Aging Step for Samples PMVE1904_1, PMVE1005_2 and PMVE1105 respectively .....	75
<b>Figure 4- 23:</b> TGA Diagram of Pure Silica Aerogel.....	76
<b>Figure 4- 24:</b> TGA Diagram of Silica Aerogel-PEPEG Composite (P1207), Addition After the Hydrolysis Step .....	77
<b>Figure 4-25:</b> TGA Diagram of Silica Aerogel-PVP Composite (PVP2408), Addition After the Hydrolysis Step .....	78

<b>Figure 4-26:</b> TGA Diagram of Silica Aerogel-PVP Composite (PVP1105), Addition During the Aging Step .....	78
<b>Figure 4-27:</b> TGA Diagram of Silica Aerogel-PVAc Composite (PVAc3011_1), Addition After the Hydrolysis Step.....	80
<b>Figure 4-28:</b> TGA Diagram of Silica Aerogel-PVAc Composite (PVAc1201_2), Addition Before the Hydrolysis Step .....	80
<b>Figure 4- 29:</b> TGA Diagram of Silica Aerogel-PVAc Composite (PVAc0702_4), Addition Before the Hydrolysis Step, Aging Without Solution .....	81
<b>Figure 4- 30:</b> TGA Diagram of Silica Aerogel-PVAc Composite (PVAc2302_3), Addition During the Aging Step .....	81
<b>Figure 4- 31:</b> TGA Diagram of Silica Aerogel-PMVE Composite (PMVE2510), Addition Before the Hydrolysis, Ethanol as the Only Solvent .....	82
<b>Figure 4- 32:</b> TGA Diagram of Silica Aerogel-PMVE Composite (PMVE1904_1), Addition Before the Hydrolysis, Acetone as the Co-Solvent .....	83
<b>Figure 4- 33:</b> TGA Diagram of Silica Aerogel-PMVE Composite (1005-2), Addition After the Hydrolysis, Acetone as the Co-Solvent .....	83
<b>Figure 4-34:</b> TGA Diagram of Silica Aerogel-PMVE Composite (PMVE1105), Addition During the Aging Step .....	84



## **NOMENCLATURE**

<b><i>TEOS</i></b>	Tetraethylorthosilicate (Tetraethoxysilane)
<b><i>PEPEG</i></b>	Polyethylene-block-polyethylene glycol
<b><i>PVP</i></b>	Poly(vinylpyrrolidone)
<b><i>PVAc</i></b>	Poly(vinyl acetate)
<b><i>PMVE</i></b>	Poly(methyl vinyl ether)
<b><i>ATR</i></b>	Attenuated Total Reflectance Spectroscopy
<b><i>TGA</i></b>	Thermal Gravimetric Analysis

**Chapter 1: INTRODUCTION**

As the lightest solid material with very low thermal conductivity and high transparency, silica aerogels have been drawing increased attention in recent years due to an increasing number of application areas. To overcome the problems faced with this material especially with its fragility, new scientific ideas are developed. Scientists started to integrate the concept of organic-inorganic hybrid materials into the area of silica aerogels. The use of silica aerogel as the inorganic matrix helped researchers to develop new materials by the incorporation of an organic entity into it. Several studies are conducted to move the subject of silica-organic composites further [6-8].

Different approaches for the synthesis of composites are adopted with diverse organic entities which would be integrated in the inorganic matrices. As one of the approaches, the organic part is attempted to be incorporated in the beginning of the synthesis by co-condensation of the organic precursors with the silica precursor [9-11]. On the other hand, the organic entity is added during the synthesis process while trying to integrate it by means of cross-linking [4, 12, 13]. Other research focused on the post-synthesis treatment namely treating the already synthesized silica aerogel matrix with organic entities [5, 14, 15].

In this study, new materials consisting of a silica aerogel as the inorganic matrix and a variety of polymers such as poly(ethylene block poly ethylene glycol) (PEPEG), poly(vinyl pyrrolidone) (PVP), poly(vinyl acetate) (PVAc) and poly(methyl vinyl ether) (PMVE) as the organic entities are synthesized through the conventional sol-gel technique. Different polymer addition steps are tested for better integration of the organic material.

Primarily a general overview about the inorganic organic hybrid materials is given in Chapter 2 for a better understanding of the following sections. Subsequently, the synthesis of the pure silica aerogel is explained prior to the information about recent studies

involving silica aerogel-polymer composites. The latter is analyzed in detail to investigate different routes and different organic materials used in the literature for the same purpose.

Experimental methods of the study are presented in Chapter 3. Starting from the pure silica aerogel synthesis, the preparation of the silica aerogel-polymer materials are explained in different sections. Consequently, the characterization methods are illustrated with a brief explanation for each of them. Physical characterization such as the density, the shrinkage and the porosity calculations of the synthesized materials are conducted along with ATR-FTIR, TGA and BET analysis to better understand the resulting properties and to confirm the polymer presence in the network. Subsequent chapter consists of the entire results for the study. It includes the images taken by a microscope, the physical characterization results along with ATR-FTIR spectra, TGA spectra and BET results.

The last chapter concludes the total work performed for this study including any discussion which could be made using the results illustrated in the previous Chapter and any future work which could be initiated to carry on this project.

In this work, composite materials are synthesized through the conventional sol-gel technique. Non studied polymers having suitable properties as the organic part are used with the silica aerogel as the inorganic matrix to synthesize new materials. Synthesized samples are then characterized to get a better understanding about the properties that they have gained or lost throughout the process.

## **Chapter 2: LITERATURE REVIEW**

### **Organic-Inorganic Hybrid Materials:**

#### **2.1 Brief Introduction about Organic-Inorganic Hybrid Materials**

Hybrid materials are becoming increasingly important due to the advantages offered by combining different entities such as inorganic, organic and even biological ones in the same network creating a multidisciplinary work [1, 16]. The combination of these different entities into one composite material is actually an old challenge which started in the beginning of the industrial era [17]. Preliminary and important inorganic-organic composite materials were derived from paint and polymer industries where the primary aim was to improve optical and mechanical properties. As the research moves forward, combining different properties into one single material then attracted more interest in this field. The number of scientific articles as well as World Intellectual Property Organization (WO) patents have increased significantly over the past 20 years indicating the growing importance of this research field [1]. The number of studies on organic-inorganic hybrid materials exploded especially very recently mainly due to the use of soft chemistry (sol-gel process) with more suitable and mild process conditions facilitating the research in this area of material synthesis. Moreover, the research focused more on the high added-value composites as there arise more application areas with the development of the technology [17]. By the synthesis of an organic-inorganic hybrid material, different properties are combined to obtain a superior one which can not be achieved with the individual constituents alone leading to a stronger application potential for the new material. The organic-inorganic hybrid materials are thus considered as candidates for several applications such as: coatings [18-20], catalysts and porous supports, adsorbents, [6, 21, 22], chemical and biomedical sensing [23, 24], photonic, optic and microelectronic [25-

27], energy and energy related membranes [28, 29], biology and medicine [30] and adhesives.

Along with the general information about the the hybrid materials theme, the basic definitions and concepts of this field should also be given. The name hybrid is referred as a general term for intimately mixed organic/inorganic composite materials [1, 31]. Ormocers (organically modified ceramics) [32], ormosils (organically modified silicates) and ceramers (ceramics modified with polymers) are some other names used for hybrid materials. If one of the components or the phases is of nanometer size, then the hybrid material is called nanocomposite. The forces existing between the constituents vary from weak (Van der Waals, Ionic or hydrogen bonding)[1] to relatively strong interactions (covalent or ionic-covalent bonds)[1] for these nanocomposite materials [31]. The varying force between the constituents representing the hybrid interface is of great importance because it determines the material homogeneity, the transparency and stability [1].

If the constituents of these hybrid materials are investigated, inorganic component of the hybrid material include inorganic metal oxides and metal-oxo-polymers producing amorphous networks, nanocrystalline networks or metal-oxo clusters [1]. Organic constituent which is usually represented by polymers is either network modifier or network former [1, 33, 34]. The introduction of this organic component into the inorganic one will be explained in detail in the following sections.

Apart from the nature of the interface and the constituents, the chemical pathway used in the preparation of the hybrid materials is also considerably important. Same components used with a different chemical pathway create composites with entirely different properties at the end.

With the most general point of view, there are mainly two different routes to prepare nanoscale hybrid materials: the top-down and the bottom-up approaches. With the top-down approach, macroscopic sized particles are reduced in size by physical means such

as grinding, heating processes and milling [35]. However, using this approach, the size of the particles is limited. Therefore, hybrid composites are generally not created through the use of top-down approach. Based on the theory of bottom-up approach, nanoscale hybrid materials are formed starting from the precursor compounds or nanobuilding blocks [1, 35]. To obtain homogeneous and nanostructured hybrid materials, the latter approach is mostly adopted.

As mentioned earlier, the soft-chemistry namely the sol-gel process which can be accepted as a bottom-up approach, has emerged as the most promising method to synthesize hybrid organic-inorganic composites [36]. Since this method involves low temperature conditions, it is accepted as the ideal route to process polymeric materials without damaging their structures. The variety of organic and inorganic components and the different strategies that are applied to the process conditions enlarge the application areas of these sol-gel derived hybrid materials [36].

## **2.2 Types of Inorganic-Polymer Composites**

Inorganic polymeric hybrid materials can be classified among the various types of organic-inorganic composites. They are synthesized by the sol-gel approach and are classified into 5 different types according to the existing interaction between the components, the macromolecular structures of composites and their preparation conditions. These types are schematized in Figure 2-1. Novak *et al.* showed that soluble and preformed polymers which are entrapped in an inorganic network form the primary type of hybrid materials (Type 1) [37]. If this preformed polymer is covalently linked to the inorganic network, then these materials constitute a second type of hybrid materials. The third type of hybrid materials is explained as mutually interpenetrating inorganic and organic networks. The fourth type differs from the previous type by the existence of covalent bonding

between the interpenetrating inorganic and organic networks. The last class is called as non-shrinking sol-gel composites among the different types of hybrid materials [37].

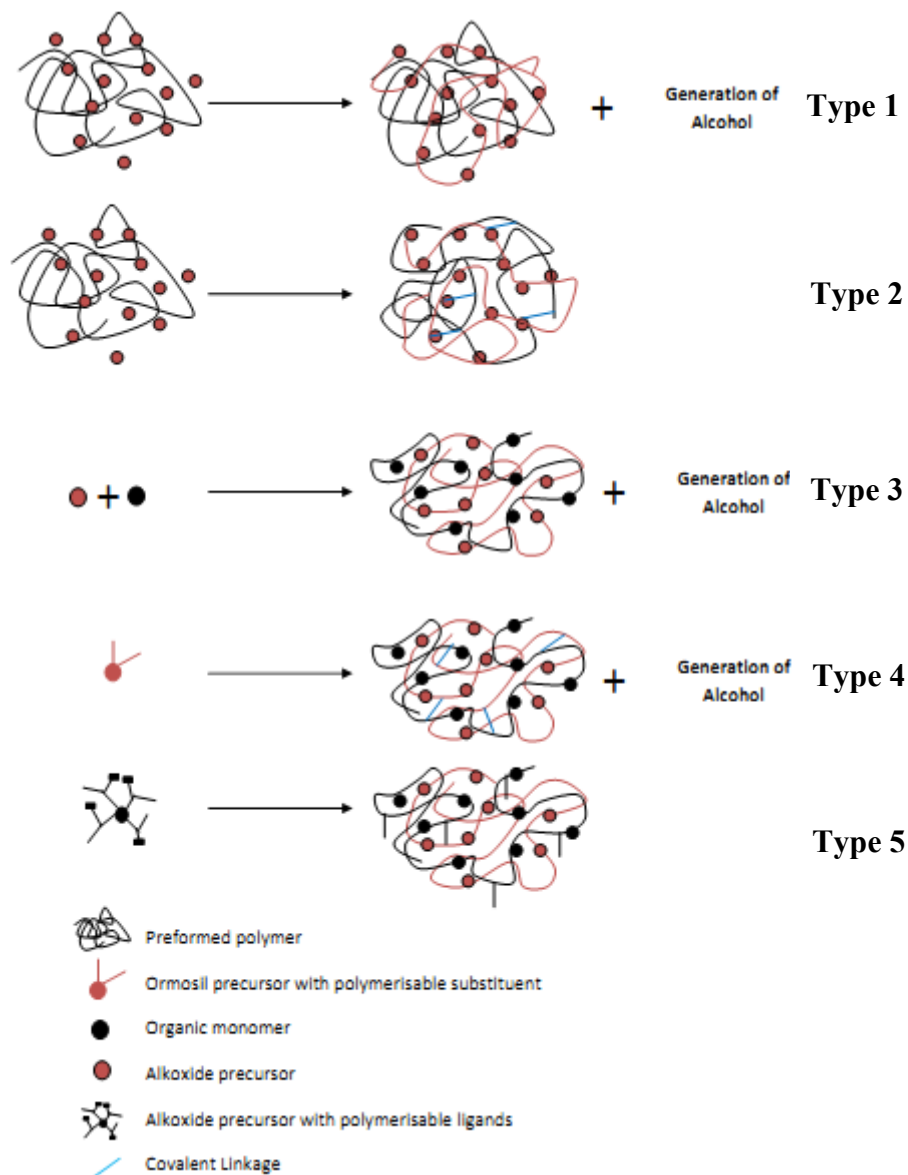


Figure 2-1: Different Types of Organic-Inorganic Polymeric Hybrid Materials. Adapted from ref. [38]

With more detailed information, the first type of hybrid materials can be prepared by using several polymers which are readily soluble and also remain soluble in the initial reaction solution containing the precursor [38]. Some organic entities such as alcohols can precipitate because of the reaction products of the precursor with the addition of the water. Therefore, it is necessary to investigate the solubility of the second phase during the chemical reactions occurring within the initial solution to obtain homogeneous composites at the end.

The second type of hybrid materials comprising the preformed polymers embedded in the inorganic network by covalent linkages can be generally synthesized by functionalizing the organic group with trialkoxysilane groups [38].

Nevertheless, it is usually difficult to find an organic material soluble in the hydrolysis solution. Therefore, the research is mostly focused on the formation of interpenetrating organic/inorganic networks covalently bonded or not. These composites are prepared by the simultaneous formation of the organic and inorganic matrices. However, addition of coupling agents thereby creating covalent linkages between these matrices can form more rigid or elastic materials [37].

The main problem for all the types of hybrid materials stated above was the reduction in dimensions of the resulting composite materials. Due to this large shrinkage values, a new type of material is prepared by using such precursors that the hydrolysis products would be polymerizable alcohols. Because all components of the solution undergo polymerization process, there will not be any constituent left for the evaporation which will cause the large shrinkage [37].

Silica aerogel-polymer composites, being the motivation of this thesis, belong to all these different types of inorganic-polymer materials depending on the preparation conditions. The reader will soon be informed about the preparation conditions leading to



silica aerogel-polymer hybrids. However, primarily how the inorganic matrix of the composites -silica aerogels- is synthesized should be understood.

### 2.3 Silica Aerogel-Polymer Composites

#### *2.3.1 Silica Aerogels*

Aerogels are becoming more appealing to scientists in recent years due to their fascinating properties. These unique properties are the result of the arrangement of their solid network. Their extremely high porosity and high surface area give them unique characteristics and make them promising candidates for various applications. These low density materials are transparent, have low thermal conductivity but are very fragile and absorb moisture which causes their degradation. The properties of silica aerogels are summarized in Table 2.1.

*Table 2.1: Properties of Silica Aerogels*

<b>Property</b>	<b>Value</b>	<b>Comment</b>
<b>Density</b>	~0.003g/cm <sup>3</sup>	Lowest density solid [2]
<b>Porosity</b>	80-99.8%	High porosity [2, 39]
<b>Surface Area</b>	500-1200 m <sup>2</sup> /g	Determined by Nitrogen Adsorption/Desorption (BET) [2, 39]
<b>Mean Pore Diameter</b>	20-150 nm	Mostly in mesoporous range [2]
<b>Thermal Conductivity</b>	0.017-0.021 W/m.K	High thermal insulation property[2, 39]
<b>Thermal Tolerance</b>	Up to 500 °C	Shrinkage starts at 500°C and increases with temperature. Melting point is 1200 °C [40]
<b>Dielectric Constant</b>	1.0-2.0	Low for a solid material [2]

<b>Sound Velocity</b>	100 m/s	One of the lowest velocities for a solids[2]
<b>Poisson's Ratio</b>	0.2	Independent of density, similar to the dense silica [40]
<b>Young's Modulus</b>	0.002-100 MPa	Very small compared to dense silica (10 <sup>4</sup> MPa) [39]
<b>Index of refraction</b>	~1.05	Low for a solid material [2]
<b>Optical Property</b>	> 90%	Transmittance Measurement at 630 nm [40]

Application areas of silica aerogels can be variable due to their different resulting properties [41]. Monolithic silica aerogels are used as Cherenkov detectors due to their good optical properties such as transparency and low refractive index [42, 43]. As these materials have very low thermal conductivity, their use as insulation materials, in space vehicles or in architecture are becoming more and more important [44-46]. Silica aerogels are also suitable for use as catalysts, sorbents and sensors because of their high porosity and low density characteristics [47-49]. Due to their favorable electrical properties, silica aerogels can also be used as dielectrics for ICs, spacers for vacuum electrodes or capacitors [50].

They are transparent, have low thermal conductivity but are very fragile at relatively low stresses depending on their preparation conditions [51]. Although the advantages brought by these materials (silica aerogels) offer a variety of application areas as mentioned in previous paragraph, the fragility of this material limits its use because it is difficult even to hold the material without damaging it. To improve the properties of silica aerogels, it is usually thought to prepare silica aerogel composite materials. Primary objective to prepare monolithic silica aerogel composites is to improve the mechanical properties along with thermal properties while keeping its transparency.

To enlarge the application areas and to improve undesirable properties of the silica aerogels, scientists started to synthesize silica aerogel composite materials with different constituents. The reader should primarily understand the synthesis conditions of the pure silica aerogels before going into details of the hybrid material preparation conditions.

Silica aerogels are prepared by sol-gel process. Primarily, after mixing the reactants, independent colloidal particles are formed and dispersed within the solution. These particles have partial internally crosslinked structures. This colloidal suspension is known as the “sol” (Fig.2-3). Later in the process, “gel” is the term given for an interconnected rigid network consisting of submicrometer sized pores filled with liquid and chains whose average length is greater than a micrometer [52]. This gel is composed of three dimensional silicon oxide arrangement filled with a liquid [53]. If the pore liquid is an alcohol used in the process, the gel is named as alcogel (Fig.2-3). The next step is to dry the alcogel to discard the liquid within its network and to obtain an aerogel (Fig.2-3). The total process requires a lot of time including gel preparation stage consisting of the wet gel synthesis, aging step which is required to strengthen the wet gel and drying stage leading to the porous aerogel structure cleaned from all the liquid [54].

### 2.3.1.1 Sol-Gel Process:

#### *2.3.1.1.1 Gel Preparation:*

As this step consists of consequent hydrolysis and condensation reactions leading to a solid network, the experimenter should understand the underlying chemistry for the development of the aerogels. Silica precursors are the starting materials of the sol-gel process. Synthesis starts with the hydrolysis of the appropriate precursor mixed with water in a suitable solvent. The hydrolysis reactions and the final point of the condensation leading to a solid network are accelerated by the addition of a catalyst. Three different procedures such as acid catalysis, base catalysis and two step acid-base catalysis are

suggested by Dorcheh and Abbasi in their study [2]. A typical two step sol-gel process is schematized in Figure 2-2.

### 2.3.1.1.2 Chemical Precursors:

When silica aerogels were first synthesized, metallic precursors were used. Currently, organic precursors such as TEOS, TMOS, and some other silica based precursors are preferred over metallic ones. These organic precursors have partial positive charges that make them less susceptible to nucleophilic attack [54]. As they also have their oxidation state equal to their coordination number, their hydrolysis and condensation kinetics are slower than metal systems. To overcome this slow kinetics, acid and/or base catalysts are frequently added to the solution.

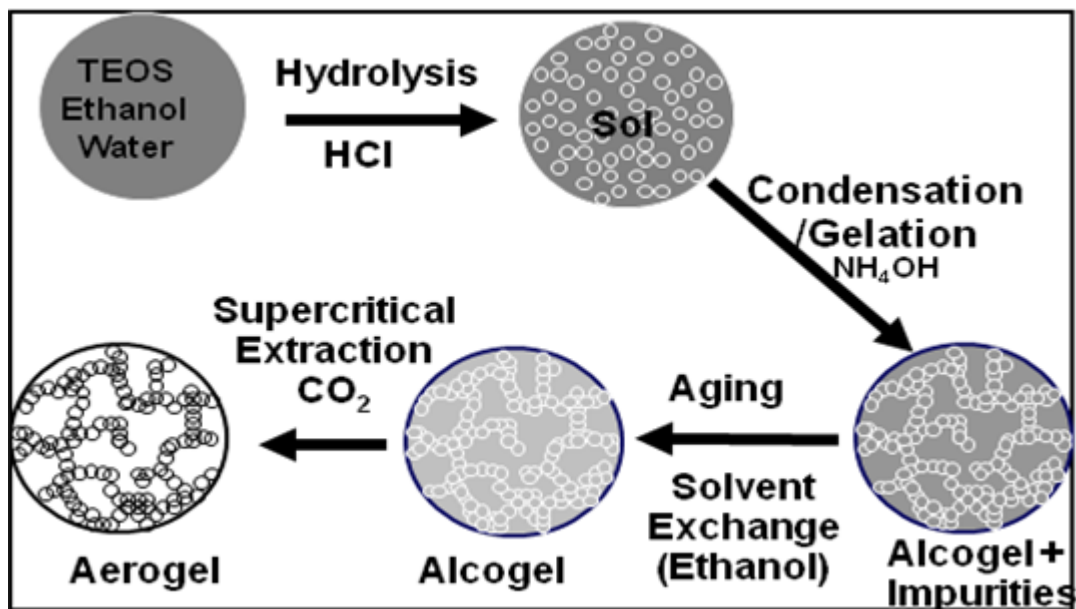
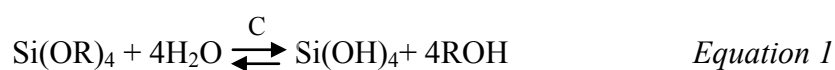


Figure 2-2: Two step acid base catalysis of silica aerogels

### 2.3.1.1.3 Hydrolysis:

Hydrolysis is the primary step of the sol-gel synthesis. With the help of a catalyst, alkoxide groups (OR) of the organic precursor  $-\text{Si}(\text{OR})_4-$  are replaced by hydroxyl groups (OH) one by one leading to the formation of the silanol groups (Si-OH) [54].

A general hydrolysis reaction of a silica precursor can be represented as follows:



where R represents the alkoxide group and C the catalyst.

The reverse process is called esterification. The replaced alkoxide group of the precursor appears in the alcohol corresponding to it. As water is immiscible with alkoxy silanes (because of the hydrophobicity of the alkoxide groups), alcohols such as ethanol and methanol are also added in the sol to achieve the miscibility between the constituents. Namely, to facilitate hydrolysis, alcohols are used as co-solvents along the water [38]. Looking at the phase diagram constituted by ethanol/water/alkoxide combination as shown in Figure 2-3, the minimum amount of alcohol that is required to achieve miscibility along the required stoichiometry between the organic precursor and water (for a homogeneous mixture) can be calculated.

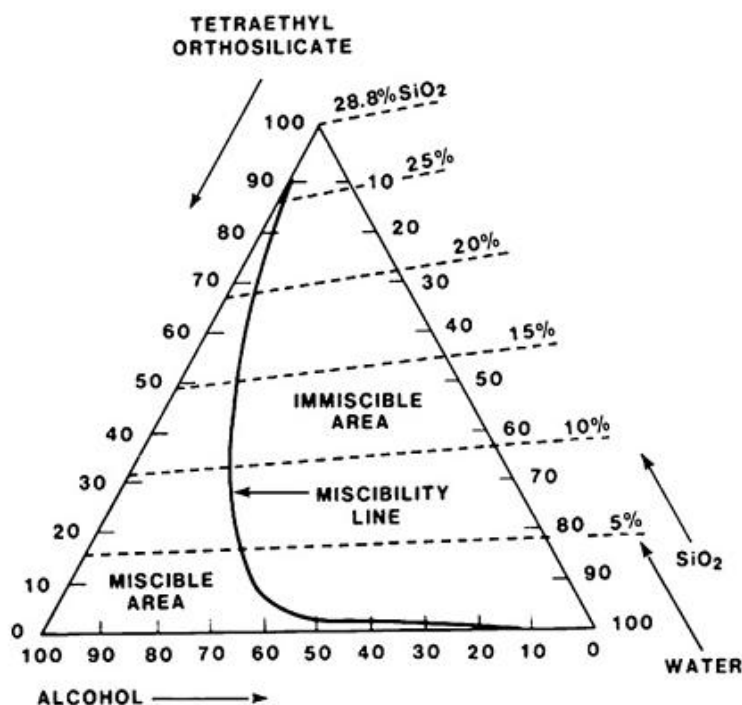


Figure 2-3: Ternary Phase Diagram of TEOS-Ethanol-Water system at 25°C. Reprinted from ref. [2] with permission from Elsevier.

Hydrolysis is performed either by the addition of an acid catalyst or a base catalyst as mentioned earlier. Rate and extent of the hydrolysis depend upon the strength and the concentration of the catalyst as well as the temperature and the choice of the solvent. Alkoxy groups tend to donate more electrons than hydroxyl groups so that as more alkoxy groups around the silicon atom are replaced by hydroxyl groups, the transition state becomes less stable and the rate of the hydrolysis decreases [38].

The effect of pH on the hydrolysis rate can be seen in Figure 2-4. Both hydrolysis and condensation reactions are accelerated with low pH values. However, the rate of hydrolysis is higher than that of condensation reactions. As the pH value increases, both reaction rates decrease. Moreover, at neutral pH, the hydrolysis rate reaches its minimum

value while the condensation rate starts to increase gradually. Based on the information gathered from this figure, the hydrolysis and condensation reactions can be arranged accordingly.

As an example, the hydrolysis of Tetramethylorthosilicate (TMOS) is faster than that of Tetraethylorthosilicate (TEOS) because TEOS has bulkier ethoxide groups (compared to methoxide groups of TMOS) that slow the process of hydrolysis [54]. Bulkier alkoxide groups exert more influence on the rate of the hydrolysis. Larger groups create more steric hindrance and they overcrowd the transition state leading to a slower reaction.

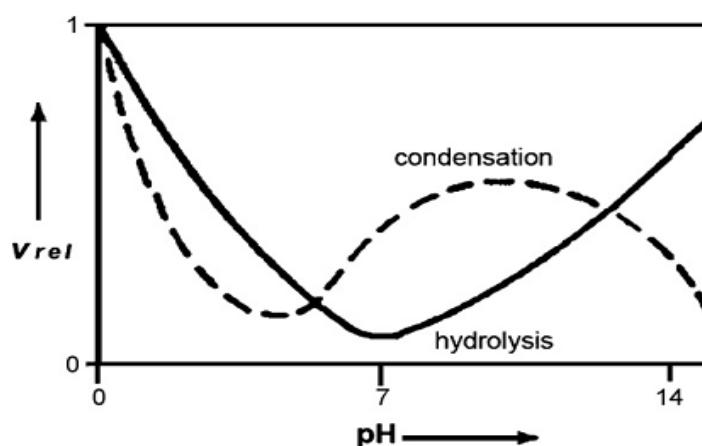
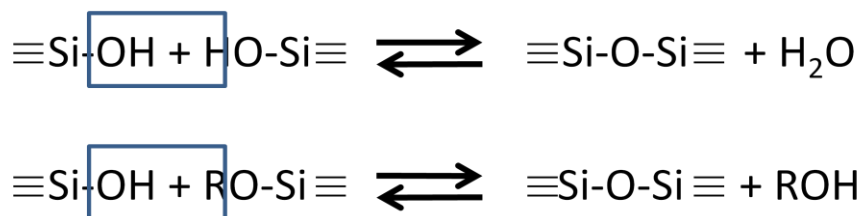


Figure 2-4: Dependence of the relative hydrolysis and condensation rates on the pH of the solution Reprinted from ref. [2] with permission from Elsevier.

#### 2.3.1.1.4 Condensation:

Condensation reactions are polymerization reactions leading to the formation of siloxane bonds ( $--\text{Si}-\text{O}-\text{Si}-$ ) [54]. These reactions are classified in two different types such as water condensation and alcohol condensation as is shown in Figure 2-5. The reverse reactions are hydrolysis and alcoholysis respectively. Condensation reactions occur simultaneously with hydrolysis reactions as soon as hydrolyzed species appear in the solution.



**Figure 2-5: Water and Alcohol Condensation Reactions respectively**

Condensation rate is dependent on the charge of the transition state and on the steric effects just like the hydrolysis [38]. Less steric crowding in the transition state or intermediate molecules can promote condensation kinetics, however; bulky groups decrease the rate of the process [54].

Condensation reaction rates have a strong pH dependency as seen in Figure 2-4. The pH of the process affects also the structure of the network along with the rate of the process. Acid catalyzed reactions result in an open, highly ramified structure followed with further hydrolysis and co-condensation reactions. The outcome of the base catalyzed reactions is a gel with larger pores between interconnected particles because of a higher condensation rate with respect to hydrolysis. The result is the formation of dense particles in a highly condensed network [37]. The dependence of the structure of the resulting gel on the pH is illustrated with Figure 2-6.



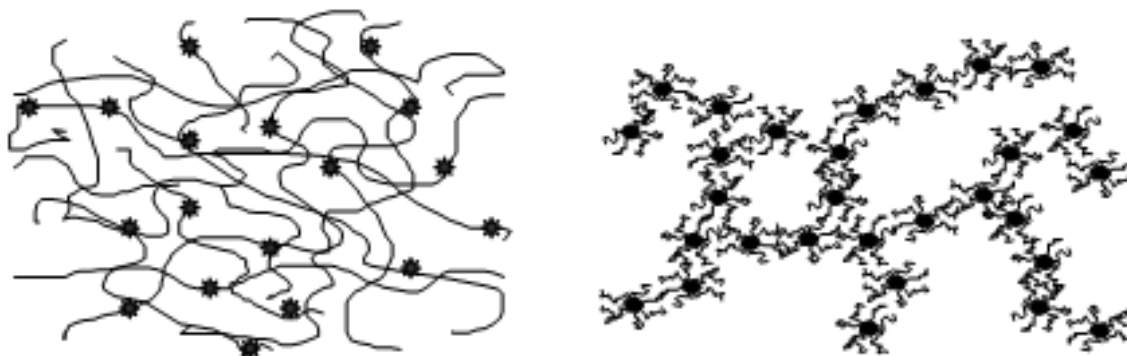


**Figure 2-6: Gel structure for acid and base catalyzed reactions respectively. Reprinted from ref. [3] with permission from Elsevier.**

#### *2.3.1.1.5 Gelation and Aging:*

In one way, gelation can be considered as the final step of the condensation reactions with a sudden, large increase in the viscosity. Gel is formed when the sol can carry a stress elastically [52]. However, at the initial gel point where the sol reaches this high viscosity and does not pour when the vessel is tipped, there are still sol particles present in the network. Further cross-linking and chemical inclusion of isolated sol particles into the network occur following gelation and results in an increase in the elasticity [38].

Aging processes, during which wet gels or alcogels are placed into suitable solutions, are applied after the gelation step. The gelation time is accepted as the moment when the last bond is formed in the chains constituting the spanning cluster [54]. After gelation occurs, condensation reactions do not stop but continue because of the flexible hydroxyl groups on the surface of the gels. When the gel is kept in its pore liquid for a period of time called aging, its structure and properties continue to change even after its gelation point [52]. Different processes such as polycondensation, syneresis, coarsening and phase transformations can take place during the aging process. Condensation

processes continue to occur within the network if the silanols are close enough to react with each other. This process increases the connectivity of the network and its fractal dimension. Syneresis which is the term used for the expulsion of liquid from the pores in alcoholic gel systems is recognized by the formation of new bonds through condensation reactions. By this way, the bridging bonds within the network increases and it causes the gel to shrink [52]. Coarsening process causes a decrease of the surface area because of the continuous precipitation and dissolution process of the network itself. Another effect of aging can be phase transformations due to the presence of isolated regions of the unreacted precursor in the porous gel. When this gel is placed into aging solution, these unreacted materials can react partially or completely producing a material with different structure and composition. If the refractive index of such material is different than that of the network, the whole sample may contain appearance properties of a phase-separated material [38].

Aging process serves to make stiffer and stronger networks by creating new bridging bonds. It is important for the resulting physical properties and also for the resulting mechanical properties which ensure the success of the drying that will follow.

#### *2.3.1.1.6 Drying:*

Drying of the alcogels is the removal of the liquid from its pores by replacing it with air. This process can be divided into several stages. Primarily, the sample shrinks by an amount equal to the volume of liquid evaporates [54]. As the drying proceeds, the gel structure becomes more stiff and strong and the shrinkage stops. At this point, the liquid starts to recede into the porous structure of the gel. Due to the small pore size, the surface tension and high capillary forces several cracks are created at this stage of the process. Furthermore, flow in the thin liquid film remaining on the pore walls to the surface followed by evaporation and also direct evaporation from the pores make the drying continue [38]. Then, the liquid becomes isolated into pockets, and the drying continues

only by evaporation of the liquid within the sample and diffusion of the vapor to the outside [54].

Although there are different methods to perform drying of the alcogels, supercritical drying is the most preferred one during which there is no capillary stress causing cracks in the resulting aerogel. In this process, an alcogel sample filled with liquid is contacted with a supercritical fluid. The supercritical fluid is able to dissolve the pore liquid therefore it reduces the capillary stresses created within the pores. By this procedure, all liquid trapped inside the pores is transferred by diffusion to the supercritical fluid phase without damaging the structure. Then, the vessel in which the extraction proceeds is depressurized. Because alcohols have good solubility in CO<sub>2</sub> which is relatively nontoxic and cheap, CO<sub>2</sub> is the most widely utilized gas in supercritical drying processes. CO<sub>2</sub> has also suitable critical conditions with critical temperature of 31.1 °C and critical pressure of 74 atm.

### ***2.3.2 Synthesis of Silica Aerogel Composites:***

Recently, the field of polymer-silica nanocomposites has been flourishing. There appeared several articles, books or reviews about this subject explaining their synthesis, characterization and application areas [6-8,55,56]. Our research focuses mainly on a certain subfield of silica nanocomposites, namely silica aerogel polymer composites.

Sol-gel process is the preferred method to synthesize silica aerogel-polymer hybrid materials because of its low temperature processing characteristics [55]. As organic materials are more sensitive to temperature changes, the low temperature process allows these components to keep their properties without being degraded. Organic-inorganic composites combine the properties such as the rigidity, the transparency, the chemical and thermal stability of an inorganic entity with the properties such as flexibility, ductility and processability, functionalisation of an organic entity [8, 16] Therefore, scientists thought to combine the advantages of organic materials with those of silica aerogels synthesizing silica aerogel polymer composites.

Apart from the low temperature processing advantages, the sol-gel mechanism allows the nanoscale mixing of the different components [38]. This intimate mixing can help to obtain transparent materials because the possibility of domain formation is reduced. Since the properties of the resulting composite would not depend only on the individual properties of the constituents but also on the phase morphology and interfacial properties, the mixing stage is of vital importance to prevent phase separation [38]. Therefore, to obtain hybrid silica aerogels, in other words, silica aerogel composites, it is required to carefully plan the cross linking reaction as well as the process conditions from the initial stage. As the structure of the silica aerogels give them these appealing physical characteristics, it should not be damaged or changed but kept the same as much as possible while preparing new composite materials involving silica aerogels [16].

Although the sol-gel process emerges as the most promising route for the synthesis of silica aerogel composites, there is still some research using different technique or different procedure for the synthesis of silica aerogel-polymer composites.

#### 2.3.2.1 Co-condensation reactions by the use of organically substituted co-precursors

One of the applied methods to synthesize silica aerogel polymer composites is to use an organo(poly)siloxane as the co-precursor [11]. Co-condensation of two or more precursors leads to the formation of a chemical bond between inorganic silica precursor and the organic co-precursor [55]. These polymers which are used as co-precursors are accepted to be suitable for the preparation of the silica aerogel-polymer composite materials due to their chemical and structural compatibility with the sol-gel process.

In the research conducted by de la Rosa *et al.*, Polymethydisiloxane (PDMS) was used as the organic precursor along with the inorganic silica precursor, tetraethylorthosilicate (TEOS), to create a hybrid silica aerogel covalently bonded to an organic group [11]. In this study, there was no solvent usage to homogenize the hydrolysis solution because aerogels were derived via high-power-ultrasound-assisted reactions. After

the pre-hydrolysis of the inorganic precursor, the polymer –PDMS- was added to the solution along with methyltriethoxysilane (MTMS) as another organic phase. Simultaneous hydrolysis of the inorganic and organic precursors resulted in a silica aerogel-polymer composite which was found to be mechanically stronger due to the formation of covalent bonds. However, the results revealed some heterogeneity in the composite material due to a phase separation between the tough silica matrix and the elastic polymer chains which resulted in plastic microcracks in the pores of the synthesized composites.

In another study, Luis Esquivias *et al.* synthesized OH-PDMS/TEOS aerogels to study the bioactivity of these hybrids [9]. Ultrasonic mixing was again used to homogenize the mixture of TEOS and OH terminated PDMS which are actually immiscible. It is also recognized that the ultrasonic mixing prevents the cyclidation of chains while increasing their cross-linking. In the final stage, the wet gels were dried in an autoclave with supercritical ethanol. Unfortunately, their work resulted in composite aerogel containing some heterogeneity with low cross-linking.

Another work of the group of Luis Esquivias, the silica aerogel polymer composite was synthesized using PDMS as the co-precursor. The mechanical properties of the new bioactive hybrid materials were investigated[10]. In their study, PDMS and MTMS were used as organic phases along with the silica precursor, TEOS. It is claimed that the introduction of the cross-linker in the silica network enhances the mechanical resistance of the material.

Aspen Aerogels also contributed in this field by the use of PDMS in their silica aerogel synthesis [57]. The researchers have chosen to use PDMS with hydroxyl end groups because of its good thermal stability and potential reactivity towards silica precursors. They investigated the physical properties such as the density and the shrinkage as well as the mechanical and thermal properties of the resulting composites. They used THF or isopropanol as the co-solvent along ethanol to dissolve PDMS and obtain a

homogeneous solution rather than using ultrasound mixing. They examined the effect of changing the process parameters, the molecular weight of the organic precursor and the aging solutions. Epoxy-PDMS was another organic precursor which was tested for the same purpose with the same process parameters. They concluded that the organic precursor incorporation in the silica network increased the flexural strength but reduced the transparency. The higher density of the synthesized materials was due to the bonding between the silica precursor and PDMS.

Hüsing *et al.* also used an organically substituted co-precursor along with the silica precursor [58]. The authors demonstrated that silica aerogel polymer composites can be synthesized by using a new sol-gel precursor such as oligo(methylvinylsiloxane). They introduced it as a co-precursor together with TEOS to obtain a silica gel polymer network at the end. The silica precursor, TEOS, was prehydrolyzed in ethanol with hydrochloric acid before the addition of the polymeric precursor. After the addition of a base catalyst, the polymeric precursor solution was added under continuous stirring. After a specified time, the sol was transferred into molds and left for gelation. Wet gels were then subjected to supercritical drying to obtain silica aerogel polymer composites. As the amount of polymeric precursor increased, the specific surface area of the composite aerogels decreased and the corresponding density increased. A higher weight loss in TGA was attributed to a higher polymer content. However, the organic weight loss was very close to the added weight of the polymeric precursor assuming there is no hydrolysis or condensation of the co-precursor. Based on this information, no high degree of cross-linking can be concluded. Though, as the higher amount of polymeric precursor leads to longer gelation times, it is concluded that the polymeric precursor interrupts the silica network formed by the silica precursor alone.

### 2.3.2.2 Liquid Phase Modification in the wet nanocomposite stage

#### 2.3.2.2.1 Diffusion Controlled Polymer Cross-Linking

There are not many polymers which are compatible with the sol-gel process. Not to be limited in a small range of polymers with similar functionalities, the research on synthesizing silica aerogel polymer composites has included the use of other components such as cross-linkers [4, 12, 13], stabilizing agents,[59] and coupling agents [60]. The use of a cross-linker to attach the polymer to the silica network appears to be one of the most commonly performed procedure. For this method, several cross-linkers are used according to their solubilities in the initial solution containing the precursor, alcohol and water or in the aging solutions.

Zhang *et al.* synthesized silica aerogel polyurethane composites via the use of a isocyanate cross-linker [61]. Inspired by the polyurethane chemistry, the authors hypothesized that the isocyanates will react with surface silanols which will mimic the polyols in the polyurethane formation. In the study, silica alcogels were prepared using either one step or two step sol-gel process and then placed into solutions containing isocyanate monomers for cross-linking. Different cross-linking solvents at different temperatures were investigated. The use of viscous solvents increased the number of solvent exchange steps because of the difficulty of full removal of the solvent from the pores. Therefore, cross-linking in volatile solvents such as acetone or acetonitrile was also performed reducing the necessity of several washing stages. During cross-linking, it was suggested that isocyanates reacted with surface silanols forming carbamates and reacted with adsorbed water to form CO<sub>2</sub> and an amine which in turn reacted with other isocyanates to extend the polymer chain. This process also created particle bridging with urethane terminated polyurea and it was confirmed by <sup>13</sup>C-NMR analysis. After supercritical drying, the silica aerogel composites were mechanically tested. It was shown that the cross-linking increased the strength of silica aerogel together with increasing

density. The reduction in surface area was explained by the fact that the polymer coating prevents the access to the porous structure beneath the first polymer layer. The resulting composites were not totally hydrophobic and did sink when placed in water; but they were not as hydrophilic as the pure silica aerogels because they did not collapse with water contact. This study has shown that the silica aerogels could also be cross-linked not only with isocyanates but with other cross-linkers as well provided that the cross-linker would react both with surface silanols and with itself.

Several research groups utilized another technique for the synthesis of cross-linked silica aerogels. They used the method of co-gelation of the silica precursor with 3-aminopropyl(triethoxysilane) (APTES). Addition of APTES functionalized the precursor with amine groups which then became connectors for cross-linking of several organic constituents [4, 12, 13] .

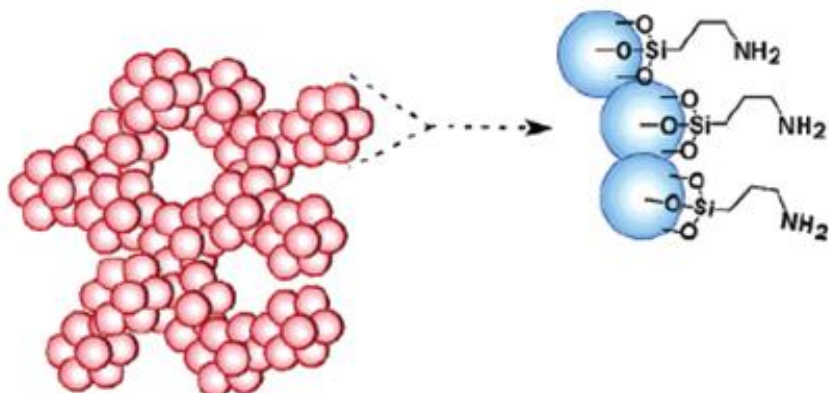


**Figure 2-7: Amine Modified Silica Surface.** Adapted from ref [4]. Copyright 2011 American Chemical Society.

Meador *et al.* have used the technique of copolymerization of Tetramethylorthosilicate (TMOS) with APTES to make use of the epoxy chemistry. Introduction of APTES in the hydrolysis solution has rendered the functionalization of surface of the silica with amine groups ready to interact with epoxies which will imitate the



role of polyfunctional amines [4]. The importance of APTES addition came from the fact that the chemical bonding between the inorganic group and the polymer will make the composite more compatible and will enhance physical properties such as mechanical strength. After the introduction of amine functionality, the alcogel was treated with di-, tri- and tetra- epoxies with various concentrations [4]. Subsequently, while the alcogels were still in the corresponding cross-linking solution, they were placed in an oven at specified temperatures for further cross-linking. After supercritical drying, composite aerogels were characterized. Density of the hybrids increased as the cross-linking increased resulting in the reduction of the surface area as expected. However, silica aerogel cross-linked with the short length epoxides had higher surface areas compared to the composites prepared with isocyanates as described previously. Tri-epoxides resulted in strongest silica aerogels due to their greater reactivity compared to other epoxides. Although the epoxide incorporation was also achieved without APTES, the density of the composites indicated that APTES addition increased the cross-linking dramatically.

Another study using the same approach was performed by Katti *et al.* for the cross-linking of silica aerogels with di- isocyanates. Just like the previously described study of Meador *et al.* [4], they modified the surface of the silica aerogels with APTES to introduce amine functionality [62]. Hexamethylene diisocyanate oligomer was used as the cross-linker. Since the hydrolysis of TMOS is faster than that of APTES, it is claimed that the amine functionality will be mostly present at the surface of the skeletal nanoparticles. It is also reported that the reaction of isocyanates with amines is faster than their reaction with hydroxyls. Therefore, the resulting polyureas are stronger than polyurethanes. After treatment with APTES, the resulting alcogels were placed into a solution containing isocyanates for cross-linking. Subsequently, the cross-linked alcogels were dried supercritically. Based on the characterization results, the cross-linking of amine functionalized silica aerogels resulted in a denser structure. However, it was suggested that

the polymer coats the surface while leaving the mesoporous voids open. The samples were characterized by Attenuated Total Reflectance Spectrometry (ATR-FTIR) and Thermal Gravimetric Analysis (TGA) for the confirmation of polymer presence. Mechanical testing showed that the silica aerogel composites were stronger compared to the unmodified, pure counterparts.

Cross-linking of amine modified silica aerogels with isocyanates using amine functionality was also investigated in two other studies [12, 63]. Meador *et al.* reported that they ameliorated their previous research [4] by extending some process parameters [12]. It was shown that both silica and cross-linker concentration had a significant effect on the final density. In that regard, these two parameters along with water concentration were varied in order to determine their effect on the amount and the length of the polymer crosslink. With an interest in the shortening the aerogel synthesis process, the number of solvent exchange steps before the polymerization was also varied to find the optimum procedure. The characterization of these cross-linked silica aerogel with di-isocyanates showed that the processing parameters had profound effects on the density, porosity, strength and the thermal conductivity. The size of the cross-links was quantified by  $^{13}\text{C}$  NMR technique to provide information about the resulting properties of the silica aerogels.

Luo *et al.* performed the same synthesis methods and then carried out dynamic compressive experiments for the resulting hybrid materials [63]. They investigated the effect of density on the mechanical properties of the composite silica aerogel by varying the cross-linking agent in the aging bath with different aging time and temperature conditions. It was reported that both the Young's modulus and compressive yield strength of the composites have increased with increasing density meaning increasing polymer concentration.

Another study performing the same procedure using polystyrene as the polymer was conducted by Ilhan *et al.* [13]. The research was focused on the preparation of a core-shell

structure with silica aerogel as the core and the polystyrene as the shell. For this purpose, the silica precursor which is TMOS in this case, was amine modified with APTES. After the attachment of styrene moieties to the amine modified silica aerogel, the styrene moieties were cross-linked with a free-radical polymerization reaction by the introduction of Azobisisobutyronitrile (AIBN) along with styrene, p-chloromethylstyrene or pentafluorostyrene. The authors reported that the free radical polymerization of polystyrene in the mesopores created interparticle tethers [13]. SEM and BET analysis supported the claim that the polymer only coats the surface without penetrating into the network and filling the mesopores.

Another research group proposed to use a silane precursor such as vinyltrimethoxysilane (VTMSH) to provide reaction sites for styrene polymerization [64]. The silica aerogels were prepared by the hydrolysis of alcohol solutions of silane components such as TMOS, VTMSH and BTMSH (to provide flexibility) together. Consequently, the water and basic catalyst were added to the mixture under continuous stirring. The wet gels were then poured into molds where the gelation took place. After gelation and succeeding aging processes, the alcogels were placed into the solution consisting of styrene moieties and an initiator. After this cross-linking step and the following solvent exchange processes, the cross-linked composites were dried supercritically. The resulting silica aerogels had higher densities with an increasing VTMSH which would lead to more cross-linked polymers. On the other hand, higher BTMSH concentration tended to decrease the density because of creating steric hindrance for polystyrene cross-linking with hexyl groups. This finding was also supported by BET analysis which showed the reduction in surface area of the composites.

Boday *et al.* modified the surface of the aerogel with a  $\alpha$ -haloester functional triethoxysilane to enable the covalent attachment of the polymer (Poly(methyl methacrylate)) on the surface [65]. As the modification agent is less reactive than the main

precursor, it was highly ensured that the surface would be covered by the agent. After the modification, the authors followed the same procedure as previous studies and placed the alcogels into solutions containing appropriate monomer and suitable catalyst for polymerization. The time of polymerization was varied to have control over the molecular weight of the polymer namely the length of the polymer chain. At the end of the polymerization, the alcogels were dried supercritically to obtain composite silica aerogels. The difference of polymer concentration between the interior and the exterior of the stronger silica aerogel composites revealed that as the polymerization proceeds there is less chance for monomers to penetrate inside the network and continue to extend the polymer chain there. The surface area reduction and the pore size shift also supported this claim.

Recently, a study conducted by Nguyen *et al.* involved the synthesis TMOS/BTMSPA ((bis(trimethoxysilylpropyl)amine) aerogels reinforced with tri-isocyanates to investigate the flexibility and elastic property changes [66]. The aim of incorporating BTMSPA to the network was to provide flexible linkages to the structure, to create reactive sites for tri-isocyanates and to serve as a base catalyst for the condensation reactions. It was reported that the silica aerogels were synthesized using one step sol-gel process using BTMSPA as the catalyst. After gelation, wet gels were immersed in a solution containing tri-isocyanates. The amine sites of BTMSPA acted as reaction sites for the polyurea conformal coating on the silica network. After treatment of the wet gels with tri-isocyanates, the gels were supercritically dried with CO<sub>2</sub>. The resulting silica aerogel composites exhibited higher mechanical strength along with more flexibility. Low concentrations of BTMSPA in the initial mixture resulted in low polymer cross-linking due to the low reaction sites for the polymer linkage. The surface area of the reinforced aerogels decreased as expected because polymer coating blocked the access of the interior porous structure for the nitrogen sorption experiment.

#### 2.3.2.2.2 Direct Addition of the Monomer in the Initial Solution for Polymer Cross-Linking

A silica aerogel-polymer cross-linked hybrid material can also be formed via the dissolution of chosen monomer in a suitable solution containing the inorganic precursor followed by the sol-gel reaction.

Leventis *et al.* used this technique for incorporation of a polymer coating on the surface of the silica aerogels [67]. They synthesized polyacrylonitrile cross-linked silica aerogels using a one pot procedure to shorten the total time of the sol-gel process. Including the monomer in the initial sol eliminated the steps associated with preparation and use of cross-linking solutions thereby reducing the time of the total process. Acrylonitrile was directly added to the initial sol together with a free radical initiator to covalently bond the polymer to the silica surface thus preventing polymer loss in any other stages of the process. They found out that there was still unreacted monomer inside the structure and they conducted post cross-linking washes to clear the composite network. After supercritical drying, opaque-white silica aerogel cross-linked polymer composites were obtained with lower surface area and higher pore radius. As the purpose of the study was not only to synthesize silica aerogel polymer composites but also to use them as a precursor for other processes, the authors did not perform any other characterizations other than density, shrinkage and porosity measurements.

Meador *et al.* in their recent paper proposed a new method similar to the one used by Leventis group [67] to shorten the process where a polymer coating is applied on a silica aerogel [68]. The authors proposed a streamlined procedure to eliminate polymer diffusion and half of the solvent exchange steps. Instead of using diffusion controlled polymer cross-linking, the paper showed a one pot procedure in which the polymer was directly added in the initial sol. Based on this point of view, the wash step before the cross-linking and the polymer diffusion steps were eliminated. The results indicated that the silica aerogel composites prepared by this method were more homogeneous with respect to the polymer

distribution. This view is supported by the extremely higher densities with extremely lower surface areas compared to the silica aerogel composites prepared by diffusion process. This is due to the complete reaction of epoxy monomers with all amine sites without being controlled by diffusion. Improved mechanical properties are also achieved by this method which represents more advantages like a shorter process with a more homogeneous distribution of the polymer coating.

Yim *et al.* used the wet gel modification step in order to prepare silica aerogel polymer composites [69]. They did neither include any cross-linker, stabilizing agents nor coupling agents in order to link the polymer to the silica network. They started from the very beginning, from the monomer to synthesize the composite. They primarily prepared the silica alcogel by hydrolyzing TMOS in acidic conditions. The subsequent distillation of this partially hydrolyzed sol to evaporate any solvent resulted in a condensed silica solution. To this solution, polymeric MDI (methyl diphenyl diisocyanate) solution was added with varying densities along with a catalyst 2-dimethylaminoethanol and a diluents, 1,4-dioxane. Absence of a basic catalyst in the condensation step increased the gelation time and also the corresponding aging processes. Resulting silica aerogel polyurethane composites were then supercritically dried to remove any residual liquid inside the pores. The final surface areas measured by BET method was only around 200 m<sup>2</sup>/g, though the researchers pointed out that the synthesized composites had low thermal conductivity and do not absorb moisture like in the case of native silica aerogels.

#### 2.3.2.3 Post-synthesis modification of the final dried product by dissolved organic species

Another method to prepare silica aerogel polymer composites is to primarily synthesize the inorganic aerogel namely silica aerogel without the polymer and then subject this aerogel to the polymer addition. The polymer is added either during the supercritical drying or after the supercritical drying stages of the sol-gel process.

### 2.3.2.3.1 Chemical Vapor Deposition Technique (CVD)

The CVD technique was first used to create silica aerogel polycyanoacrylate composites by Boday *et al.* [5]. They synthesized base-catalyzed silica aerogels and exposed them to nitrogen containing methyl cyanoacrylate. Cyanoacrylate esters readily polymerize upon adsorption on the surface containing adsorbed water or nucleophilic substituents. In addition, their relatively high vapor pressure makes them ideal candidates for CVD approach. As a result of the CVD reactions, the surface of the silica aerogels was homogeneously coated with polycyanoacrylate which was confirmed by SEM analysis. However, the treatment with acetone proved that the polymers which are formed on the surface were not covalently attached because they were all removed with the solvent. The polymer coating had reduced the aerogel transparency, even had lead to opaque aerogels. Because of the high numbers of initiators on the surface, namely high concentration of adsorbed water, very long polymer chains could not be formed. The increase in density, the reduction in surface area, the opaqueness and the polymer leaching with acetone contact were not compatible with improvements in the mechanical properties and unexpected increase in the surface hydrophobicity. It is suggested that a reduction in the surface initiators should lead to strong aerogel composites with smaller increase in density and less decrease in surface area.

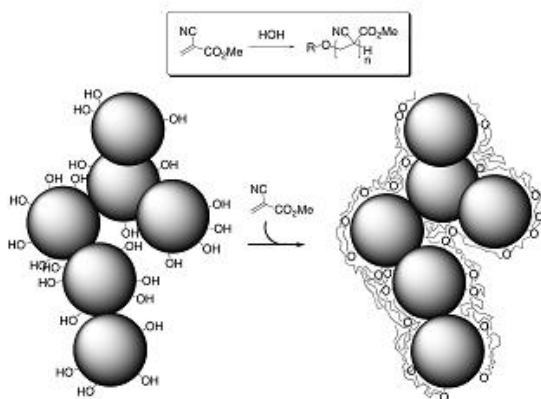


**Figure 2-8: CVD Deposition and Subsequent Polymerization of Methyl Cyanoacrylate On the Surface of Silica Aerogels. Reprinted with permission from ref [5]. Copyright 2011 American Chemical Society.**

Another study of Boday *et al.* on the chemical vapor deposition method presents an improvement for the attachment of polycyanoacrylate on the surface of the silica aerogels [14]. They considered the method proposed by Meador *et al.*, [4, 12] in order to aminate the surface of the aerogel before the cross-linking reactions. The silica precursor, TMOS was treated with APTES to prepare silica aerogels with amine groups on the surface. In order only to leave amine groups on the surface, the wet gels were then treated with Hexamethyldisiloxane (HMDS) which reacted with silanols and residual water. Due to this reasoning, they expected to have only amine groups which will initiate the polymerization of cyanoacrylates deposited by CVD method. The modification of the silica aerogel surface would result in higher molecular weight chains deposition. After copolymerization with APTES and surface silylation, the wet gels were dried supercritically prior to the CVD method. The dried silica aerogels were then treated with dry nitrogen gas saturated with methyl cyanoacrylates in a reaction chamber. Varying the time of the exposure to the monomer saturated gas stream gave the control of the density of the composite aerogels.



Although the composites were again opaque and had lower surface areas, resistance of the polymer to the extraction with acetone indicated that the covalent bonding was achieved successfully. As the concentration of the amine groups on the surface increased, the heterogeneity of the polymer deposition appeared. The amine groups prevented the penetration of the polymer inside the porous structure restricting it only on the surface creating a dense crust. However, the strength of the aerogels increased so significantly that they could be cut in specific shapes without breaking.

Further studies conducted by Boday *et al.* in the field of silica aerogel polymer composite synthesis by CVD method presents new strategies to prepare the hybrid material [15]. In this study, the authors chose to use hexylene- and phenylene bridged polysilsesquioxanes as the silica precursor. It was reported that the hydrophobic organic bridging groups of the polysilsesquioxanes reduced adsorbed water concentration on the surface available for polymerization reaction. This fact was confirmed by contact angle measurements and also by thermal gravimetric analysis. Due to the reduced amount of water available for the initiation of the polymerization, polymers with higher molecular weights were obtained at the end of the preparation process. However, similar to one of the previous studies of Boday *et al.* [5], chemical vapor deposition of cyanoacrylate followed by its polymerization on the hexylene or phenylene bridged polysilsesquioxanes aerogels resulted in weak bonds between the polymer and the surface of the aerogel. Polymers attached to the surface of the aerogels were easily extracted with acetone as mentioned previously [5]. Although the polymer chains were not covalently attached to the silica network, the composites had higher flexural strengths with increasing densities. The surface area of the CVD processed composites was lower than unmodified ones. However, it was still higher than the specific surface area of pure silica aerogels subjected to chemical vapor deposition method.

#### 2.3.2.4 Addition of molecular, but non-reactive compounds to the precursor solution

##### *2.3.2.4.1 Addition before the hydrolysis*

Addition of the organic species to the initial hydrolysis solution is another method supported by the scientists to prepare silica aerogel polymer composites. Despite the fact that there are more studies on silica xerogels, some research has been conducted to synthesize silica aerogel polymer composites using this technique. Premachandra *et al.* investigated the preparation of sulfopolybenzobisthiazole-silica composite [70]. In their study, they chose a thermally-stable, high temperature resistant aromatic polymer, polybenzobisthiazole which was also sulfonated to increase its reactivity towards the inorganic phase. They firstly prepared a polymer solution containing sulfopolybenzobisthiazole, methanol and tributylamine. Afterwards, they added the silica precursor and a coupling agent in this solution under continuous stirring. After a specified amount of time, water was also added to the solution to initiate hydrolysis. The silica content of the final sol was varied to obtain different densities of composite aerogels. After gelation and solvent exchange steps, the wet composite gels were subjected to supercritical drying by CO<sub>2</sub>. As a result of mechanical characterization, the authors indicated that the brittleness of the native silica aerogels was reduced significantly by the polymer incorporation.

Another contribution to this method of silica aerogel-polymer synthesis was performed by Novak *et al.* [71]. Several polymers were screened for this study and three of them which were poly(2-vinylpyridine), (PVP), polym[methyl methacrylate-co-(3-trimethoxy-silyl)propyl methacrylate)] (PMMA-TMSPM) and silanol terminated poly(dimethylsiloxane) (PDMS) were found to be suitable for the process. The mentioned polymers were dissolved in appropriate solvents used for the sol-gel process and directly added to the sol before the hydrolysis. After gelation and solvent exchange steps, the wet composites were dried supercritically with CO<sub>2</sub>. The research group also investigated in

situ polymerization of a vinyl polymer simultaneously with the sol-gel condensation reaction. Free radical polymerization of N,N-dimethylacrylamide with a corresponding cross-linking agent was initiated in situ with the sol-gel process. This method allowed the formation of two interpenetrating network concurrently. The paper summarizes the characterization results of PVP-silica aerogel composites; however, properties of composites with other polymers were not mentioned. The PVP incorporation reduced the hydrophilic character of silica aerogel and its shrinkage while strengthening the network. Although the composites were transparent, their porosity and surface area were not characterized.

Similar to the process of functionalization of silica network with APTES described previously (See Section 1.3.2.2), the organic phase, the polymer can also be functionalized with amines through the treatment with 3-Isocyanatopropyltriethoxysilane [57]. The synthesis of these silica aerogel polyoxyethylene composites is performed using a procedure similar to the one which is described elsewhere [72]. Simultaneous hydrolysis and condensation with the silica precursor led to the formation of covalent bonds between the organic and the inorganic phases. The resulting composites were transparent and had improved mechanical properties. Higher molecular weight polymers resulted in better mechanical properties, but reduction in the transparency limited the molecular weight of polyoxyethylene which can be used in this process. The maximum molecular weight which can be incorporated without losing the transparency was determined and subsequent experiments including the mechanical and thermal testings were performed accordingly.

#### *2.3.2.4.2 Addition after the hydrolysis*

Another approach to synthesize silica aerogel polymer composites is the addition of the organic material after the hydrolysis of the silica precursor. By this way, the polymeric entity has less chance to interfere with the hydrolysis reaction.

Silica aerogel films were also used for the preparation of silica aerogel polymer composite materials [73]. In this work, the researchers synthesized PDMS hybrid silica aerogel thin films which are reinforced by nanofibers embedded by the electrospinning technique. PDMS based polyurethane was the polymer used for the nanofiber electrospinning. The silica precursor was firstly hydrolyzed in an acidic medium and then silanol terminated PDMS oligomers were added to the hydrolysis solution. After the addition of a base catalyst, gelation kinetics was tested to find a suitable time for the nanofiber electrospinning process in which polymer would be embedded in the matrix. After the gelation of the polymer embedded films, wet films were aged and then subjected to solvent exchange with ethanol before supercritical drying. The resulting materials were silica aerogel polymer thin film composites. Although the reinforced aerogels were no more transparent after the integration of the polymer, they showed high surface areas with large pore volumes. SEM images demonstrated that the polymer nanofibers were well dispersed within the silica film and this rendered the silica film flexible while keeping the high porosity and the low thermal conductivity characteristics of the native silica aerogel.

#### 2.3.2.5 Use of single source precursors in which the organic entity is a part of the network forming species

The synthesis route consisting of the use of a precursor which has the organic entity as its integral part was patented in 2010 by Ou *et al.* [74]. The invention provides specific examples for the synthesis procedures of reinforced silica aerogel monoliths. Silica aerogels are reinforced by triethoxysilyl terminated linear polymers which are prepared by the reaction of the polymer with 3-Isocyanatopropyltriethoxysilane in a suitable solvent. Primarily, linear polymers were end capped with trialkoxysilyl functions. Subsequently, the modified polymer was added to the hydrolysis solution within its solvent. After gelation which was accelerated with the addition of a base, the wet gels were supercritically dried to

obtain silica aerogel polymer composites. It is claimed that the polymer is covalently attached to the silica network via Si-C bonds.

Loy and Shea investigated the preparation of bridged polysilsesquioxanes silica aerogels in their study [75]. In this work, the organic constituent was a part of the network forming species. The molecular building block used in this procedure had an organic framework attached to two or more trifunctional silyl groups by carbon-silicon bonds. Sol-gel process leads to the polymerization of such monomers which will then form bridged polysilsesquioxanes. Monomers were hydrolyzed under acidic conditions after having dissolved in a suitable solvent with an excess amount of water. As hydrolysis and condensation proceeded, branched polysilsesquioxanes grew in size and the viscosity of the sol increased. Before the gelation, the sol was poured in a mold to have a distinct shape. Supercritical drying of these wet gels led to composite aerogels.

Hüsing *et al.* studied the development of novel siloxane-silica nanocomposite aerogels from a single component precursor [58]. Primarily, oligo methyl(2-triethoxysilyl)ethyl siloxane was synthesized via the hydrosilation reaction between oligomethylvinyl siloxane with triethoxysilane in the presence of a platinum catalyst in toluene. Subsequently, the general procedure of a sol-gel process was applied. The polymeric precursor was primarily dissolved in ethanol followed by the hydrolysis via the addition of the acid catalyst and water. The homogeneous and transparent sol was poured into molds and left for gelation. The wet gels were then dried supercritically without being subjected to aging and solvent exchange steps. After performing the drying procedure, white monolithic aerogels with high densities (in the range of 0,8-1,1 g/cm<sup>3</sup>) and up to %55 shrinkage are obtained. Porosity and the specific surface areas of these materials could not be measured by BET because of the inaccessibility of the micropores to nitrogen.

### **2.4 Silica Xerogel-Polymer Composites**

Even though our research focuses on the silica aerogel-polymer composites, it is necessary to review silica xerogel-polymer composites which will form the basis of other hybrid materials for our investigation. The only and most important difference in these studies on the synthesis of silica-polymer composites is the lack of the supercritical drying step. Performing ambient pressure drying or any other drying processes results in a less porous structure with higher shrinkage values and lower surface areas. Experimenting the supercritical drying for most of these materials will lead to better properties. Therefore, it is important to investigate the synthesis conditions of these materials to form a basis for the preparation of silica aerogel-polymer composites.

Poly(vinyl alcohol) [76, 77], poly(imide) [78, 79], poly(methyl methacrylate) [60], poly(ethylene oxide) [80], poly(vinyl acetate) [81] or poly(ether amide) [82] are some polymers used in the preparation of silica xerogel composites. Since it was possible to synthesize silica xerogel composites with these polymers by adding them directly to the hydrolysis solution, it would be interesting to test these polymers with silica aerogels. Ionescu *et al.* investigated the incorporation of the poly(vinyl alcohol) in the silica network by adding the polymer dissolved in water in the precursor solution [77]. By firstly preparing the mixture consisting of the silica precursor and the ethanol as the solvent, the researchers added the PVA dissolved in water to this initial mixture. After a specified hydrolysis time in an acidic medium, the sol was left for gelation. Because one step sol-gel procedure was used, the gelation of the sol took several weeks. After gelation, the wet gels were dried at 60 °C and then subjected to heat treatments at higher temperatures. The microstructure of the resulting hybrid xerogels was qualitatively evaluated by the use of small angle neutron scattering (SANS) technique. It was concluded that an increase in the thermal treatment temperature as well as an increase in the molecular mass due to the polymer addition caused a significant change in the microstructure fractal behavior [77].

The sample which was subjected to the highest heat treatment temperature was found to have the smoothest surface.

Polyimide was another polymer incorporated by the same route followed by Ionescu *et al.* [77]. Ragosta and Musto investigated in detail organic-inorganic hybrid materials based on silica-polyimide components in their review [79]. Polyimides were determined as suitable for this process because they can be obtained via polyamic acid precursors which are soluble in water. For the preparation of silica-polyimide composite materials, primarily polyamic precursor solution is prepared. The silica precursor was then added to this solution in order to perform hydrolysis and polycondensation reactions with the addition of a suitable catalyst. The sol was then film cast by drying the solvent and subjected to curing at elevated temperatures. The heating started the imidization reactions to convert polyamic acid to polyimide along with the cross-linking of the siloxane constituents forming the silica network.

The use of a coupling agent is another method proposed to cross-link silica xerogels with polymers [60]. However, in this approach, the coupling agent is incorporated directly to the heat treated gel, but not added in the hydrolysis solution. The so called coupling agent was responsible to bond to the silanol groups of the surface of the gel as well as to bond to the active sites of the monomer. After the impregnation of the coupling agent dissolved in the specified alcohol, the gels were firstly dried before the introduction of the monomer. The monomers were impregnated on the heat treated gels by simply immersion of the gels successively in different concentrations of the monomer catalyzed solution by benzoyl peroxide. Curing was applied in order to allow for polymerization of monomer on the gels. Excess poly(methyl methacrylate) –PMMA- was removed only by grinding and polishing the gel [60].

Wojcik *et al.* conducted a study on the synthesis of poly(ethylene oxide) silica xerogel composites [80]. The polymer, being soluble in water, was directly added to the

initial hydrolysis solution. The sol was filtered to clear the solution from the precipitates of the polymer during hydrolysis. The gelation occurred without the addition of any catalyst. The resulting wet gels were dried at their gelation temperature (50°C) and then at a higher temperatures for several days. The molecular weight of the polymer and the water/alkoxide ratio were varied in order to optimize the synthesis conditions. Higher water content led to higher skeletal densities with higher internal porosities for an increasing molecular weight whereas lower ratios resulted in lower densities for an increasing molecular weight. Higher water ratios allowed faster and more complete hydrolysis of TEOS thereby indicating a higher degree of hydrogen bonding between silanols and the ether oxygens of the polymer. FTIR spectra confirmed the physical differences obtained at the end of the synthesis and thermal gravimetric analysis indicated the presence of the polymer within the network through the corresponding weight losses.

In another study, Wojcik et al. investigated the preparation of silica xerogel PVAc composites[81]. The polymer was added to the initial hydrolysis solution along with the other components. The polymer weight ratio was varied between 2% and 50%. The resulting composites had higher flexural strengths, were less brittle and had improved hydrophobicity compared to the pure counterparts.

Another polymer tested for the synthesis of composites xerogels was poly(ether amide) [82]. Primarily, 4-aminophenyl ether and 1,3-phenyldiamine were reacted with terephthaloyl in dimethylacetamide to produce amide chains. Then these amide chains were functionalized with carbonyl groups and subsequently reacted with aminophenyl trimethoxysilane (APTMOS). The consequent hydrolysis and condensation reactions of the silica precursor and alkoxy groups of APTMOS formed chemical bonds between polyamide chains and the silica network. The results showed a greater mechanical strength and thermal stability for the composite films compared to those of the pure polymer.



Some other studies were also conducted on the synthesis the silica xerogel polymer composites using a method in which the polymer was added after the hydrolysis of the silica precursor. Polyethylene glycol [83], polyethylene-block- polyethylene-glycol [84], poly(vinyl pyrrolidone) [85], poly(vinyl acetate) [86] were some polymers tested with this synthesis method. Using this technique, Martin *et al.* tried to incorporate a water soluble polymer, polyethyleneglycol, into the aerogel network, by primarily hydrolyzing TEOS with presence of an acid catalyst and water and then adding this solution into different PEG containing solutions [83]. They reported that the PEG concentration in the final aerogel allows the manipulation of the macropore size. They mainly investigated physical, mechanical and acoustic properties of the composite material prepared by the sol-gel route. The authors showed that PEG addition rendered silica aerogels softer, whiter and more opaque. Increasing pore size caused a reduction in surface area and also changed the transparency of the materials. Density of the composites was still around the same value even if the PEG concentration was different. It was concluded that the solid silica matrix should have been changing with a changing polymer amount addition. By structural change of the solid matrix, PEG addition increased the mechanical stability and acoustic velocity at low concentrations. However, increasing the PEG concentration beyond a certain value weakened the matrix and resulted in slower acoustic velocities.

Another polymer used in the same approach was a derivative of PEG, polyethylene-block- polyethylene-glycol (PEPEG) which is soluble in water-alcohol mixtures [84]. Due to its small molecular weight, it is referred as an oligomer rather than a polymer. As in the case with PEG, the silica precursor TEOS is hydrolyzed for 24 hours before the addition of the oligomer. The composite alcogels were dried in an oven at 50 °C, 100 °C and 150 °C successively. Although the shrinkage of the gels was negligible after the second heat treatment, the heating at 50 °C caused 70% shrinkage in the resulting composites. Kulkarni *et al.* reported that the surface area and the pore size of the silica aerogel were significantly

affected by the addition of PEPEG. The oligomer is expected to fill the pores leading to an increase in the pore size which in turns reduces the surface area. After a certain amount which was determined to be 10% of polymer ( $m_{\text{PEPEG}}/m_{\text{TEOS}} = 0.1$ ), the oligomer disrupted the matrix so much that a monolithic composite could not be obtained. Until a certain amount of oligomer, the mechanical properties of the silica xerogel composites were found to increase with an increase in the oligomer concentration. Based on this information, it was concluded that PEPEG was not acting as a bridging element to complete the matrix but probably stayed trapped in the matrix [84]. The condensation of Si-OH species between themselves was faster than a condensation which could occur between the labile glycol groups of PEPEG and Si-OH groups. Therefore, the silica chain formation occurred first and oligomers stayed trapped in the matrix. Steric hindrance of PEPEG chains was found to prevent the interlinking of silica matrix to some extent and led to greater interparticle pores.

Wei *et al.* synthesized silica aerogel poly(vinyl pyrrolidone composites) –PVP-prepared using the same method [85]. Being soluble in the ethanol, the solvent of the process, PVP was another good candidate for the preparation of the silica aerogel polymer composites. The polymer dissolved in ethanol was introduced to the process after the hydrolysis of the silica precursor TEOS, in an acidic medium. After the polymer addition and subsequent gelation of the composites, the alcogels were treated with trimethylchlorosilane (TMCS) for surface modification. The replacement of surface -OH groups with -OSiCH<sub>3</sub> groups of TMCS has rendered the alcogels hydrophobic before the ambient pressure drying. The resulting composite silica aerogels had higher densities not only because of the polymer incorporation but also because of the ambient pressure drying causing larger shrinkage. The surface area was increased surprisingly. However, the generation of micropores was a good explanation for this phenomenon based on the packing and aggregation of polymer nanoparticles. PVP reduced the pore size by occupying a portion of the mesopore portion along with generating a small portion of

micropores. The authors also tested the thermal stability of the composite material by taking TGA measurements. It was observed that the silica aerogels undergo a weight loss at the decomposition temperature of the polymer indicating its presence within the network.

Another polymer tested for the silica aerogel polymer composite synthesis because of its good solubility in water-ethanol mixture is poly(vinyl acetate) [86]. Beaudry, Klein and McCauley prepared silica aerogel composites by primarily hydrolyzing TEOS in an acidic medium. After hydrolysis, PVAc was added to the sol for another 24 hours of mixing. For increasing condensation rate with a decrease in the hydrolysis rate, formamide was also added to the sol before pouring the sol into the molds. Because of the fast gelation, resulting structure of the wet gels consisted of larger mean pore sizes. Larger pores reduced the capillary stress effect during the ambient pressure drying leading to reduced shrinkage. Reduction in density with increasing polymer content revealed the presence of interaction such as the hydrogen bonding between the phases. Based on their characterization results, the authors concluded that there exists hydrogen bonding between the silanols and the OH groups of the polymer chain. As the decomposition temperature determined from the thermal gravimetric analysis was not so higher than that of native PVAc, it is not expected to have strong covalent bonds within the network.

## Chapter 3: EXPERIMENTAL METHODS AND CHARACTERIZATION TECHNIQUES

### 3.1 Pure Silica Aerogel Synthesis

In this study, pure silica aerogels were synthesized using a two-step sol-gel procedure using Tetraethylorthosilicate (TEOS) (from Alfa Aesar 98% purity) as the silica precursor, HCl (from Riedel-de Haen with 37% purity) as the acid catalyst and NH<sub>4</sub>OH (from Aldrich 2.0 M in ethanol) as the condensation catalyst. Primarily, an equal weight percent solution containing EtOH (from Merck with 99.9% purity) and TEOS was prepared. Afterwards, water and acid catalyst were added to obtain a pH of around 2.0 to initiate hydrolysis under continuous stirring. After a specified time of hydrolysis (approximately 40 minutes), the condensation catalyst was added until the pH of the solution reaches 5.5 to start the condensation reactions which eventually lead to gelling of the solution. Before gelation takes place, the solution was poured into cylindrical molds with a diameter of 12.3 mm. The amount of reactants used in the process is shown in Table 3.1.

Table 3.1 Amounts of reactants used in a typical procedure

Compound	Amount added in the sol	Amount (moles)
TEOS	1 g.	Corresponds to 0.0048 moles
EtOH	1 g.	Corresponds to 0.0217 moles to obtain a 50 wt. %solution of TEOS and EtOH
H <sub>2</sub> O	0.34 g	Corresponds to 0.189 moles for a 4:1 molar ratio of H <sub>2</sub> O/TEOS

HCl/EtOH Solution (0.048M)	0.2 ml	Corresponds to $9.6 \times 10^{-6}$ moles of HCl and 0.0033 moles of EtOH
NH <sub>4</sub> OH/EtOH Solution (0.1M)	0.5 ml	Corresponds to $5 \times 10^{-5}$ moles of NH <sub>4</sub> OH and 0.0085 moles of EtOH

The completion of gelation was confirmed by tilting the mold to monitor its increasing viscosity until no more movement of the sol was observed. As the wet gels were still fragile just after the gelation and could be broken while trying to get them out of the mold, at least 15 minutes were waited before the next step of the process. Subsequently, the wet gels were taken out from the molds and placed in an aging solution consisting of equivolume mixture of water and ethanol. One has to be fast enough to take the gel out of the mold and place it in the solution in order avoid evaporation of the pore liquid and to prevent crack formation. The aging solution in a closed container was placed in the oven at 323K for 24 hours before transferring the alcogels into pure ethanol. The purpose of the aging alcogels in water-ethanol solution is to improve their mechanical strength via hydrolysis and condensation reactions of unreacted tetraethylortosilicate remaining on the alcogels. The replacement of water-ethanol solution with pure ethanol is called the solvent exchange step. The pure ethanol solution in which alcogels were kept for 3 more days at room temperature serves to remove all impurities from the pores along with minimization of water concentration within the pores. In order to extract ethanol from the pores of the wet gels, drying with supercritical CO<sub>2</sub> was used. This supercritical drying process was conducted as 313.2 K and 90 bar. The resulting silica aerogels were transparent, brittle and hydrophilic. The schematic representation of the whole process is given in Figure 3-1.

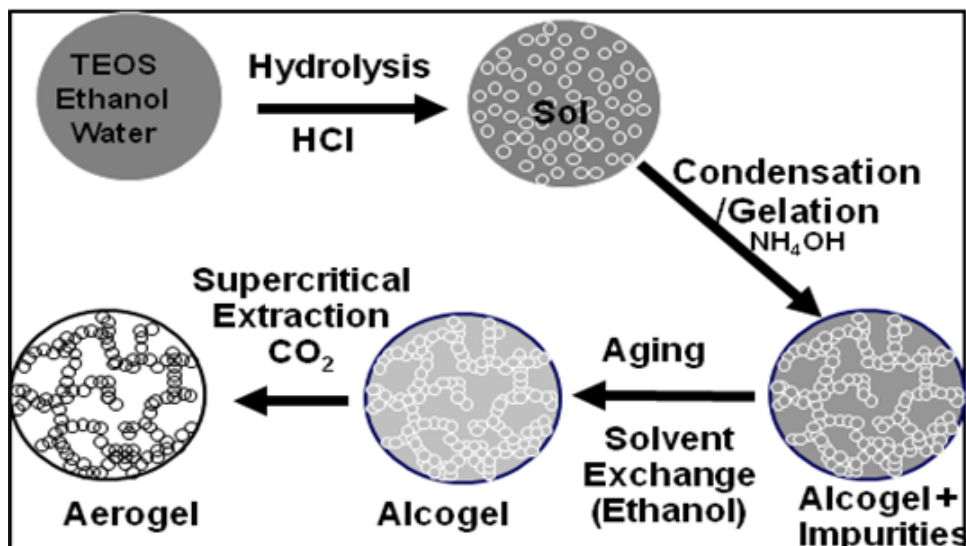


Figure 3-1: Schematic Representation of the Silica Aerogel Synthesis Procedure Using Two-Step Sol-Gel Method

### 3.2 Preparation of Silica Aerogel-Polymer Composites

In this study, four different polymers were chosen for the incorporation in the silica aerogel for the preparation of hybrid materials. These polymers were poly(vinyl acetate) (100000 g/mol molecular weight, from Aldrich), Poly(vinylpyrrolidone) (10000 g/mol molecular weight, from Aldrich), poly(ethylene-block-polyethylene glycol) (575 g/mol molecular weight from Aldrich) and poly(methyl vinyl ether) (equal weight percent in water solution, from Aldrich). Three different procedures such as the addition of the polymer before the hydrolysis, before the condensation (after the hydrolysis) and during the aging step were followed to synthesize composite materials. The hydrolysis time was increased if required in the case of introducing the polymer prior to the hydrolysis for a better dispersion and a better homogeneity. If the polymer was added before the condensation step, the solution was left under continuous stirring for at least 1 hour after the usual hydrolysis time until the base catalyst addition. This additional time was expected

to help the complete dissolution and uniform dispersion of the polymer. The synthesis of the silica aerogel composite in the wet gel stage namely during the aging required higher duration for the aging step ranging from 5 days up to the two weeks. The rest of the procedure such as the amount of reactants, the initial hydrolysis time, the aging temperature and the supercritical drying conditions remained unchanged unless it is stated otherwise in the following sections 3.2.1, 3.2.2, 3.2.3 and 3.2.4. The mass percentage of the polymer stated was calculated with respect to the mass of TEOS in the initial hydrolysis solution. (i.e. 10% of polymer indicates  $m_{\text{polymer}}/m_{\text{TEOS}} = 0.1$ )

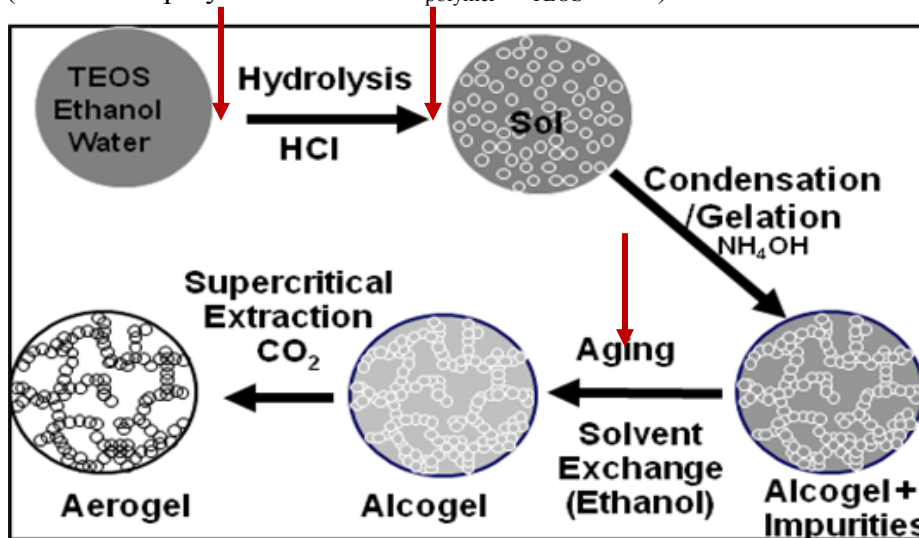


Figure 3-2: The Schematic Representation of Silica Aerogel Polymer Composites With Different Addition Steps Indicated by Red Arrows

### 3.2.1 Silica Aerogel PEPEG Composite Synthesis

Polyethylene-block-polyethylene glycol was chosen as the organic phase because of the higher compressive modulus of its polyethylene chains and the labile glycol group which is expected to bind to the surface silanols of the silica aerogels [84]. The polymer was added either before the hydrolysis or before the condensation step or during the aging step. The mass of the polymer is changed from 1% to 6% which was calculated with

respect to the mass of the tetraethylortosilicate, the silica precursor. To increase the homogeneity of the solution, 24 hours of hydrolysis time was also experimented.

For the procedure including the incorporation of the polymer in aging step, the specified amount of polymer was added in the pure ethanol solution. This polymer containing solution was used in the solvent exchange step in order to perform liquid phase modification of the wet gel. The remaining part of the procedure was followed as usual.

### 3.2.2 Silica Aerogel Poly(vinylpyrrolidone) Composite Synthesis

Poly(vinyl pyrrolidone) was selected for the silica aerogel polymer composite synthesis process because of its compatibility with the process conditions. As the solubility of the named polymer is high in ethanol-water mixtures, its addition did not create any problem in the progress of the procedure. The organic entity was added in the sol-gel process just before the hydrolysis, before the condensation or during the aging steps. Because of the high solubility of the PVP, there was no issue regarding to the homogeneity of the solution. The amount of polymer was varied between %0.5 and %20 with respect to the mass of TEOS as stated earlier in this section.

### 3.2.3 Silica Aerogel Poly(vinyl acetate) Composite Synthesis:

Poly(vinyl acetate) was again selected for the silica aerogel polymer composite synthesis process because of its compatibility with the process conditions similar to the poly(vinyl pyrrolidone). It was expected that the polymer forms hydrogen bonds with the silanol groups via its hydroxyl end group. The solubility of poly(vinyl acetate) in ethanol was found to be lower than the solubility in acetone. Based on this information, the solvent of the process was replaced half and half or completely by acetone. However, the aging solution composition and the pure ethanol used in the solvent exchange step were not modified. For several experiments, the aging step was performed without the aging solution. The wet gels were directly placed in oven at 323 K within their molds after



gelation. The solvent exchange step prior the supercritical drying was skipped for the mentioned case of synthesis conditions.

#### 3.2.4 Silica Aerogel Poly(methyl vinyl ether) Composite Synthesis

Poly(methyl vinyl ether) was bought as a solution as 50 wt. % in H<sub>2</sub>O and used as received. The mass of the water which will be added to the hydrolysis solution was calculated according to the water mass coming from the polymer solution. Because of the water content, the maximum mass of the polymer was limited to around 3% of polymer with respect to TEOS except for the addition during the aging step. The composites were prepared by the usual sol-gel method by using ethanol or ethanol/acetone mixture as the solvent. The polymer was added either before/after hydrolysis or during the aging step.

### **3.3 Characterization of Silica Aerogel Polymer Composites**

#### 3.3.1 Monolithicity, Bulk Shrinkage, Density and Porosity

After the supercritical drying, silica aerogel composites were mostly monolithic, some of them possessed several cracks and a few of them were completely cracked. Depending on the synthesis conditions with different addition steps, aging procedures and types of the polymers, the transparency of the silica aerogel composites varied. The results of the appearance of the silica aerogel composites are given in Section 4.1 of the Chapter 4.

The volume shrinkage of the composites was measured comparing the volumes before (labeled as alcogel) and the after the supercritical drying (labeled as aerogel). The volume shrinkage was measured as follows:

$$\Delta V = (V_{\text{alcogel}} - V_{\text{aerogel}}) / V_{\text{alcogel}} \quad \text{Equation 2}$$

The dimensions of the samples in the alcogel or aerogel conditions were measured with the help of a caliper for most accurate results.

The density of the hybrid materials was measured by simply dividing the final mass of the aerogel by its volume.

The porosity of the prepared samples was calculated based on the density of the sample using the following equation where  $\rho_{\text{SiO}_2}$  was accepted as the density of pure silica ( $2.19 \text{ g/cm}^3$ ) ( $\rho_{\text{SiO}_2} = \rho_{\text{skeletal}}$ ) and  $\rho_{\text{aerogel}}$  was the bulk density of the composite calculated previously:

$$\text{Porosity (\%)} = (\rho_{\text{skeletal}} - \rho_{\text{bulk}}) / \rho_{\text{skeletal}} \quad \text{Equation 3}$$

The corresponding theoretical pore volume which will also be compared with the value found by BET measurements was calculated as follows:

$$\text{Pore Volume} = (1 / \rho_{\text{bulk}}) - (1 / \rho_{\text{skeletal}}) \quad \text{Equation 4}$$

The difference between the pore volumes found theoretically and experimentally (by BET analysis) indicates approximately the pore volume which could not be measured by BET analysis (See Section 3.3.2). It includes the microporous and macroporous regions [40].

### 3.3.2 Surface Area Measurements by BET

The BET method is named after the names of Stephen Brunauer, P.H. Emmett and Edward Teller who extended the Langmuir's kinetic theory to multilayer adsorption [87]. This is the most commonly used technique to determine the aerogel porosity, namely the average pore size diameter, the pore size distribution, the specific surface area and the pore volume. Basic working principle of BET technique depends on the physical adsorption of an inert gas inside the pores. Nitrogen is the most commonly used BET gas because of its inertness to chemical reactions and its availability in the form of liquid. The theory assumes that the uppermost adsorbate layer is in dynamic equilibrium with the vapor. If there is more than one layer, then the upper layer would be in equilibrium with the vapor and so

forth. Because the equilibrium is dynamic, the locations of surface sites covered by one or more layer can change but the number of molecules will not [87].

In this study, the average pore size and the specific surface area of the silica aerogel-polymer composites was measured by using BET equipment Micromeritics ASAP 2020.

The system includes two separate internal vacuum systems which are designed for sample analysis and sample preparation respectively. The apparatus has two sample preparation ports for degassing purposes and one sample analysis port. To be able to obtain accurate results, the weight of the sample should be determined accurately before analysis. Most samples absorb moisture or any other contaminants when contacted with atmosphere. Therefore, the sample should be cleaned from all these contaminants via degassing before the analysis. The term “degas” refers to the process of placing the sample under vacuum and heating it to clean it out. In this study, the degas temperature used was 353K for silica aerogel polymer composites and the degas duration as one day in order not to damage the heat sensible polymers inside the composite. After degassing, the true weight of the sample is determined for the analysis. The sample is allowed to interact with the adsorbate which is the atmosphere chosen for the analysis. The pressure is continuously measured until a stable reading is achieved where the equilibrium would have been reached.

While the BET results will be given in chapter 4, the effect of polymer addition in different steps of the sol-gel process will be discussed in chapter 5.

### 3.3.3 Infrared Spectroscopy, IR

Infrared Spectroscopy is the method used to identify the chemical structure of the analyzed sample by measuring the light absorbed by different types of vibrations in molecules. The peaks appearing on the IR spectrum gives insight about the composition of the material as each chemical group or chemical bond corresponds to a different peak. Although each molecule has its own characteristic IR spectrum, it is confirmed that certain

atom groups have bands at the same (or near) frequency regardless what type of bonds have the rest of the molecule [88]. These overlapping bands may lead to some misinterpretations if the entire spectrum is not analyzed completely.

In this study, ATR-FTIR measurements were performed using the apparatus Thermoscientific Nicolet IS10. For ATR analysis, no sample preparation is required. A small piece of sample (only a few milligram) is placed between a crystal of high refractive index and a clamp constructed of a metal tip. The infrared radiation is sent through the crystal towards the sample at a specified angle for total reflection. The radiation beam can only penetrate into the sample a few wavelengths of light such as between 0.5 to 2.0 microns. This penetrating beam is termed as the evanescent wave. During this penetration, the chemical bonds of the sample absorb some of the evanescent wave. The attenuated reflected beam is directed towards the detector that would result in the IR spectra of the sample.

In this work, ATR spectroscopy was used for each silica aerogel-polymer sample to identify characteristic peaks of the polymers used in the experiments. The spectra of the hybrid materials were also compared with the pure silica aerogel spectra and the pure polymer spectra if available.

#### 3.3.4 Thermal Gravimetric Analysis, TGA

In Thermal Gravimetric Analysis (TGA), the mass of the sample is measured as a function of temperature increase. A constant heating rate or a non-linear temperature program can be used. The sample can also be kept at constant temperature while recording the mass change as a function of time. The atmosphere used in the analysis depends on the type of sample to be analyzed. The atmosphere can be reactive, oxidative ( $O_2$  or air) or inert (Helium, Argon).

The interpretation of TGA experiment is performed by analyzing TGA curve together with DTG curve. TGA curve is displayed as a percent mass change as a function

of temperature or time. DTG curve can be explained as the first derivative of TGA curve and it shows the rate at which the mass changes. The mass variations within the sample during the analysis are seen as step changes in TGA curves and downward or upward peaks in the DTG curve.

Weight loss may result from evaporation of residual moisture or solvent remaining in the sample, but at higher temperatures such as from the beginning of 200 °C-300°C, it may arise from the polymer decomposition.

In this study, TGA analysis was performed using the apparatus with the model Exstar SII TG/DTA6300. TGA analysis is used in order to compare the weight changes of the composites with that of pure silica aerogel or that of pure polymer if available. The decomposition temperature was identified in the TGA analysis results of the silica aerogel samples to determine the polymer presence. The different weight percent polymer addition was also compared to determine if any change in the weight loss occurs due to the polymer weight. The samples were heated until 900 °C with a constant heating rate 10 °C /min with synthetic air as the atmosphere.

## **Chapter 4: RESULTS & DISCUSSION**

### **4.1 Photographic Images of Silica Aerogel Polymer Composites**

In this section, several images of the synthesized silica aerogel-polymer composites are presented. Although the images give general information about the polymer incorporation related to the transparency, more concrete conclusions are drawn by coupling these images with the other characterization results. For each polymer, numerous photographs are given for each different synthesis conditions.

#### *4.1.1 Silica Aerogel-PEPEG Composites*

Silica aerogel-PEPEG composites were white-opaque materials with non uniform distribution of the polymer for several samples. The non homogeneity is due to the low solubility of the polymer in the sol-gel mixture. The mixture of polymer with the initial hydrolysis sol resulted in a white emulsion with some polymer particles remaining insoluble in the mixture. The addition of the base to the solution to accelerate the condensation and subsequent gelation of the samples resulted in the phase separation in the wet gel (Fig. 4-1). On the other hand, a longer hydrolysis time (up to 24 hours) led to homogeneous samples, however the samples were opaque (Fig. 4-2). Longer hydrolysis led to better homogeneity allowing the white polymer particles disperse evenly in the sol.

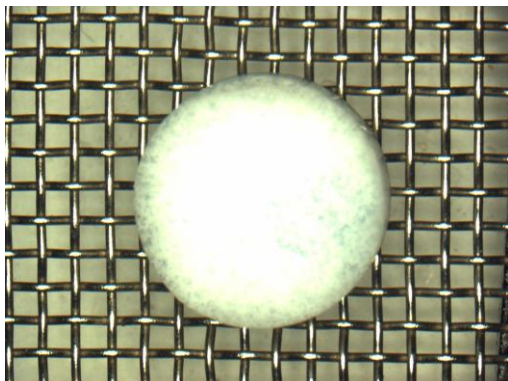


**Figure 4-1: Silica Aerogel-PEPEG Composite (Addition Before the Hydrolysis Step)**

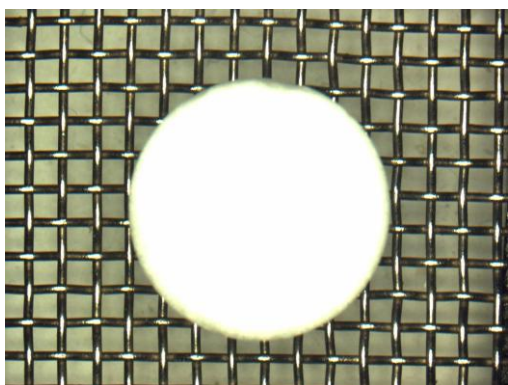


**Figure 4-2: Silica Aerogel-PEPEG Composite (Addition Before the Condensation Step)**

#### 4.1.2 Silica Aerogel-PVP Composites

The silica aerogel-PVP composites were prepared using the all possible addition routes. While the addition before the hydrolysis and before the condensation steps resulted in translucent or white-opaque materials (Fig. 4-3), the addition during the aging step led to transparent composites with a slightly yellowish colour (Fig. 4-4). Poly(vinyl pyrrolidone) has a high solubility in ethanol-water mixtures. However, the presence of the base solution caused the polymer to precipitate from the sol immediately. Therefore, polymer addition before the hydrolysis and before the condensation steps resulted in phase separated materials. Longer hydrolysis time again led to better homogeneity but white-opaque samples. On the other hand, the polymer addition during the aging step to eliminate the

direct contact of the polymer with the base solution did not change transparency of the aerogels. The silica aerogel-PVP samples remained transparent after the aging and drying steps. With this approach, it is anticipated to have hydrogen bonding between the OH groups of PVP and the surface silanols. Therefore, it is expected that the polymer remains on the surface like a coating. A slight yellowish colour which does not hinder the transparency suggests that this hypothesis may be true.

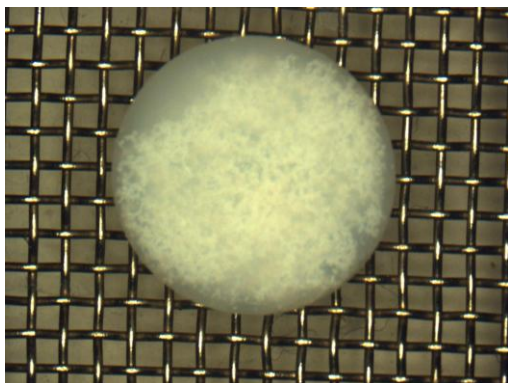


**Figure 4-3: Silica Aerogel-PVP Composite (Addition Before the Condensation Step)**

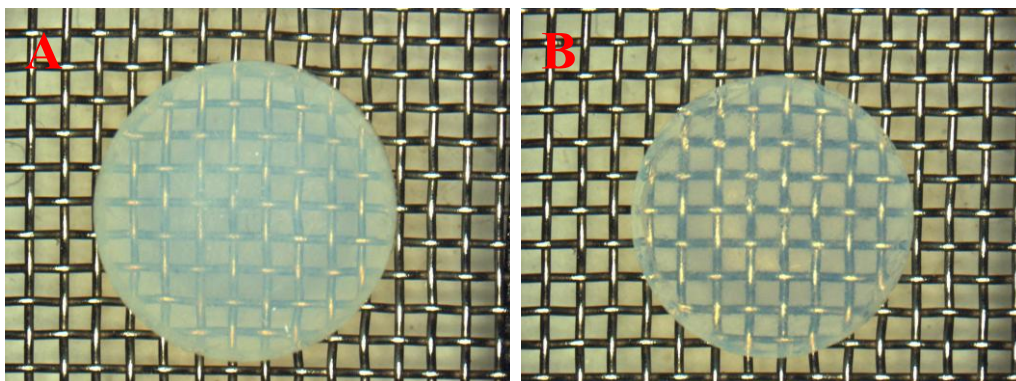


**Figure 4-4: Silica Aerogel-PVP Composites (Addition During the Aging Step). A) Higher Amount of Polymer Addition B) Lower Amount of Polymer Addition**

#### 4.1.3 Silica Aerogel-PVAc Composites

PVAc incorporation in the synthesis process of the silica aerogel gave the most promising results. A high solubility of PVAc in the initial sol and in acetone as the second



co-solvent facilitated the incorporation of PVAc in the aerogel network. As the polymer has a similar refractive index with silica aerogel, the resulting composites did not lose their transparency with all experiments where polymer was added in different stages of the sol-gel process. Different additions steps, different but smaller polymer masses or different aging conditions mostly resulted in transparent or translucent composites. As the mass of the polymer which was added either before the hydrolysis or before the condensation step increased, the transparency of the composite decreased prominently. It is concluded that there is a limit on the amount of polymer which can be incorporated into the silica network. Beyond a certain amount, the sample becomes opaque due to the filling of the pores with the polymer. However, similar to the case with PVP, the resulting composites synthesized by the addition of the polymer during the aging step were totally transparent. Based on this result, it can be concluded either that the polymer remains on the surface by the hydrogen bonding or the polymer incorporation is very low while being insufficient to modify the transparency. Further conclusions will be drawn along with ATR-FTIR and BET analysis.

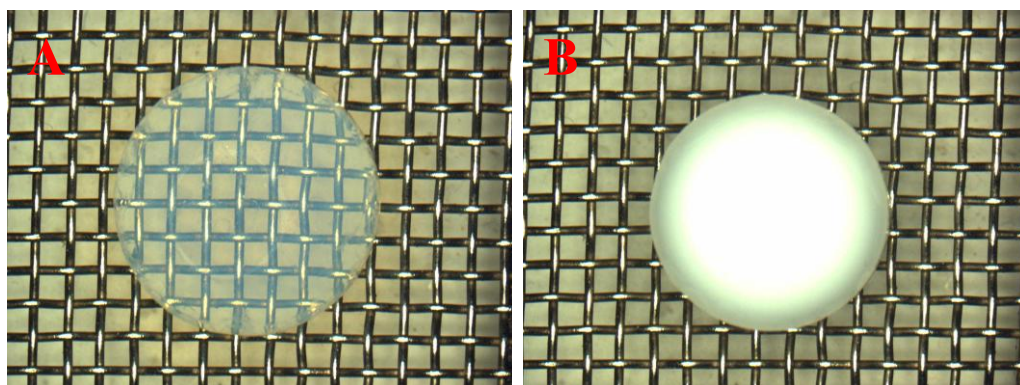


**Figure 4-5: Silica Aerogel-PVAc Composites (Addition Before the Hydrolysis Step). A) Lower Amount of Polymer Addition, B) Higher Amount of Polymer Addition**

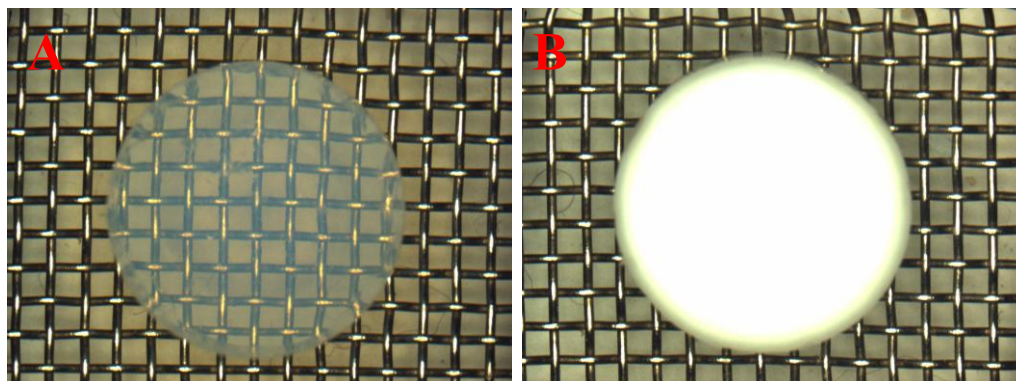


**Figure 4-6: Silica Aerogel-PVAc Composites (Addition After the Hydrolysis Step). A) Lower Amount of Polymer Addition, B) Higher Amount of Polymer Addition**

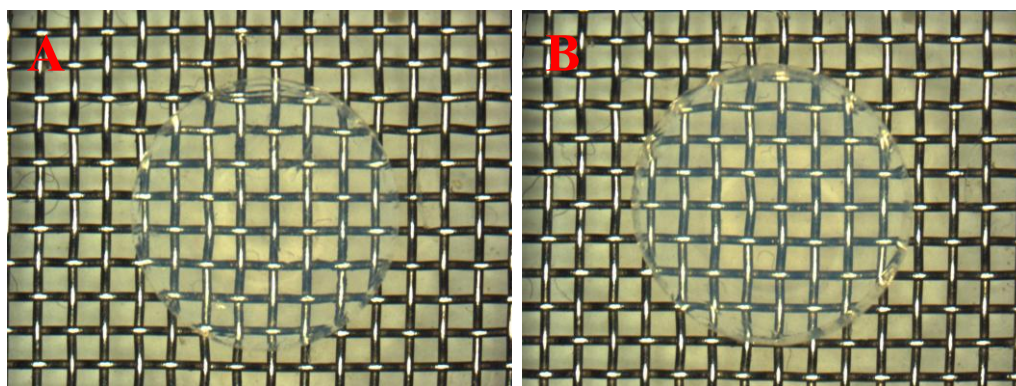


**Figure 4-7: Silica Aerogel-PVAc Composites (Addition During the Aging Step). A) Higher Amount of Polymer Addition, B) Lower Amount of Polymer Addition.**

#### 4.1.4 Silica Aerogel-PMVE Composites

To synthesize silica aerogel-PMVE composite materials, all possible addition routes were again tested. Primarily, ethanol was used as the solvent like in the previous experiments. Although the monolithic-crack free samples were obtained, the composites were opaque as it is seen from the Figure 4-8. Then, acetone was also tested along with ethanol to determine the effect of this co-solvent on the resulting composites. The use of acetone as a co-solvent along ethanol changed completely the transparency of the sample. Although the ethanol as the single solvent led to completely white-opaque aerogels, the addition of acetone transformed the composites to transparent materials (Fig. 4.8). This

can be the result of a better solubility of the polymer in acetone rather than in ethanol. Like the other experiments, beyond a certain amount of polymer, the samples were not homogeneous and phase separation was observed. (Fig. 4-9).

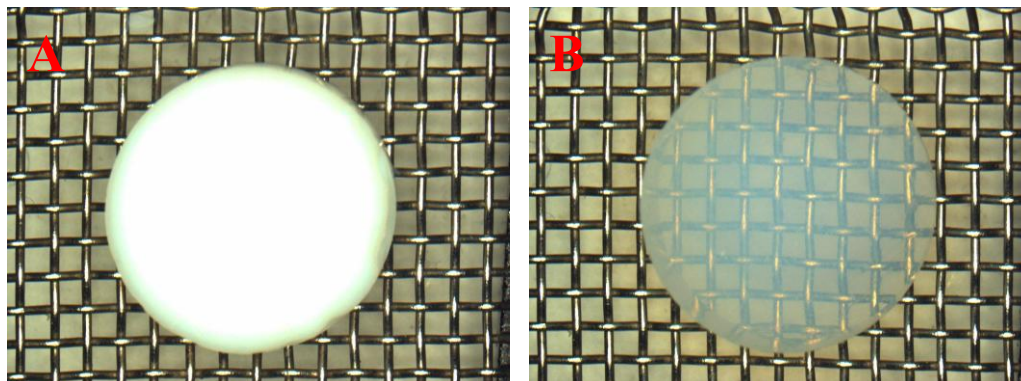


**Figure 4-8: Silica Aerogel-PMVE Composites (Addition Before the Hydrolysis Step), A) Ethanol as the only solvent B) Acetone as the co-solvent along ethanol**

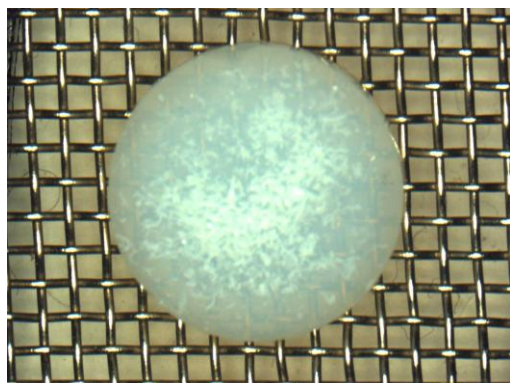


**Figure 4-9: Silica Aerogel-PMVE Composites (Addition Before the Hydrolysis Step), Acetone as the co-solvent along ethanol (Polymer Amount is higher compared with Fig. 4-8).**

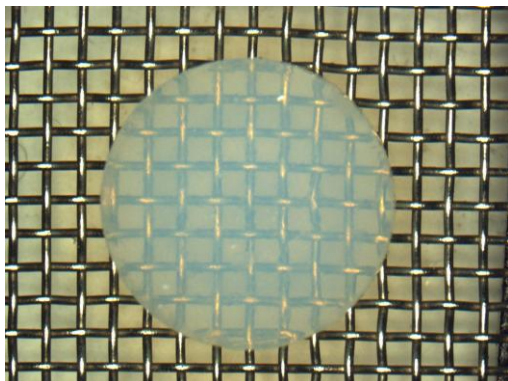


Figure 4-10: Silica Aerogel-PMVE Composite (Addition After the Hydrolysis Step)

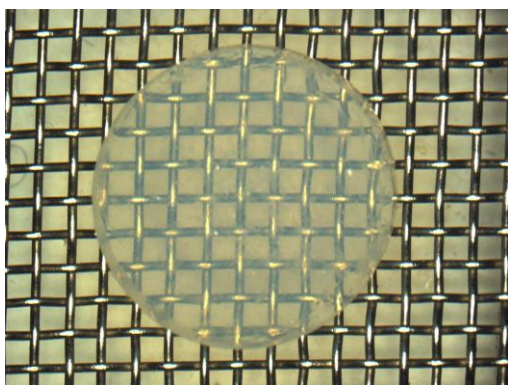


Figure 4-10: Silica Aerogel-PMVE Composite (Addition During the Aging Step)

## 4.2 Physical Characterization Results

### 4.2.1 Bulk Density of the Composites

The bulk density of composites differed from one trial to the other one consisting of different polymers, different addition steps or different polymer amounts. The density range for composites containing PEPEG was between 0.131 and 0.302 g/cm<sup>3</sup>. Those containing PVP had a similar range between 0.174 and 0.357 g/cm<sup>3</sup>. The silica aerogel PVAc composites had a wider density range such as 0.121 and 0.467 g/cm<sup>3</sup>. The lightest composites were those which contained PMVE as the polymeric material. The density range of these composites was between 0.116 and 0.246 g/cm<sup>3</sup> only.



Shrinkage was found to be the main factor affecting the density as expected. The more the samples shrank, the more the density increased due to a more compact structure. Moreover, shrinkage was affected by many other factors such as the type of the polymer, the amount of the polymer, the addition step of the polymer and the corresponding aging conditions.

In the case of PEPEG-silica aerogel composites, the smallest density was obtained when the polymer was added during the aging step. These samples were as transparent as pure silica aerogels. Moreover, polymer precipitates have been observed in the aging solution. Therefore, it can be concluded that the resulting sample did not contain PEPEG. Furthermore, it can be said that the PEPEG incorporation was not achieved with the addition during the aging step. Otherwise, there is not a general trend for the density of the silica aerogel-PEPEG composites. The highest density is achieved if the hydrolysis time is lengthened to one day instead of 40 minutes for a better dispersion of the polymer. However, the long hydrolysis time also caused some solvent loss due to the evaporation resulting in a more saturated solution. This also leads to an increase in the final density of the material.

The density of the silica aerogel PVP composites did not change significantly when the addition of the polymer was before the hydrolysis or before the condensation (after the hydrolysis step). The same amount of polymer addition in these two different steps resulted in similar densities. The amount of polymer in the addition during the aging step also affects the density. However, the amount of silica aerogel placed in the aging solution varied from one experiment to the other. Therefore, a good trend can not be seen with the results obtained. UV-VIS Spectroscopic results with Nanodrop indicated that there is a limit in the polymer amount which can be incorporated on the silica aerogel. After a certain period of time which is determined to be around 12 days in our study, there was no or little change in the concentration of the aging solution. This result indicated that the surface of

the aerogel becomes saturated with the polymer after a specified period of time. The UV-VIS Spectroscopy results are given in the Appendix A.

In the case of silica aerogel PVAc composites, the density increased for the samples aged in the molds. As these samples shrank more than the others, their density was found to be greater than all the materials synthesized for this study. Apart from this visible result, there was neither a general trend for the density changes within the different samples. This is mainly due to the polymer dissolution during the aging. When the polymer amount is increased more than 10% , the resulting composites had a density lower than the samples containing less amount of polymer.

For silica aerogel PMVE composites, there was not a change in density between the addition steps for the same amount of polymer. In addition, the polymer amount did not affect the density of the resulting samples. The composition of aging solution was varied for 3 of the samples and the results indicated that the water concentration of the aging solution affects final density. As the concentration of water in the aging solution increased, the density was found to decrease.

#### 4.2.2 Volumetric (or Linear) Shrinkage of Composites

The shrinkage of the silica aerogel-polymer composites was calculated volumetrically or linearly depending on the data available.

The linear shrinkage of the silica aerogel PEPEG composites was around 20 %, with 17.6 as the smallest and 26.4% as the highest shrinkage values. The amount of polymer which is added or the addition step had no apparent effect on the shrinkage of the composites.

The silica aerogel-PVP composites shrank less compared to samples prepared with PEPEG. This result can be due to the better integration of PVP in the network than PEPEG as it is also seen with the subsequent analysis. The composites with PVP had shrinkage values mostly around 18% with 13.60% as the smallest and 24.60% as the highest.

Shrinkage values for silica aerogel-PVAc composites were mostly determined volumetrically. As more experiments were performed for the synthesis of this composite, the shrinkage value range is very wide for the samples. The materials which were not placed in the aging solution after the gelation had very high shrinkage values up to 60%. This is because of the unfinished hydrolysis and condensation reactions. The aging solution containing water serves to terminate the hydrolysis and condensation reactions which are undergoing even after the gelation. When this step is skipped to prevent polymer dissolution, the samples shrink more than usual even if they contain higher amount of polymer. Apart from the samples which were not subjected to the aging solutions, the synthesized materials had very diverse shrinkage values were not following a trend.

The samples prepared with poly(methy vinyl ether) have the smallest shrinkage values among the entire set of samples. In addition, the samples prepared with the use of acetone as the co-solvent showed smaller shrinkage. This can be attributed to the fact that the polymer has a higher solubility in acetone which serves to better integrate it into the silica matrix.

The shrinkage of the composites is found to be dependent on the mass of the polymer. As the amount of the polymer increases, the volumetric or linear shrinkage of the materials tend to decrease. However, several samples with high polymer content deviate from this pattern. Based on the fact there were polymer precipitates in the base of the beaker at the end of the synthesis and the changing transparency of the aging solution due to polymer dissolution, it is concluded that the amount of polymer remaining in the network decreases. Therefore, the increase in shrinkage values when there is a high amount of polymer is expected. The network can have become saturated with the polymer so that higher amounts did not get into the network.

The density values along with linear or volumetric shrinkage results of all samples can be found at the Appendix B.

#### 4.2.3 Porosity of Composites

The porosity of the samples was determined using the Equation 3 stated in Section 3.3.1. The synthesized composites exhibited different porosity values depending on the preparation conditions and the type of the polymer used. However, the porosity remained higher than %80 among all samples except those which are produced without being subjected to the aging step in the water-ethanol solution. The more the samples shrank, the more their porosity decreased. It is claimed that the shrinkage causes the samples to pack more thereby creates a more compact structure with less porosity. The porosity values of all samples can be found at the Appendix B.

#### 4.2.4 Pore Volume of Composites

The pore volume of composites is calculated using the Equation 4 mentioned in Section 3.3.1. This value is compared with the second experimental pore volume found by BET analysis when available. The difference between these values indicates the volume of the pores covered by macro- and micropores because BET analysis does not include the volume of such of pores. Based on the results, a larger polymer resulted in a greater volume of pores that are micropores and macropores. This is an apparent result because of the fact that the polymer disrupts the silica matrix causing the pores to expand or to contract.

The corresponding theoretical pore volumes are given in the Appendix B.

### **4.3 ATR-FTIR Spectra Results**

ATR-FTIR Spectrometry gives more convincing results about the polymer incorporation in the network. If the polymer is present in the network or it is bonded to the surface of the network, the corresponding peaks belonging to the polymer appear in the spectra. Nevertheless, there are some complications which lead to the misinterpretation of the spectra. Overtones, combination of bonds, Fermi or hydrogen bonding within the sample affect the location of the peak in the spectra or its intensity. The interaction or



repulsion of the bonds shifts the actual location to nearby wavelengths in the spectrum. Therefore, the corresponding peak should be searched not only at the specific wavelengths but in the closest neighborhood for a precise interpretation. In addition, although the spectrum does not give a definite quantitative result, the intensity of the peaks gives general information about the amount of the polymer in the network.

Silica aerogel's spectrum is analyzed together with the spectra of composites to recognize any difference which is appearing. The main bonding of silica aerogel is silicon-oxygen covalent bonds as expected. This intense band is found mainly in the 1200-1000  $\text{cm}^{-1}$  wavenumber range. The bonding which is observed around 1095-1089  $\text{cm}^{-1}$  and the shoulder at 1200  $\text{cm}^{-1}$  accounts for the asymmetric stretching vibrations of Si-O-Si [89]. The symmetric stretching of the same band appears at 800  $\text{cm}^{-1}$  while its bending mode is observed at 469-467  $\text{cm}^{-1}$ . The broad band appearing at higher wavenumbers such as from 3000 to 3500  $\text{cm}^{-1}$  belong to the overlapping of OH stretching bands of hydrogen bonded water molecules and SiO-H stretching of surface silanols hydrogen bonded to molecular water. The peak appearing at around 960  $\text{cm}^{-1}$  is due to the SiO stretching vibrations. Adsorbed water molecules have a corresponding peak at around 1650  $\text{cm}^{-1}$ . The weak peak appearing around 1380  $\text{cm}^{-1}$  is assigned to the CH stretching modes of the non-hydrolyzed ethoxy groups.

#### 4.3.1 Silica Aerogel-PEPEG Composites

In the case of PEPEG addition, the presence of the polymer is recognized by the symmetrical and asymmetrical stretching of  $\text{CH}_2$  bonds around 2850  $\text{cm}^{-1}$ . Another clue would be the vibration of Si-O-C bonds if their peaks' positions were not overlapping with those of Si-O-Si bonds [84]. CH stretching modes appearing around 1450  $\text{cm}^{-1}$  are assigned to the polymer since they are not present in the pure silica aerogel spectrum.

In Figure 4-11, the spectrum corresponding to the composites prepared by varying amounts of PEPEG added after the hydrolysis step is presented. If the section between

1500-1300  $\text{cm}^{-1}$  is analyzed, the peak with a very low intensity appearing at 1450  $\text{cm}^{-1}$  for both samples but not for the silica aerogel can be attributed to the CH stretching modes of the polymer. The band at 1650  $\text{cm}^{-1}$  for both sample together with the pure silica aerogel are assigned to the OH stretching vibrations. This can also come from the OH group of the polymer itself due to the increase of the intensity of the peak with the increasing polymer content.

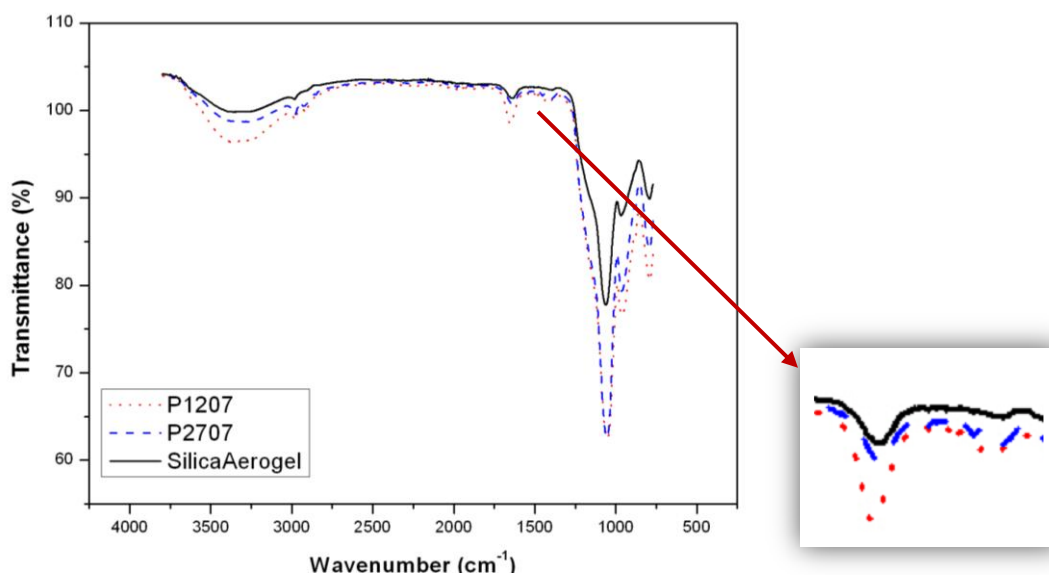


**Figure 4-11: ATR Spectrum of Silica Aerogel-PEPEG Composites (Addition After the Hydrolysis Step), Increasing Polymer Mass for the Samples P2707 and P1207 respectively**

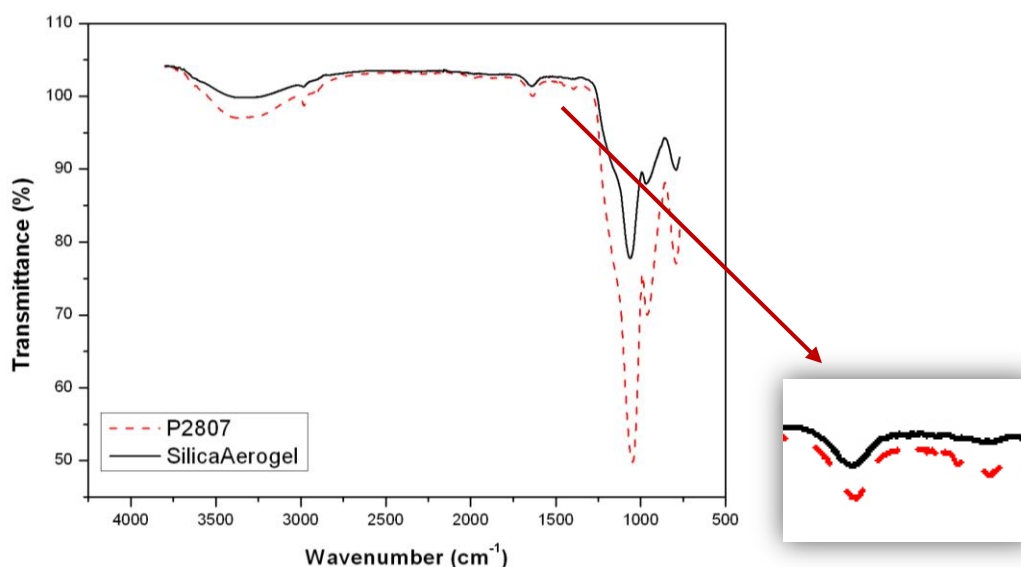


**Figure 4-12: ATR Spectrum of Silica Aerogel-PEPEG Composites (Addition During the Aging Step)**

#### 4.3.1 Silica Aerogel-PVP Composites

The presence of PVP within the composite is more easily identified due to the characteristic peaks of the polymer itself which are separated from the pure silica aerogel peaks.

Pure polymer has many characteristic peaks that are easy to recognize in the spectrum. The peaks between 3300 to 3500 cm<sup>-1</sup> belong to the adsorbed water and those around 1450 cm<sup>-1</sup> are related to CH<sub>2</sub> deformation and bending. The peaks appearing at around 2950 cm<sup>-1</sup> come from the stretching of CH<sub>2</sub> or CH. However, the major identification peaks are those which appear at 1650 and 1295 cm<sup>-1</sup> belonging to C=O and C-N respectively [85]. The locations of these characteristic peaks vary in a smaller range of wavenumbers due to other interactions within the sample.

In the following figures, spectra of composites obtained using different amount of PVP addition after the hydrolysis step or during the aging step and the same amount of

polymer addition at different steps is illustrated. The zoomed section indicates the polymer presence with the carbonyl band at high polymer contents around  $1650\text{ cm}^{-1}$  and the C-N stretching around  $1295\text{ cm}^{-1}$  or with an increasing intensity of the peak for the CH stretching mode around  $2890\text{ cm}^{-1}$ . An increasing polymer concentration in the aging solution resulted in an increase of polymer content of the silica aerogel as seen in Figure 4-14 by the increasing intensity of the peaks. On the other hand, for the same but smaller amount of polymer addition for different steps indicates that the polymer incorporation was not achieved in very high amounts for the addition during aging (See Fig. 4-15). To incorporate the polymer during the aging step, a higher concentration of polymer in the aging solution is required. Neither of the peaks appearing in the spectrum is significant because of the low polymer amount. Addition of lower mass of the polymer was not sufficient for polymer incorporation.

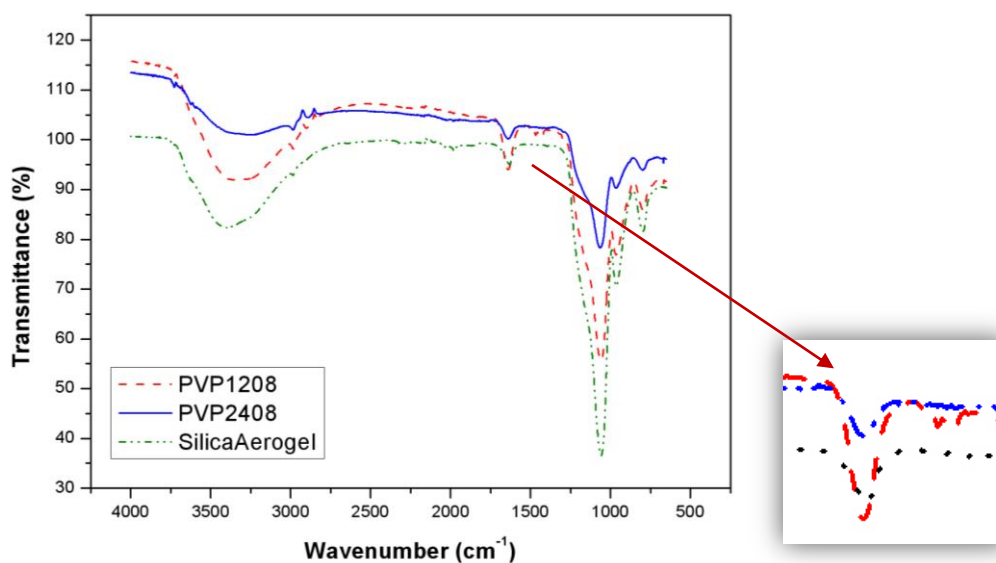


**Figure 4-13: ATR Spectrum of Silica Aerogel-PVP Composites (Addition After the Hydrolysis Step) Increasing Polymer Mass for the Samples PVP2408 and PVP1208 respectively**

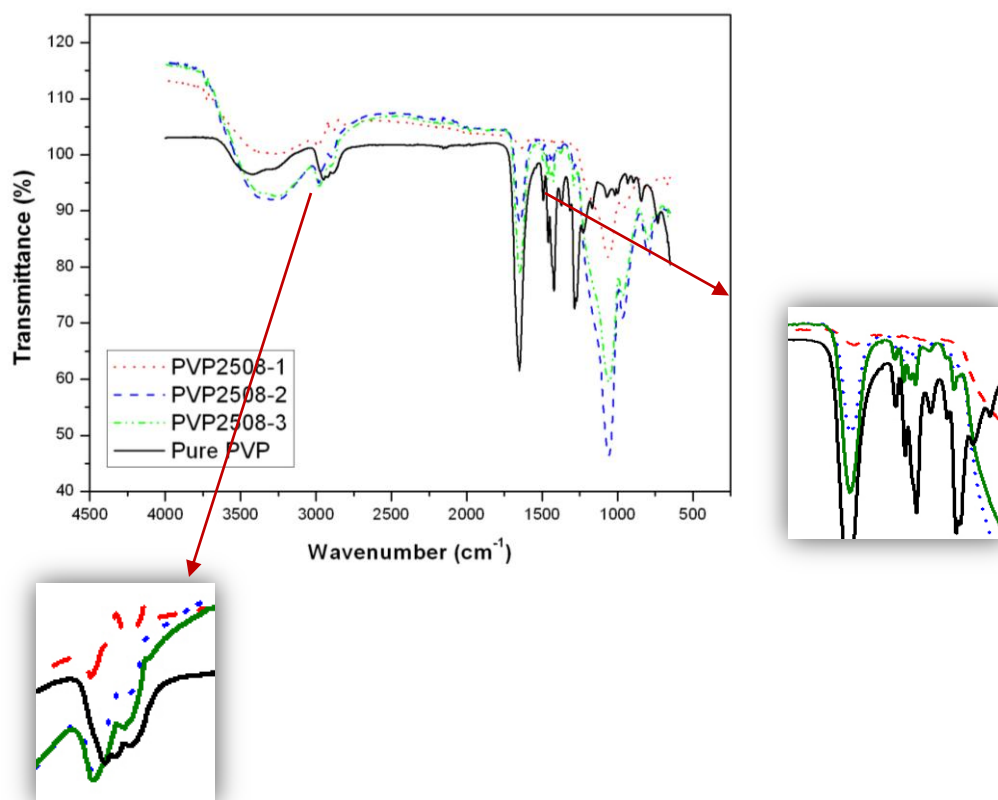


**Figure 4-14: ATR Spectrum of Silica Aerogel-PVP Composites (Addition During the Aging Step), Increasing Polymer Mass for the Samples PVP2508\_1,PVP2508\_2 and PVP2508\_3 respectively**

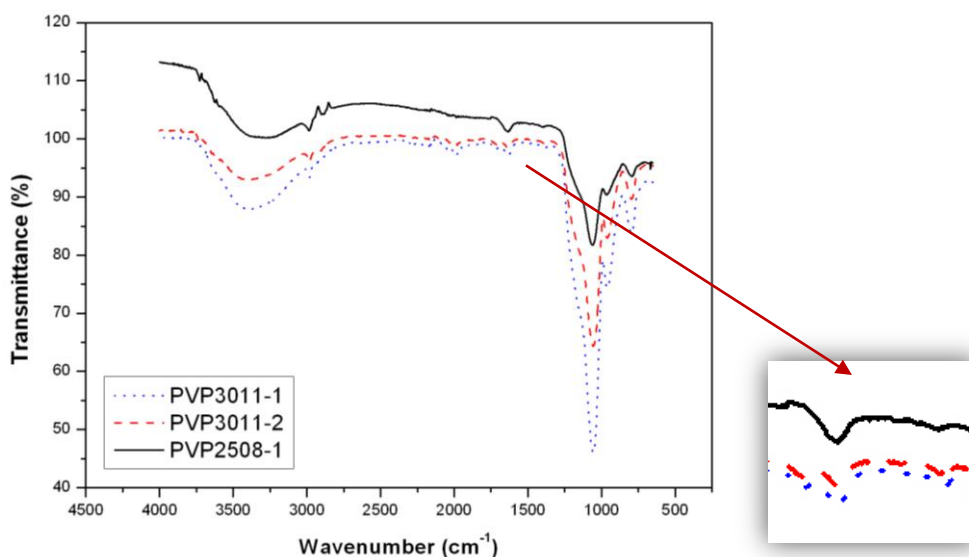


**Figure 4- 15:** ATR Spectrum of Silica Aerogel-PVP Composites, (Similar Amount of Polymer Addition) Addition Before the Hydrolysis Step, Addition After the Hydrolysis Step, Addition During the Aging Step for Samples PVP3011\_2, PVP3011\_1 and PVP2508\_1 respectively

#### 4.3.2 Silica Aerogel-PVAc Composites

The presence of the polymer is again confirmed by its characteristic peaks appearing in the spectra. The main peak belonging to PVAc is the one appearing at around  $1650\text{ cm}^{-1}$  and is related to the carbonyl stretching of the polymer. However due to the overtones and overlapping of peaks of  $\text{SiO}_2$  (appearing at around  $1640$  and  $1870\text{ cm}^{-1}$ ) and also hydrogen bonding occurring between silanol groups of the silica and OH groups of PVAc, the location of this characteristic band is shifted to longer wavenumbers.

In the following figures, different amount of polymer addition for the same addition step or different addition steps for the similar polymer amounts are illustrated for comparison. As mentioned previously, the carbonyl band location is seen at longer wavenumbers namely at around  $1750\text{ cm}^{-1}$ . Some samples do not contain such a characteristic band indicating that either the polymer amount was not sufficient or the

entire polymer amount which is added was not incorporated into the matrix. The effect of the use aging solution is showed in Fig. 4-19. Based on this spectrum, it can be concluded that PVAc added before the aging step was extracted by the aging solution. The spectrum of the composite where there was no use of aging solution shows a more significant carbonyl band indicating higher amount of polymer content.

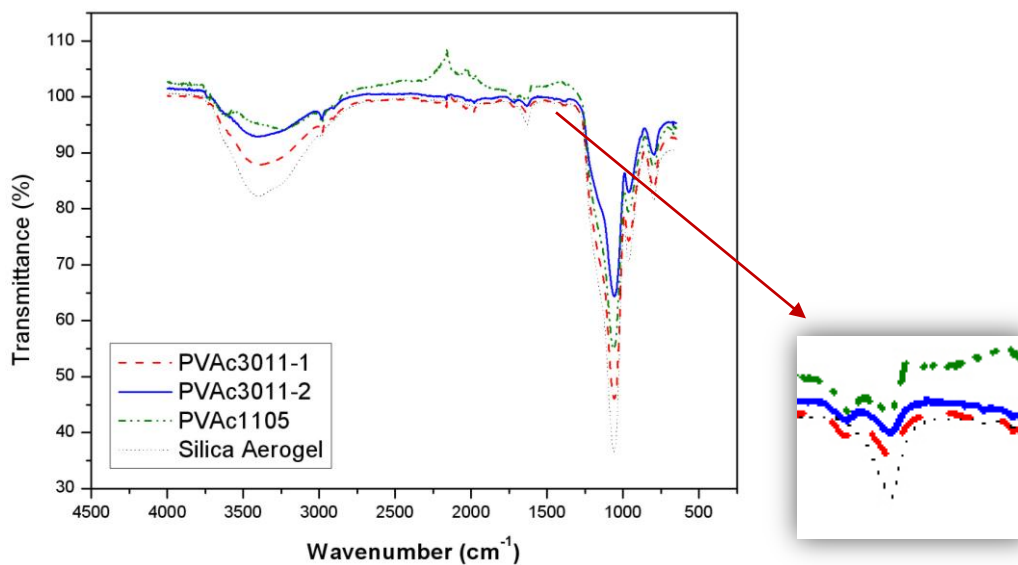


**Figure 4-16: ATR Spectrum of Silica Aerogel-PVAc Composites (Similar Amount of Polymer Addition) Addition Before the Hydrolysis Step, Addition After the Hydrolysis Step, Addition During the Aging Step for Samples PVAc3011\_2, PVAc3011\_1 and PVAc1105 respectively**

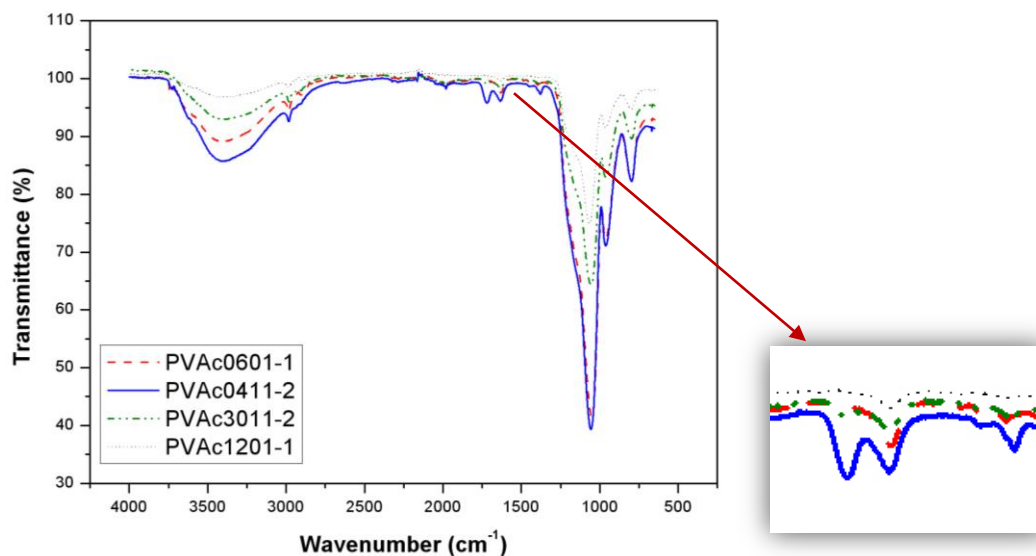


Figure 4-17: ATR Spectrum of Silica Aerogel-PVAc Composites, (Polymer Addition Before the Hydrolysis Step), Increasing Polymer Mass for the Samples PVAc0601\_1, PVAc0411\_2, PVAc3011\_2 and PVAc1201\_1 respectively

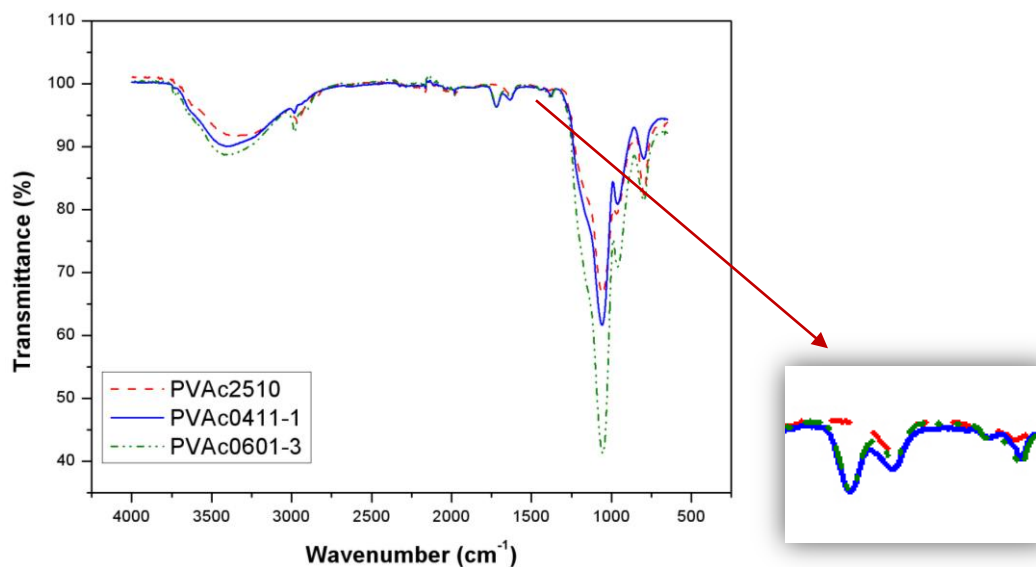


Figure 4-18: ATR Spectrum of Silica Aerogel-PVAc Composites (Polymer Addition After the Hydrolysis Step), Increasing Polymer Mass for the Samples PVAc2510, PVAc0411\_1, PVAc0601\_3 respectively.



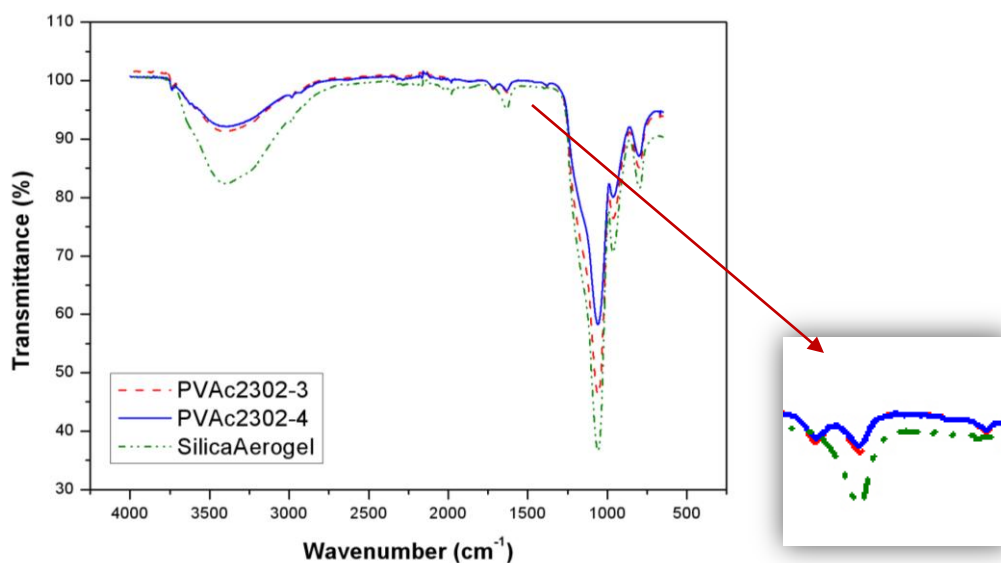


Figure 4-19: ATR Spectrum of Silica Aerogel-PVAc Composites (Polymer Addition During the Aging Step), Increasing Polymer Mass for the Samples PVAc2302\_3, PVAc2302\_4 respectively.

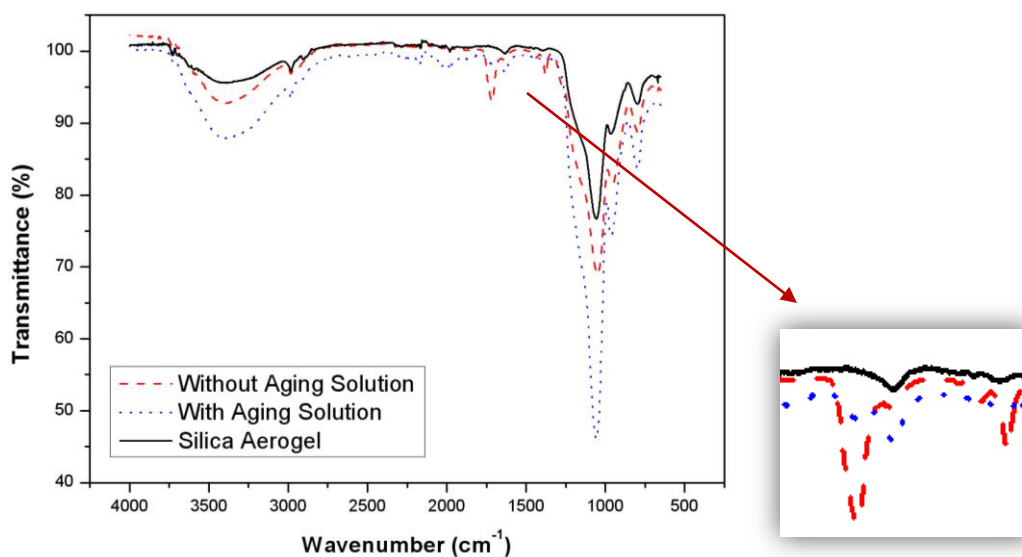


Figure 4-20: ATR Spectrum of Silica Aerogel-PVAc Composites, Aging With and Without Solution

#### 4.3.4 Silica Aerogel-PMVE Composites

The peaks belonging to poly(methyl vinyl ether) are not easy to identify in the IR spectra of the silica aerogel composite because some of its peaks are overlapping with those of the pure silica aerogel. If the high frequency region is analyzed, PMVE has four distinctive absorption bands around  $2900\text{ cm}^{-1}$ . The bands at  $2880$ ,  $2930$  and  $2975\text{ cm}^{-1}$  belong to CH stretching of  $\text{CH}_2$  groups and that around  $2820\text{ cm}^{-1}$  is due to the methoxy chain CH stretching [90]. Another CH stretching is seen at around  $1450\text{ cm}^{-1}$ .

The IR spectra results are given in the following figures. The peak appearing around  $2900\text{ cm}^{-1}$  has four different shoulders as mentioned before. In addition, the weak peaks appearing around  $1450\text{ cm}^{-1}$  indicate the CH stretching vibrations. However, these bands do not constitute strong evidence about the polymer presence in the composite. The IR spectra should be analyzed along with TGA analysis in order to confirm the polymer presence within the composite sample.

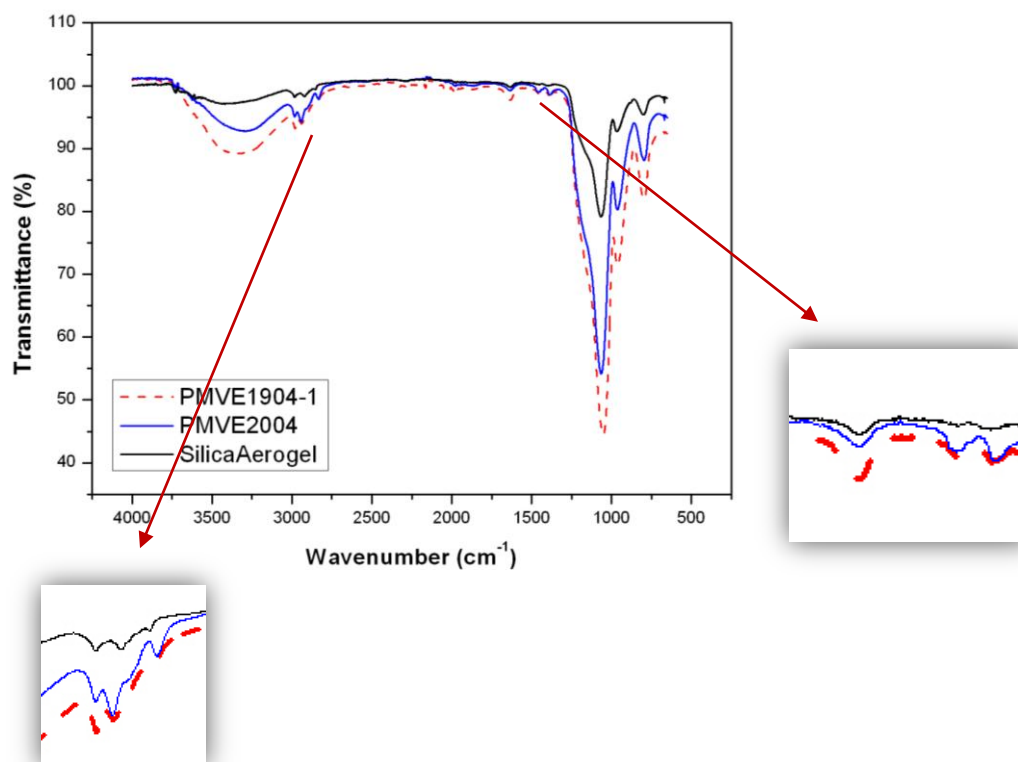
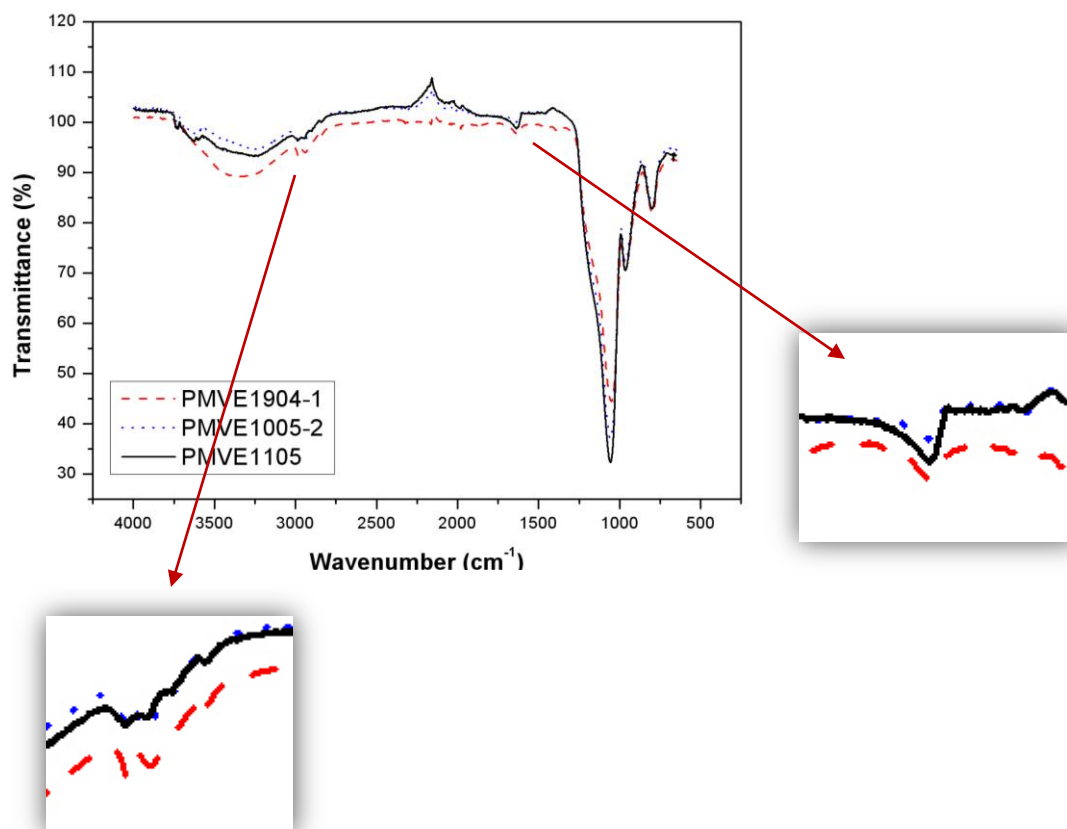


Figure 4-21: ATR Spectrum of Silica Aerogel-PMVE Composites, (Polymer Addition Before the Hydrolysis Step), Increasing Polymer Mass for the Samples PMVE1904\_1 and PMVE2004 respectively



**Figure 4-22:** ATR Spectrum of Silica Aerogel-PMVE Composites, (Similar Amount of Polymer Addition) Addition Before the Hydrolysis Step, Addition After the Hydrolysis Step, Addition During the Aging Step for Samples PMVE1904\_1, PMVE1005\_2 and PMVE1105 respectively

#### 4.4 TGA Results

TGA analysis is performed for this study in order to confirm the presence of the polymer in the synthesized material. Even though TGA does not give a precise quantitative result, it gives a good estimation about the polymer amount in the network by percent mass. The mass of the pure silica aerogel is not reduced more than 6 to 8 % in the same TGA analysis. Based on this information, the greater mass losses are attributed to the polymer in the network. TGA spectra of pure polymers are also illustrated, in order to determine the specific temperatures at which the major mass losses may occur.

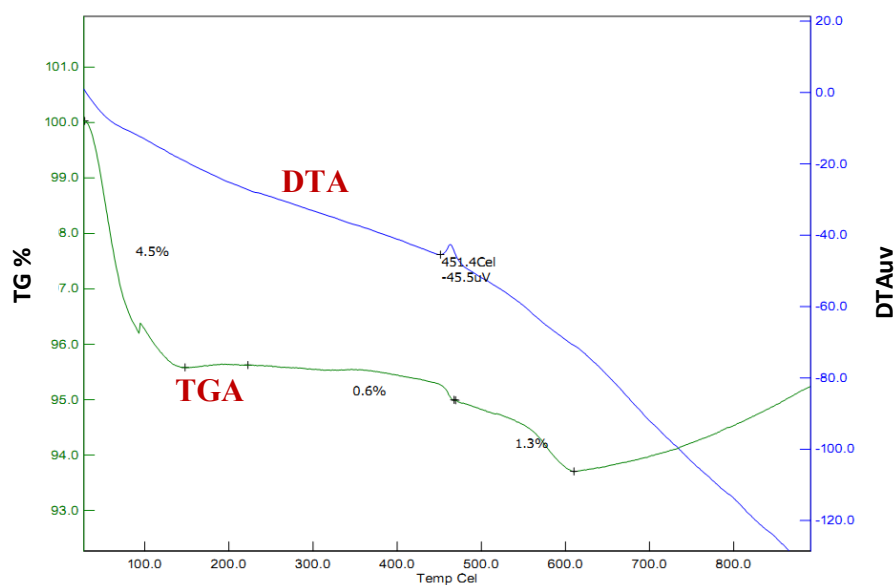


**Figure 4- 23: TGA Diagram of Pure Silica Aerogel**

#### 4.4.1 Silica Aerogel PEPEG Composites

One TGA diagram is given for the silica aerogel-PEPEG Composites (See Fig. 4-23). The second mass loss which appears around 200°C is mostly attributed to the mass loss of the polymer. The polymer decomposition usually starts after 200 °C which is also the case in this spectrum. The total mass is reduced by 20 % which is a much higher value than the value obtained with the silica aerogel alone. This can be attributed to the presence of the polymer in the silica aerogel.

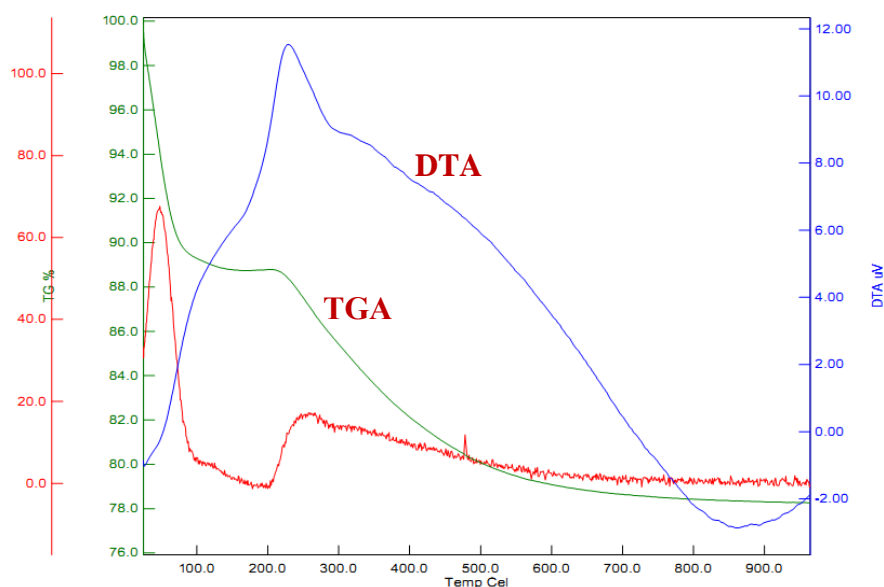


**Figure 4- 24: TGA Diagram of Silica Aerogel-PEPEG Composite (P1207), Addition After the Hydrolysis Step**

#### 4.4.2 Silica Aerogel PVP Composites

The results of thermal gravimetric analysis for silica aerogel-PVP samples are seen in the following figures. TGA of pure polymer shows that that the main mass losses start after 300 °C even though there appears to have some reduction in the mass at the beginning of the heating process. This temperature (300 °C) is stated as the decomposition temperature of the polymer itself. If the spectra of the composites are analyzed, the losses occurring especially after 300 °C belong mainly to the polymer. The spectrum of PVP1105 (Fig.4-24) shows the result with the 44.5% mass loss in total. The polymer was added during the aging step for this sample. Based on the TGA results, it can be concluded that the polymer mass is about 35% of the total mass of the composite. The polymer is either hydrogen bonded to the surface silanols or is entangled within the pores.

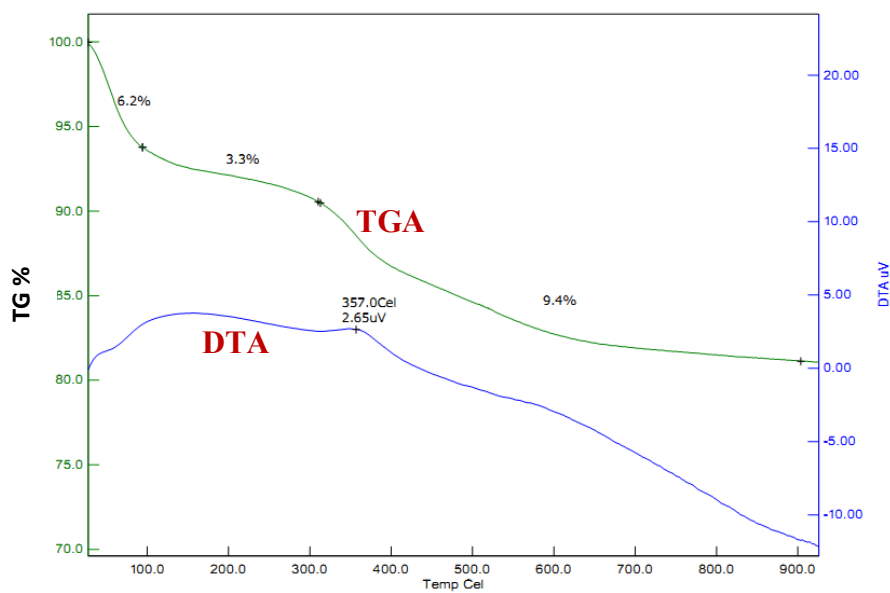


Figure 4-25: TGA Diagram of Silica Aerogel-PVP Composite (PVP2408), Addition After the Hydrolysis Step

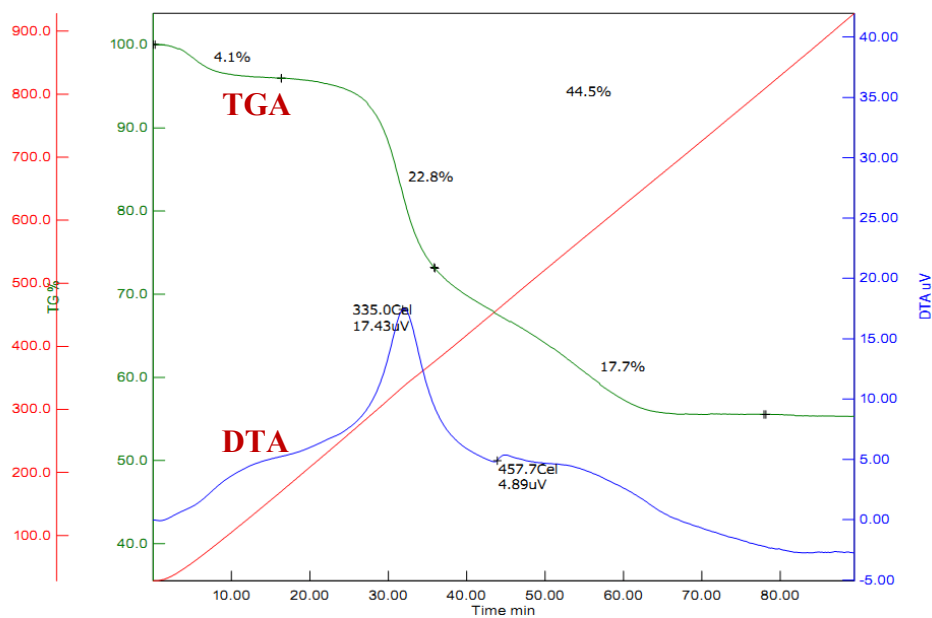


Figure 4-26: TGA Diagram of Silica Aerogel-PVP Composite (PVP1105), Addition During the Aging Step

#### 4.4.3 Silica Aerogel PVAc Composites

The thermal gravimetric results for the silica aerogel-PVAc composites are given subsequently. Based on the TGA diagram of the pure polymer, the major mass loss starts around 300°C. Any mass loss occurring around and after 300 °C can be attributed to the presence of polymer in the sample if the total mass loss exceeds 6%. There may also be some unreacted ethoxy groups present in the network, and the mass losses occurring after the specified temperature can also be attributed to the presence of these groups. Therefore, the total mass loss should be larger than the mass loss occurring with the pure silica aerogel for the confirmation of the polymer presence.

Although the mass of the added polymer was much smaller in the case of aging without solution, the TGA diagram shows that the integration of the polymer is more successful if the alcogels are not placed into aging solutions. Apart from the spectrum obtained for the composites without the aging solution, the mass loss of the analyzed samples does not differ significantly.



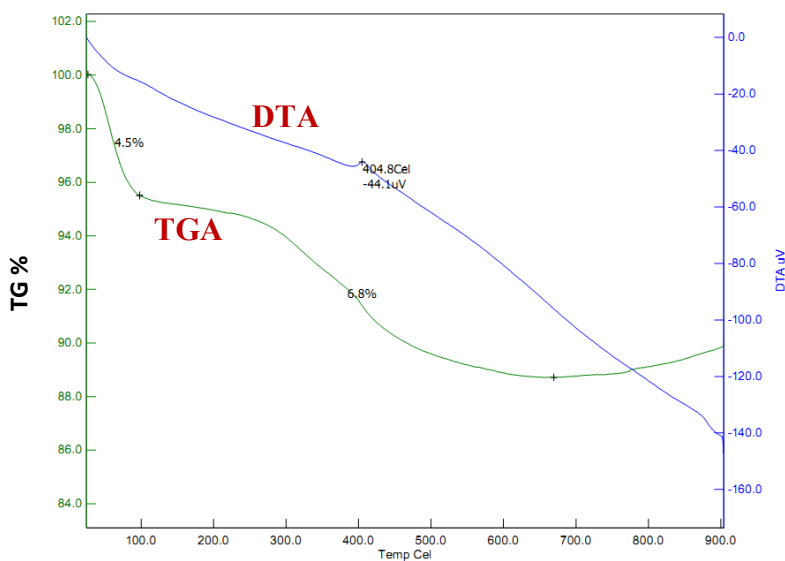


Figure 4-27: TGA Diagram of Silica Aerogel-PVAc Composite (PVAc3011\_1), Addition After the Hydrolysis Step

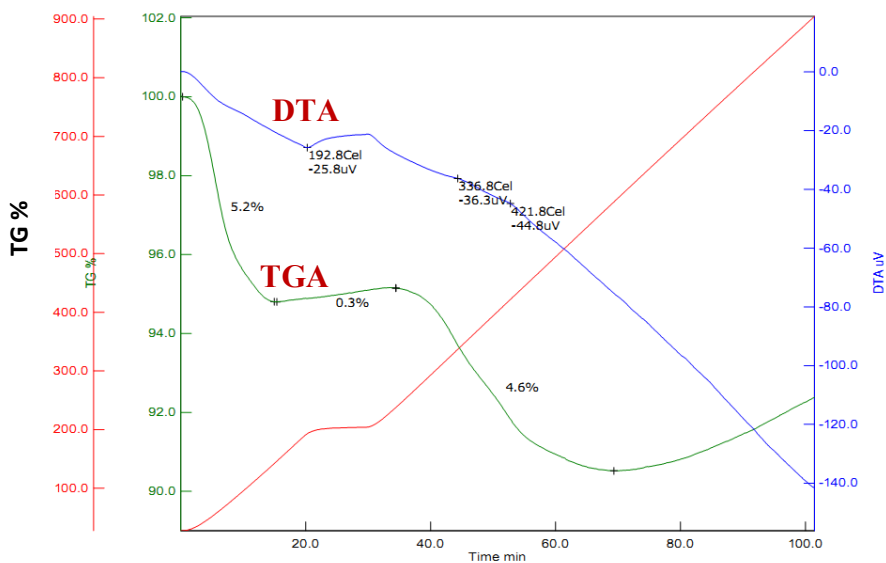


Figure 4-28: TGA Diagram of Silica Aerogel-PVAc Composite (PVAc1201\_2), Addition Before the Hydrolysis Step

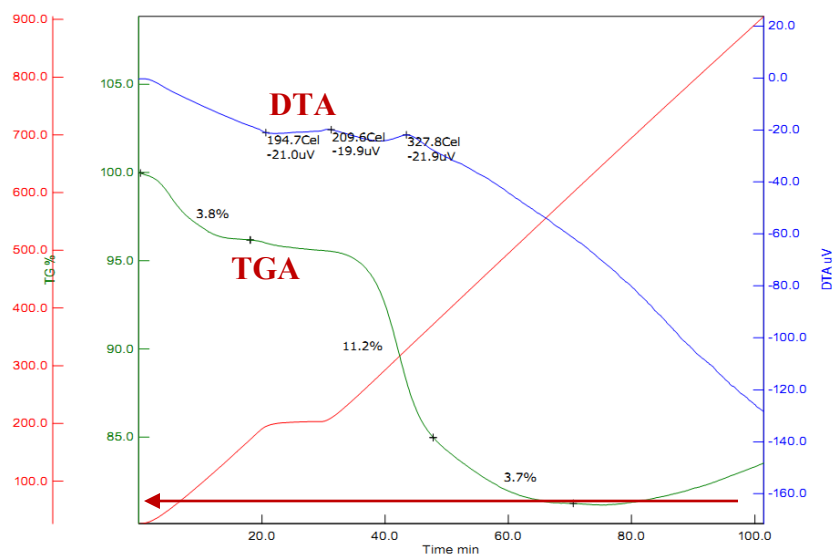


Figure 4- 29: TGA Diagram of Silica Aerogel-PVAc Composite (PVAc0702\_4), Addition Before the Hydrolysis Step, Aging Without Solution

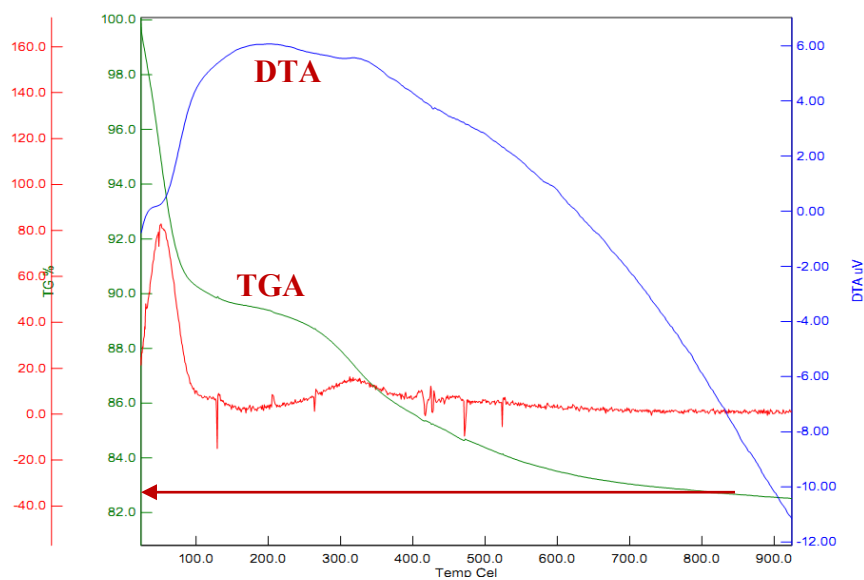
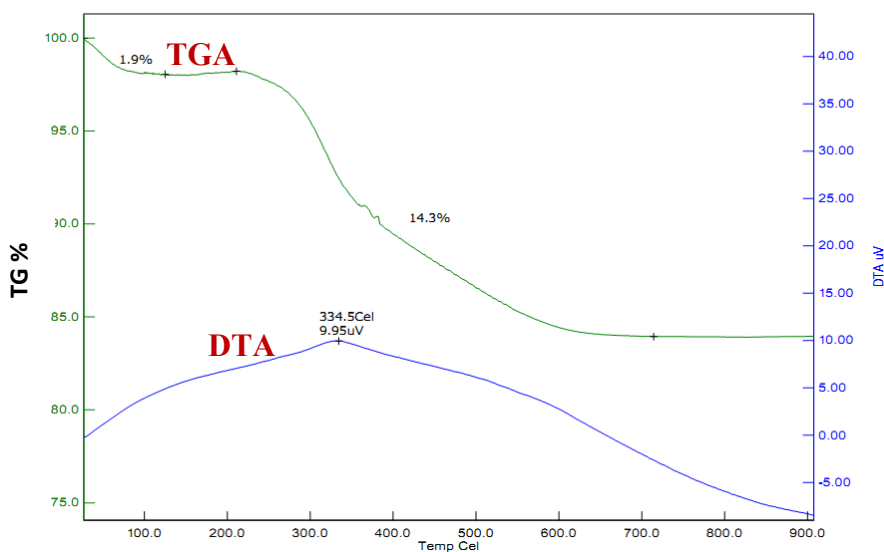


Figure 4- 30: TGA Diagram of Silica Aerogel-PVAc Composite (PVAc2302\_3), Addition During the Aging Step

#### 4.4.4 Silica Aerogel PMVE Composites

In the case of silica aerogel-PMVE composites, the use of acetone as the co-solvent has no apparent effect on the polymer incorporation into the network. For the same amount of added polymer, the mass loss does not differ using different solvents. On the other hand, the mass loss attributed to the adsorbed water and ethanol in the sample is smaller for these samples. The other main mass loss is mostly assigned to the polymer as the total mass loss is greater than the one obtained with pure silica aerogel. The polymer addition after the hydrolysis step (before the condensation step) seems to have a greater mass loss indicating a higher polymer amount (See Fig. 4-31). Although this sample had a higher density among others, the IR spectra of the same sample had no apparent difference from the others. On the other hand, the major characteristic peaks of PMVE are not separable from the peaks of silica aerogel. Therefore, TGA analysis gives a better understanding about the polymer incorporation for these samples.



**Figure 4- 31: TGA Diagram of Silica Aerogel-PMVE Composite (PMVE2510), Addition Before the Hydrolysis, Ethanol as the Only Solvent**

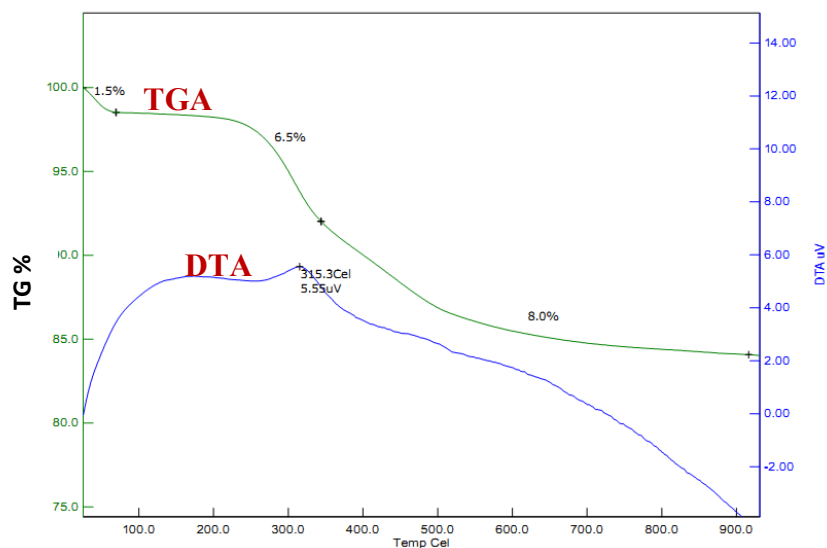


**Figure 4- 32: TGA Diagram of Silica Aerogel-PMVE Composite (PMVE1904\_1), Addition Before the Hydrolysis, Acetone as the Co-Solvent**

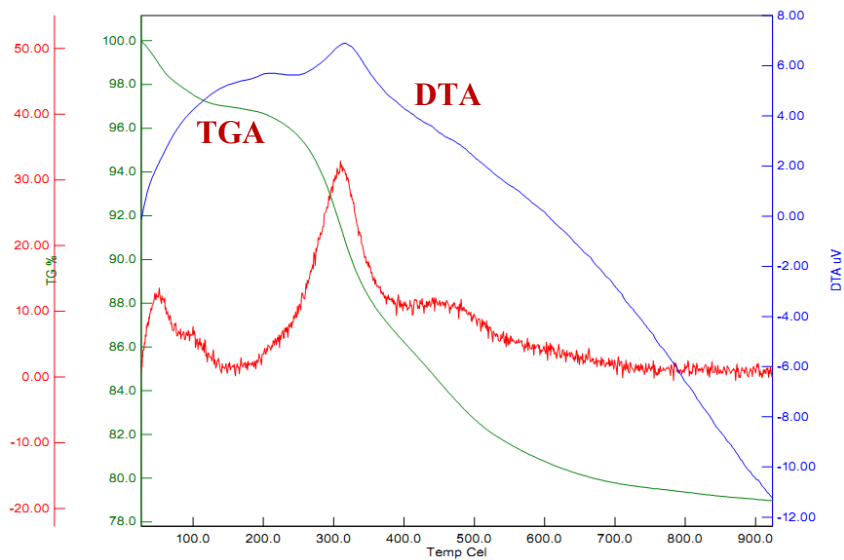


**Figure 4- 33: TGA Diagram of Silica Aerogel-PMVE Composite (1005-2), Addition After the Hydrolysis, Acetone as the Co-Solvent**

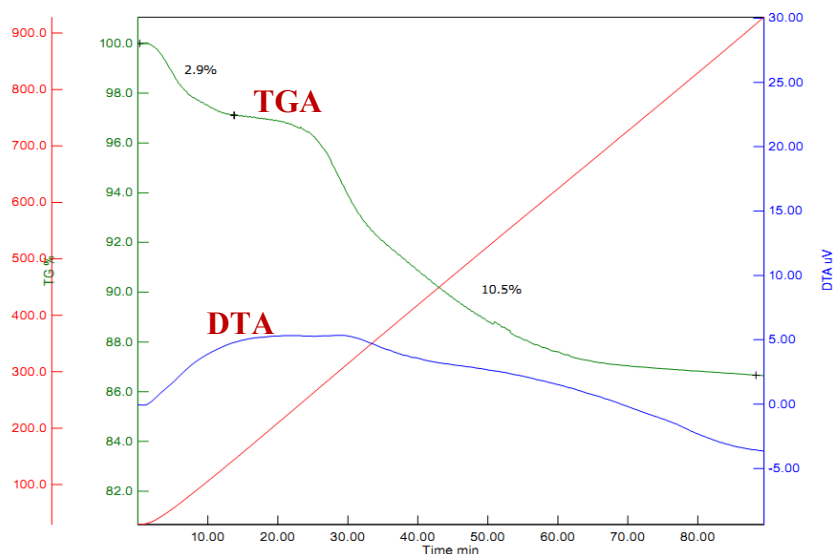


**Figure 4-34: TGA Diagram of Silica Aerogel-PMVE Composite (PMVE1105), Addition During the Aging Step**

#### **4.5 BET Results**

BET analysis is another method used to characterize the synthesized silica aerogel-polymer composites. The specific surface areas, the desorption average pore radius and the pore volumes of the composite samples are compared with the values obtained for the pure silica aerogel. Any large difference in the mentioned parameters indicates the presence of the polymer. The reduction or increase in the specified results give a general impression about how the polymer is present within the samples, namely it is whether entangled within the pores or attached on the surface.

The specific surface area of the composites is not changed significantly with the addition of the polymer before and after the hydrolysis step. The surface area remained as a high value which is around 800-900  $\text{m}^2/\text{g}$  even if the mass of polymer which is added to the sol is 20% of the mass of the precursor. In addition, the average desorption pore radius of

the composite samples is found to be greater than the pore radius of the pure silica aerogel. The polymer can somehow enter in the pore while enlarging it. Moreover, it can also be said that the polymer had disrupted the network causing the smaller pores to collapse and form larger pores for the polymer access. However, it is a question of how the pore is enlarged without damaging the surface area. In addition, if the total micropore area is analyzed for these samples, it is observed that the corresponding area is around %1 of the total surface area or so small that it could not have been measured. This result suggests that the polymer should have filled the pores and reduced the area of the microporous region.

In the case of aging without solution, the specific surface area of the composites tends to decrease with an increasing average pore radius. This is due to a more compact structure resulting from greater shrinkage. The decrease in the pore volume of these samples from 2.8 cm<sup>3</sup>/g to 2.1 cm<sup>3</sup>/g can be explained mainly by the difference in this shrinkage value of these samples compared with that of the pure silica aerogels. As the samples were not subjected to the aging, the network strengthening which would have prevented the large shrinkage was not performed.

On the other hand, the polymer addition during the aging step ended up with different results. The specific surface area of the composites were halved whereas the average desorption pore radius were increased. Larger pores caused a decrease in the surface area of the synthesized samples. The polymer is expected to coat the surface while decreasing the surface area and entering the pores while enlarging them. This information together with the reduction in the total pore volume of these samples can be attributed to the filling of the larger pores with the polymers. A slightly smaller total pore volume indicates the covering of larger pores with the polymer.

#### ***4.6 Unified Results and Discussion***

When all the characterization results mentioned in this chapter are combined and analyzed together, a more thorough understanding is obtained.

Several silica aerogel-PEPEG composites had higher densities indicating that polymer should be integrated in the silica network. However, due to the loss of transparency and non-homogeneity, it is concluded that the polymer is not bonded to or evenly distributed in the silica network. It may only stay entangled in the pores while disrupting the usual silica network distribution. Due to the overlapping of characteristic polymer bands with those of silica aerogel, the IR spectrum does not give concrete information about the polymer presence. The weak peaks appearing in the spectrum are attributed to the polymer but more definite results should be obtained.

The results of silica aerogel-PVP composites were more promising compared with composites which are prepared with PEPEG. Greater densities than the pure silica aerogel, intense and characteristic peaks on the IR spectrum and apparent mass losses in TGA spectrum confirm the polymer presence in the network. The remaining transparency and high porosity of the composites materials prepared by the addition of the polymer during the aging step is one of the qualifications demanded for these materials. Although the specific surface area of these samples was halved, the values were still within the high range of 500-600 m<sup>2</sup>/g.

The composites synthesized with PVAc as the organic part were other promising candidates for this study. The high solubility of PVAc especially in the acetone which is used as the co-solvent facilitated the incorporation of this material in the network. The similar refractive index with silica aerogel helped to develop transparent materials even if the polymer is added either before or after the hydrolysis step. The characteristic carbonyl band is mostly apparent in the IR spectra giving a good confirmation about the polymer presence. The corresponding TGA results also support the polymer presence although the mass losses are lower than those obtained with silica aerogel-PVP composites. The remaining high surface area and the desorption pore radius make these samples good candidates for the future of this study.

The last composites which are synthesized with PMVE were also successful according to the results. However, the use of acetone as the co-solvent was a necessity rather than a choice for these samples. The use of acetone made the samples appear transparent while not changing any other properties. It was also difficult to interpret the IR spectrum of these samples because of the fact that the bands of the polymer were overlapping with those of pure silica aerogel. However, the TGA results confirm the polymer existence in the sample along with slightly higher densities compared with native silica aerogel.



## Chapter 5: CONCLUSION

In this study, novel inorganic-organic hybrid materials consisting of silica aerogel as the inorganic part and different polymers as the organic part are synthesized. We have demonstrated that several addition steps such as the addition before the hydrolysis, after the hydrolysis (before the condensation) or during the aging step are suitable for the polymer incorporation in the host matrix which is synthesized through the sol-gel process.

Among all tested polymers, it is argued that poly(vinyl acetate) and poly(methyl vinyl ether) were promising candidates for the addition before and after the hydrolysis and poly(vinyl pyrrolidone) was a promising candidate for the addition during the aging step.

The density, the porosity and the shrinkage analysis indicated that the polymer incorporation affects the resulting physical properties. It is concluded that polymer addition increases the density; however the corresponding porosities remained greater than 80%. In addition, the density changes do not follow a general trend leading to a conclusion that the polymer incorporation has a limitation. After a certain amount of polymer, the silica network is saturated so that the matrix can not accept any other organic entity in it. Shrinkage of the composites is found to be mostly dependent on the aging conditions rather than the polymer addition. However, increasing polymer amount tends to decrease the shrinkage because of the strengthening of the network.

Moreover, most of the synthesized composite aerogels, especially the ones for which the polymer is added during the aging step are transparent. The polymer integration did not change the appearance of the native silica aerogels. It is claimed that the phase separation which occurred for several samples disrupted the transparency of the composites.

ATR-FTIR investigations on the synthesized samples clearly showed that the novel materials contain corresponding polymers, based on the characteristic peaks of the polymers which are emerging in the spectra.

Furthermore, TGA analysis of the resulting materials gives a general impression about the amount of polymer which is still present in the network after the total process. The more there is weight loss at the end of the analysis, the more it is expected to have a larger amount of polymer within the network. In addition, it is claimed that the polymer addition during the hydrolysis steps does not significantly change the pore characteristics of the native silica aerogel together with the specific surface area. Conversely, the addition of the polymer during aging step caused the specific surface area to decrease with increasing average pore radius. It is concluded that the addition during the aging step coats the surface of the synthesized aerogel with the polymer. The corresponding polymer enters the pores while enlarging them. The enlargement of the pores in turn reduces the specific surface area. However, because observed differences between the BET results of pure silica aerogels and silica aerogel-polymer composites were not significant, there should not be a large difference between their pore structures. Based on this suggestion, it can be estimated that the newly synthesized composite materials should possess similar distinctive properties related to the pores structure of silica aerogels like the low thermal conductivity.

The silica aerogel-polymer composites should be further analyzed as a future work. The thermal and mechanical properties of the synthesized samples need to be understood for a deeper analysis. These properties are the ones which are mostly required for the use of silica aerogels in a variety of application areas. Any improvement in the mechanical properties along with thermal properties will widen the use of these materials in a variety of applications. Another approach could be the test of other diverse polymers with different functionalities to be able to find the most suitable candidates for the synthesis of silica aerogel polymer composites. It is also suggested to conduct studies consisting of the same

polymers used in this thesis but with different molecular weights. The effect of the molecular weight on the final properties of the silica aerogel composites should be analyzed with promising polymer candidates.

**REFERENCES:**

1. Sanchez, C., K.J. Shea, and S. Kitagawa, *Recent progress in hybrid materials science*. Chemical Society Reviews, 2011. **40**(2): p. 471-472.
2. Soleimani Dorcheh, A. and M.H. Abbasi, *Silica aerogel; synthesis, properties and characterization*. Journal of Materials Processing Technology, 2008. **199**(1-3): p. 10-26.
3. Morris, C.A., et al., *Modifying nanoscale silica with itself: a method to control surface properties of silica aerogels independently of bulk structure*. Journal of Non-Crystalline Solids, 2001. **285**(1-3): p. 29-36.
4. Meador, M.A.B., et al., *Cross-linking Amine-Modified Silica Aerogels with Epoxies: Mechanically Strong Lightweight Porous Materials*. Chemistry of Materials, 2005. **17**(5): p. 1085-1098.
5. Boday, D.J., et al., *Formation of Polycyanoacrylate–Silica Nanocomposites by Chemical Vapor Deposition of Cyanoacrylates on Aerogels*. Chemistry of Materials, 2008. **20**(9): p. 2845-2847.
6. Saegusa, T., *Organic Polymer-Silica Gel Hybrid: A Precursor of Highly Porous Silica Gel*. 1991. **28**(9): p. 817 - 829.
7. Pomogailo, A.D., *Hybrid polymer-inorganic nanocomposites*. RUSS CHEM REV, 2000. **69**(1): p. 53-80.
8. Zou, H., S. Wu, and J. Shen, *ChemInform Abstract: Polymer/Silica Nanocomposites: Preparation, Characterization, Properties, and Applications*. ChemInform, 2008. **39**(52): p. no-no.
9. Esquivias L., M.-F.V., Piñero M., de la Rosa-Fox N., Ramírez J., González-Calbet J., Salinas A., Vallet-Regí M., *Bioactive organic-inorganic hybrid aerogels*. Materials Research Society, 2005.
10. Victor Morales-Flórez, J.A.T.-F., R. Mendoza-Serna, Manuel Piñero, Nicolás de la Rosa-Fox, A. Santos, Luis Esquivias, *Mechanical Properties of Bioactive Hybrid Organic/Inorganic Aerogels*. Key Engineering Materials, 2009. **423**: p. 155-160.
11. de la Rosa-Fox, N., et al., *Nanoindentation on hybrid organic/inorganic silica aerogels*. Journal of the European Ceramic Society, 2007. **27**(11): p. 3311-3316.
12. Meador, M.A.B., et al., *Structure–Property Relationships in Porous 3D Nanostructures as a Function of Preparation Conditions: Isocyanate Cross-Linked Silica Aerogels*. Chemistry of Materials, 2007. **19**(9): p. 2247-2260.
13. Ilhan, F., et al., *Hydrophobic monolithic aerogels by nanocasting polystyrene on amine-modified silica*. Journal of Materials Chemistry, 2006. **16**(29): p. 3046-3054.

14. Boday, D.J., et al., *Strong, Low-Density Nanocomposites by Chemical Vapor Deposition and Polymerization of Cyanoacrylates on Aminated Silica Aerogels*. ACS Applied Materials & Interfaces, 2009. **1**(7): p. 1364-1369.
15. Boday, D., et al., *Strong, low density, hexylene- and phenylene-bridged polysilsesquioxane aerogel-polycyanoacrylate composites*. Journal of Materials Science, 2011: p. 1-7.
16. Hüsing, N. and S. Hartmann, *Inorganic–Organic Hybrid Porous Materials*, in *Hybrid Nanocomposites for Nanotechnology*. 2009, Springer US. p. 1-41.
17. Sanchez, C., et al., *Designed Hybrid Organic–Inorganic Nanocomposites from Functional Nanobuilding Blocks*. Chemistry of Materials, 2001. **13**(10): p. 3061-3083.
18. Wen, J., V.J. Vasudevan, and G.L. Wilkes, *Abrasion resistant inorganic/organic coating materials prepared by the sol-gel method*. Journal of Sol-Gel Science and Technology, 1995. **5**(2): p. 115-126.
19. Frings, S., et al., *Organic-inorganic hybrid coatings for coil coating application based on polyesters and tetraethoxysilane*. Progress in Organic Coatings, 1998. **33**(2): p. 126-130.
20. Messori, M., et al., *Flame retarding poly(methyl methacrylate) with nanostructured organic-inorganic hybrids coatings*. Polymer, 2003. **44**(16): p. 4463-4470.
21. Wight, A.P. and M.E. Davis, *Design and Preparation of Organic–Inorganic Hybrid Catalysts*. Chemical Reviews, 2002. **102**(10): p. 3589-3614.
22. Wen, J., et al., *Preparation of Highly Porous Silica Gel from Poly(tetramethylene oxide)/Silica Hybrids*. Chemistry of Materials, 1997. **9**(9): p. 1968-1971.
23. Dave, B.C., et al., *Sol-gel encapsulation methods for biosensors*. Analytical Chemistry, 1994. **66**(22): p. 1120A-1127A.
24. Scully, P.J.B., L.; Bolyo, J.; Dzyadevych, S.; Guisan, J. M.; Fernandez-Lafuente, R.; Jaffrezic-Renault, N.; Kuncova, G.; Matejec, V.; O'Kennedy, B.; Podrazky, O.; Rose, K.; Sasek, L.; Young, J. S., *Optical fiber biosensors using enzymatic transducers to monitor glucose*. Measurement Science and Technology, 2007. **18**(10): p. 3177-3186.
25. Houbertz, R., *Laser interaction in sol-gel based materials--3-D lithography for photonic applications*. Applied Surface Science, 2005. **247**(1-4): p. 504-512.
26. Houbertz, R., et al., *Investigations on the generation of photonic crystals using two-photon polymerization (2PP) of inorganic–organic hybrid polymers with ultra-short laser pulses*. physica status solidi (a), 2007. **204**(11): p. 3662-3675.
27. Houbertz, R., et al., *Inorganic–Organic Hybrid Polymers for Information Technology: from Planar Technology to 3D Nanostructures*. Advanced Engineering Materials, 2003. **5**(8): p. 551-555.

28. Di Noto, V., et al., *Structure, properties and proton conductivity of Nafion/[(TiO<sub>2</sub>)]·(WO<sub>3</sub>)<sub>0.148</sub>]/TiO<sub>2</sub> nanocomposite membranes*. *Electrochimica Acta*, 2010. **55**(4): p. 1431-1444.
29. Di Noto, V., et al., *New inorganic-organic proton conducting membranes based on Nafion® and [(ZrO<sub>2</sub>)·(SiO<sub>2</sub>)<sub>0.67</sub>] nanoparticles: Synthesis vibrational studies and conductivity*. *Journal of Power Sources*, 2008. **178**(2): p. 561-574.
30. Avnir, D., et al., *Enzymes and Other Proteins Entrapped in Sol-Gel Materials*. *Chemistry of Materials*, 1994. **6**(10): p. 1605-1614.
31. Wojcik, A.B. and L.C. Klein, *Transparent Organic/Inorganic Hybrid Gels: A Classification Scheme*. *Applied Organometallic Chemistry*, 1997. **11**(2): p. 129-135.
32. Haas, K.-H. and H. Wolter, *Synthesis, properties and applications of inorganic-organic copolymers (ORMOCER®s)*. *Current Opinion in Solid State and Materials Science*, 1999. **4**(6): p. 571-580.
33. Philipp, G. and H. Schmidt, *New materials for contact lenses prepared from Si- and Ti-alkoxides by the sol-gel process*. *Journal of Non-Crystalline Solids*, 1984. **63**(1-2): p. 283-292.
34. Sanchez, C., Ribot, F. , *Design of hybrid organic-inorganic materials synthesized via sol-gel chemistry*. *New Journal of Chemistry*, 1994. **18**(10): p. 1007-1047.
35. Haas, K.H., *Hybrid Inorganic–Organic Polymers Based on Organically Modified Si-Alkoxides*. *Advanced Engineering Materials*, 2000. **2**(9): p. 571-582.
36. Fidalgo, A., et al., *Hybrid Silica/Polymer Aerogels Dried at Ambient Pressure*. *Chemistry of Materials*, 2007. **19**(10): p. 2603-2609.
37. Novak, B.M., *Hybrid Nanocomposite Materials—between inorganic glasses and organic polymers*. *Advanced Materials*, 1993. **5**(6): p. 422-433.
38. Wright, J.D., Sommerdijk, A.J.M, *Sol-Gel Materials Chemistry and Applications*. *Advanced Chemistry Texts*. Vol. 4. 2001: CRC Press.
39. Hüsing, N. and U. Schubert, *Aerogels*, in *Ullmann's Encyclopedia of Industrial Chemistry*. 2000, Wiley-VCH Verlag GmbH & Co. KGaA.
40. Gerona, M.M.i., *Silica Aerogels: Synthesis and Characterization*. 2002, University of Barcelona. p. 273.
41. Hrubesh, L.W., *Aerogel applications*. *Journal of Non-Crystalline Solids*, 1998. **225**: p. 335-342.
42. Cantin, M., et al., *Silica aerogels used as Cherenkov radiators*. *Journal Name: Nucl. Instrum. Methods*, v. 118, no. 1, pp. 177-182; Other Information: Orig. Receipt Date: 31-DEC-74; Bib. Info. Source: NL (Netherlands (sent to DOE from)), 1974: p. Medium: X.
43. Buzykaev, A., et al., *Aerogels with high optical parameters for Cherenkov counters*. *Nuclear Instruments and Methods in Physics Research Section A: Accelerators, Spectrometers, Detectors and Associated Equipment*, 1996. **379**(3): p. 465-467.

44. Rubin, M. and C.M. Lampert, *Transparent silica aerogels for window insulation*. *Solar Energy Materials*. **7**(4): p. 393-400.
45. Zhu, Q., Y. Li, and Z. Qiu, *Research Progress on Aerogels as Transparent Insulation Materials*, in *Challenges of Power Engineering and Environment*, K. Cen, Y. Chi, and F. Wang, Editors. 2007, Springer Berlin Heidelberg. p. 1117-1121.
46. Long, J.W. and D.R. Rolison, *Architectural Design, Interior Decoration, and Three-Dimensional Plumbing en Route to Multifunctional Nanoarchitectures*. *Accounts of Chemical Research*, 2007. **40**(9): p. 854-862.
47. Pajonk, G.M., *ChemInform Abstract: Aerogel Catalysts*. *ChemInform*, 1991. **22**(33): p. no-no.
48. Ward, D.A. and E.I. Ko, *Preparing Catalytic Materials by the Sol-Gel Method*. *Industrial & Engineering Chemistry Research*, 1995. **34**(2): p. 421-433.
49. *Molecular oxygen sensors based on photoluminescent silica aerogels*. *Journal of Non-Crystalline Solids*, 1998. **225**: p. 343-347.
50. Owens, B.B., Passerini, S., Smyrl, W.H. , *Lithium ion insertion in porous metal oxides*. *Electrochimica Acta*, 1999. **45**: p. 215-224.
51. Randall, J.P., M.A.B. Meador, and S.C. Jana, *Tailoring Mechanical Properties of Aerogels for Aerospace Applications*. *ACS Applied Materials & Interfaces*, 2011. **3**(3): p. 613-626.
52. Hench, L.L. and J.K. West, *The sol-gel process*. *Chemical Reviews*, 1990. **90**(1): p. 33-72.
53. Rakesh P. Patel., N.S.P., Ajay M Suthar, *An Overview of Silica Aerogels*. *International Journal*, 2009. **1**(4): p. 1052-1057.
54. Brinker, C.J., Scherer, G. W., *Sol-Gel Science: The Physics and Chemistry of Sol-Gel Processing*. 1990, London: Academic Press, Inc.
55. Wen, J. and G.L. Wilkes, *Organic/Inorganic Hybrid Network Materials by the Sol-Gel Approach*. *Chemistry of Materials*, 1996. **8**(8): p. 1667-1681.
56. Saegusa, T., *Organic/inorganic polymer hybrids*. *Macromolecular Symposia*, 1995. **98**(1): p. 719-729.
57. Begag, J.M.R., et al., *Affordable Window Insulation with R-10/inch Rating*. 2004. p. Medium: ED.
58. Hüsing, N., et al., *Novel Siloxane-Silica Nanocomposite Aerogels and Xerogels*. *Journal of Sol-Gel Science and Technology*, 2003. **26**(1): p. 73-76.
59. Liu, Y., et al., *Preparation and Characterization of Porous Silica Films by a Modified Base-Catalyzed Sol-Gel Process Containing PVA: I. The Precursor Solution Synthesis*. *Journal of Sol-Gel Science and Technology*, 2002. **25**(2): p. 95-101.

60. Pope, E.J.A., Asami, M., Mackenzie, J. D., *Transparent silica gel-PMMA composites*. Journal of Materials Research, 1989. **4**: p. 1018-102.
61. Zhang, G., et al., *Isocyanate-crosslinked silica aerogel monoliths: preparation and characterization*. Journal of Non-Crystalline Solids, 2004. **350**: p. 152-164.
62. Katti, A., et al., *Chemical, Physical, and Mechanical Characterization of Isocyanate Cross-linked Amine-Modified Silica Aerogels*. Chemistry of Materials, 2005. **18**(2): p. 285-296.
63. Luo, H., H. Lu, and N. Leventis, *The compressive behavior of isocyanate-crosslinked silica aerogel at high strain rates*. Mechanics of Time-Dependent Materials, 2006. **10**(2): p. 83-111.
64. Nguyen, B.N., et al., *Tailoring Elastic Properties of Silica Aerogels Cross-Linked with Polystyrene*. ACS Applied Materials & Interfaces, 2009. **1**(3): p. 621-630.
65. Boday, D.J., et al., *Mechanically reinforced silica aerogel nanocomposites via surface initiated atom transfer radical polymerizations*. Journal of Materials Chemistry, 2010. **20**(33): p. 6863-6865.
66. Nguyen, B.N., et al., *Elastic Behavior of Methyltrimethoxysilane Based Aerogels Reinforced with Tri-Isocyanate*. ACS Applied Materials & Interfaces, 2010. **2**(5): p. 1430-1443.
67. Leventis, N., et al., *Click Synthesis of Monolithic Silicon Carbide Aerogels from Polyacrylonitrile-Coated 3D Silica Networks*. Chemistry of Materials, 2010. **22**(9): p. 2790-2803.
68. Meador, M.A.B., et al., *Epoxy Reinforced Aerogels Made Using a Streamlined Process*. ACS Applied Materials & Interfaces, 2010. **2**(7): p. 2162-2168.
69. Yim, T.-J., S. Kim, and K.-P. Yoo, *Fabrication and thermophysical characterization of nano-porous silica-polyurethane hybrid aerogel by sol-gel processing and supercritical solvent drying technique*. Korean Journal of Chemical Engineering, 2002. **19**(1): p. 159-166.
70. Premachandra, J.K., Kumudinie, C., Mark, J.E., Dang, T.D., Arnold, F.E., *Preparation and Properties of Some Hybrid Aerogels From a sulfopolybenzobisthiazole-silica Composite*,. Journal of Macromolecular Science, Part A, 1999. **36**(1): p. 73-83.
71. Novak, B.M., D. Auerbach, and C. Verrier, *Low-Density, Mutually Interpenetrating Organic-Inorganic Composite Materials via Supercritical Drying Techniques*. Chemistry of Materials, 1994. **6**(3): p. 282-286.
72. Schwertfeger, F., W. Glaubitt, and U. Schubert, *Hydrophobic aerogels from Si(OMe)<sub>4</sub>/MeSi(OMe)<sub>3</sub> mixtures*. Journal of Non-Crystalline Solids, 1992. **145**: p. 85-89.



73. Li, L., et al., *Flexible Nanofiber-Reinforced Aerogel (Xerogel) Synthesis, Manufacture, and Characterization*. ACS Applied Materials & Interfaces, 2009. **1**(11): p. 2491-2501.
74. Ou, D.L., Gould, G. L. , *Aerogels Containing Silicon Bonded Polymers*. 2010, ASPEN AEROGELS INC.
75. Loy, D.A. and K.J. Shea, *Bridged Polysilsesquioxanes. Highly Porous Hybrid Organic-Inorganic Materials*. Chemical Reviews, 1995. **95**(5): p. 1431-1442.
76. Nakane, K., et al., *Properties and structure of poly(vinyl alcohol)/silica composites*. Journal of Applied Polymer Science, 1999. **74**(1): p. 133-138.
77. Ionescu C., S.C., Balasoiu M., Popovici M., Enache C., Kuklin A., Islamov A., Kovale Y., Almásy L., *Investigation of silica-PVA xerogel microstructure evolution during thermal treatment by sans experiment*. Acta Periodica Technologica, 2004. **2004**(35): p. 95-101.
78. Chen, Y. and J.O. Iroh, *Synthesis and Characterization of Polyimide/Silica Hybrid Composites*. Chemistry of Materials, 1999. **11**(5): p. 1218-1222.
79. Ragosta, G., Musto, P., *Polyimide/silica hybrids via the sol-gel route: High performance materials for the new technological Challenges*. Express Polymer Letters, 2009. **3**(7): p. 413-428.
80. Wojcik, A.B., A. Ting, and L.C. Klein, *High molecular weight poly(ethylene oxide)/silica hybrids by the sol-gel process*. Materials Science and Engineering: C, 1998. **6**(2-3): p. 115-120.
81. Klein, A.B.W.a.L.C. *Transparent poly(vinyl acetate)-silica gels by a sol-gel process in Passive Materials for Optical Elements II*. 1993 San Diego, CA, USA Proc. SPIE.
82. Sarwar, M., S. Zulfiqar, and Z. Ahmad, *Poly (ether amide) and silica nanocomposites derived from sol-gel process*. Journal of Sol-Gel Science and Technology, 2008. **45**(1): p. 89-95.
83. Martin, J., et al., *Mechanical and acoustical properties as a function of PEG concentration in macroporous silica gels*. Journal of Non-Crystalline Solids, 2001. **285**(1-3): p. 222-229.
84. Kulkarni, M.M., et al., *Microstructural and mechanical properties of silica-PEPEG polymer composite xerogels*. Acta Materialia, 2006. **54**(19): p. 5231-5240.
85. Wei, T.-Y., S.-Y. Lu, and Y.-C. Chang, *Transparent, Hydrophobic Composite Aerogels with High Mechanical Strength and Low High-Temperature Thermal Conductivities*. The Journal of Physical Chemistry B, 2008. **112**(38): p. 11881-11886.
86. Beaudry, C.L., L.C. Klein, and R.A. McCauley, *Thermal weight loss of silica-poly(vinyl acetate) (PVAc) sol-gel composites*. Journal of Thermal Analysis and Calorimetry, 1996. **46**(1): p. 55-65.

- 
87. Lowell, S., Shields, J. E., *Powder Surface Area and Porosity* 3rd ed. Particle Technology Series. Vol. 2. 1991: Springer. 268
  88. Robert M. Silverstein, F.X.W., David J. Kiemle, *Spectrometric Identification of Organic Compounds* 7th ed. 2005, Hoboken, NJ John Wiley & Sons. 502.
  89. Al-Oweini, R. and H. El-Rassy, *Synthesis and characterization by FTIR spectroscopy of silica aerogels prepared using several Si(OR)<sub>4</sub> and R''Si(OR')<sub>3</sub> precursors*. Journal of Molecular Structure, 2009. **919**(1-3): p. 140-145.
  90. Jabbari, E. and N.A. Peppas, *Use of ATR-FTIR to study interdiffusion in polystyrene and poly(vinyl methyl ether)*. Macromolecules, 1993. **26**(9): p. 2175-2186.

## **APPENDIX A:**

### **UV-VIS Spectroscopy Results for Poly(vinyl pyrrolidone) concentration in ethanol**

In this Appendix A, UV-VIS Spectroscopy Results of Poly(vinyl pyrrolidone) is given. This analysis is performed to monitor the polymer concentration in the aging solution. Based on the polymer mass remaining on the solution, the mass of the polymer which would be on the surface of the silica aerogel is concluded.

Primarily, a calibration curve is obtained with several dilutions of the first polymeric solution. The strongest peak of the polymer appeared at around 220 nm. All the measurements are taken at this same wavelength for better accuracy.

In the Figure A-1, the calibration curve representing the concentration of PVP in ethanol versus the absorbance is given.

To obtain the calibration curve, 5 different dilutions are prepared based on the first aging solution. The following measurements of the absorbance are taken in subsequent days to monitor the reduction in the polymer concentration. Consequent Figure A-2 and Figure A-3 visualize the decreasing trend of the polymer concentration in several days. It is seen that the polymer concentration tends to decrease after several days of waiting. The reduction in polymer concentration gets smaller and smaller after the second week. It is assumed that after the second week the polymer concentration remains almost constant.

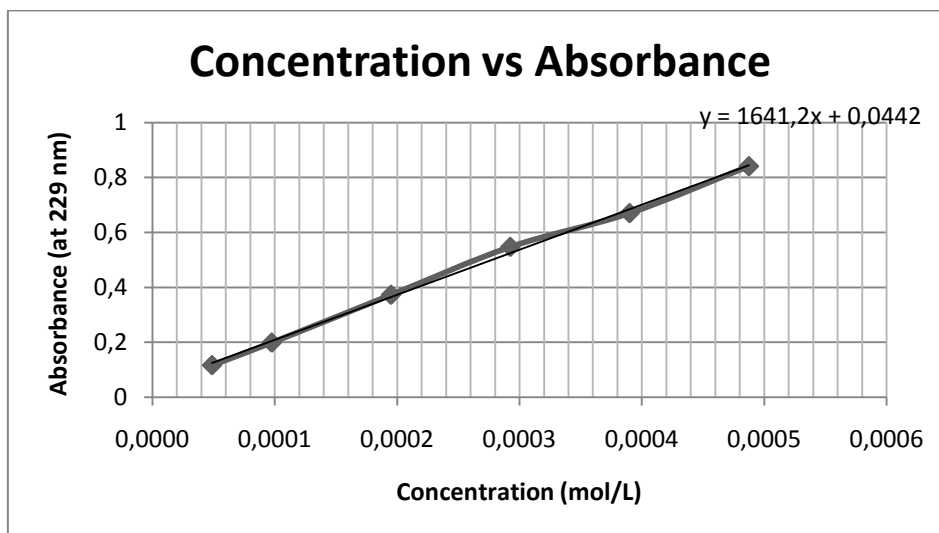


Figure A-1: Calibration Curve Representing Polymer Concentration versus UV-VIS Absorbance

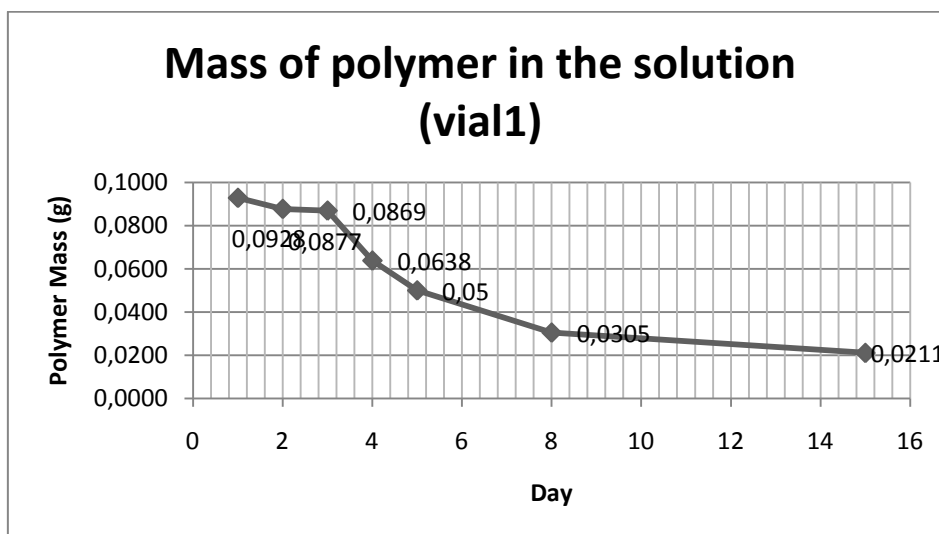


Figure A-2: Mass of the Polymer Remaining in the Aging Solution 1 With Respect to Days

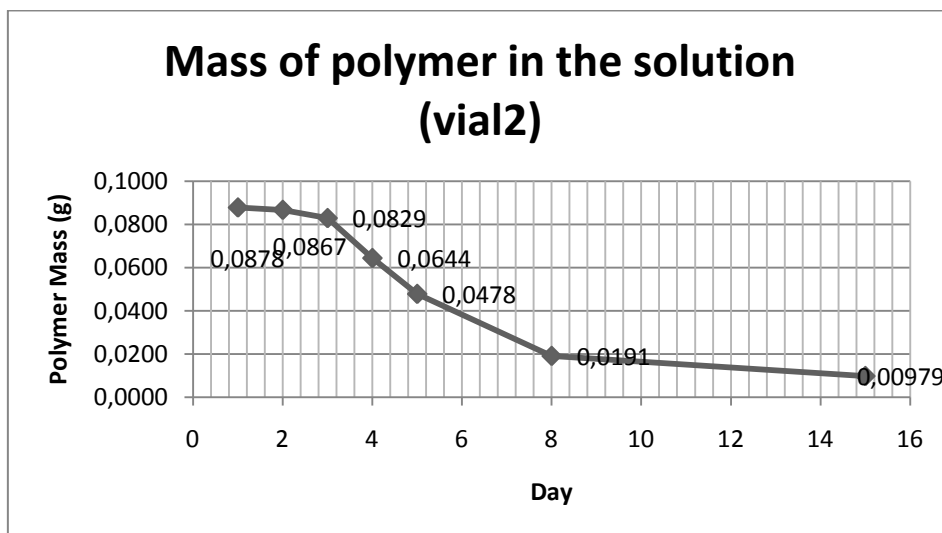


Figure A-3: Mass of the Polymer Remaining in the Aging Solution 2 With Respect to Days

## APPENDIX B:

Appendix B represents the entire density and shrinkage results for the synthesized samples. The density is measured by simply dividing the mass of the corresponding sample by its volume. The dimensions of the sample are measured with the help of a caliper for a better accuracy. The shrinkage values indicated in bold are those which represent the linear shrinkage values. The remaining results are measured volumetrically.

The porosity of the samples is measured using equation 3 mentioned in Section 3.3.1 of this thesis. The theoretical pore volumes are calculated using the equation 4 mentioned in Section 3.3.1 and the experimental pore volumes based on BET results are illustrated if available.

*Table B-1: Density and Shrinkage Results for Silica Aerogel-PEPEG Composites*

Sample Name	Density (g/cm <sup>3</sup> )	Shrinkage (%)	Porosity	Pore Volume Theoretical	Pore Volume Experimental
P1207	0,277	<b>23,6</b>	89,63	3,95	3,29
P1507_1	0,202	<b>19,2</b>	90,78	4,49	
P1507_2	0,238	<b>26,4</b>	89,13	3,75	
P1907	0,234	<b>25,6</b>	89,32	3,82	
P2707	0,302	<b>21,07</b>	86,21	2,85	2,88
P2807	0,131	<b>19,6</b>	94,02	7,18	
P1409	0,168	<b>17,7</b>	92,33	5,50	
P1509	0,237	<b>24</b>	89,18	3,76	

*Table B-2: Density and Shrinkage Results for Silica Aerogel-PVP Composites*

<b>Sample Name</b>	<b>Density (g/cm<sup>3</sup>)</b>	<b>Shrinkage (%)</b>	<b>Porosity</b>	<b>Pore Volume Theoretical</b>	<b>Pore Volume Experimental</b>
PVP2107_1	0,185	<b>18,67</b>	91,55	4,95	
PVP2107_2	0,19	<b>19,2</b>	91,32	4,81	
PVP1108	0,192	<b>19,47</b>	91,23	4,75	
PVP1208	0,216	<b>18,4</b>	90,14	4,17	2,62
PVP2408	0,357	<b>24,8</b>	83,70	2,34	
PVP2508_1	0,203	<b>22,8</b>	90,73	4,47	
PVP2508_2	0,195	<b>18,6</b>	91,10	4,67	
PVP2508_3	0,232	<b>18,4</b>	89,41	3,85	2,66
PVP2609_1	0,218	<b>18,4</b>	90,05	4,13	
PVP2609_2	0,177	<b>17,6</b>	91,92	5,19	3,64
PVP3011_1	0,174	<b>13,6</b>	92,05	5,29	
PVP3011_2	0,174	<b>14</b>	92,05	5,29	
PVP1105	0,168	15,96	92,33	5,50	3,51

*Table B-3: Density and Shrinkage Results for Silica Aerogel-PVAc Composite*

<b>Sample Name</b>	<b>Density (g/cm<sup>3</sup>)</b>	<b>Shrinkage (%)</b>	<b>Porosity</b>	<b>Pore Volume Theoretical</b>	<b>Pore Volume Experimental</b>
PVAc2510	0,187	17,6	91,46	4,89	
PVAc0411_1	0,152	-	93,06	6,12	3,12
PVAc0411_2	0,185	-	91,55	4,95	3,75
PVAc3011_1	0,169	-	92,28	5,46	
PVAc3011_2	0,175	-	92,01	5,26	3,62
PVAc0601_1	0,159	28,67	92,74	5,83	3,72
PVAc0601_2	0,156	15,44	92,88	5,95	4,39
PVAc0601_3	0,155	13,38	92,92	5,99	3,53
PVAc1201_1	0,174	17,8	92,05	5,29	
PVAc1201_2	0,166	15,63	92,42	5,57	
PVAc0202_1	0,149	14,64	93,20	6,25	
PVAc0202_2	0,138	10,98	93,70	6,79	

PVAc0202_3	0,128	17,22	94,16	7,36	
PVAc0302_1	0,152	19,94	93,06	6,12	
PVAc0302_2	0,158	20,2	92,79	5,87	
PVAc0302_3	0,158	17,89	92,79	5,87	
PVAc0302_4	0,151	25,87	93,11	6,17	
PVAc0302_5	0,168	15,19	92,33	5,50	
PVAc0302_6	0,164	18,91	92,51	5,64	
PVAc0702_1	0,447	40,48	79,59	1,78	
PVAc0702_2	0,461	31,9	78,95	-	
PVAc0702_3	-	-	-	-	
PVAc0702_4	-	-	-	-	
PVAc1602_2	-	34,3	-	-	2,65
PVAc1602_3	-	-	-	-	
PVAc1602_4	0,383	40,41	82,51	-	1,90
PVAc2302_1	0,184	26,92	91,60	4,98	
PVAc2302_2	0,187	17,28	91,46	4,92	
PVAc2302_3	0,144	12,14	93,42	6,49	3,93
PVAc2302_4	0,142	7,51	93,52	6,59	4,22
PVAc0703_1	0,364	62,48	83,38	2,29	1,64
PVAc0703_2	0,251	41,42	88,54	3,53	
PVAc0703_3	0,294	53,1	86,58	2,94	2,27
PVAc0703_4	0,353	59,21	83,88	2,38	
PVAc1603_1	0,412	<b>47,18</b>	81,19	1,97	
PVAc1603_2	0,317	<b>43,34</b>	85,53	2,70	
PVAc1105	0,121	15,5	94,47	7,81	

Table B-4: Density and Shrinkage Results for Silica Aerogel-PMVEComposites

Sample Name	Density (g/cm <sup>3</sup> )	Shrinkage (%)	Porosity	Pore Volume Theoretical	Pore Volume Experimental
PMVE2510	0,246	<b>22,4</b>	88,77	3,61	
PMVE1904_1	0,145	6,48	93,38	6,44	4,36
PMVE1904_2	0,16	7,19	92,69	5,79	
PMVE1904_3	0,17	19,64	92,24	5,43	



---

PMVE2004	0,151	3,26	93,11	6,17	
PMVE1005_1	0,144	18,43	93,38	6,44	
PMVE1005_2	0,157	7,73	92,88	5,95	4,30
PMVE1105	0,116	14,52	94,70	8,16	4,86

**VITA**

Zeynep Ülker was born in İzmir, Turkey, on November 9, 1984. She received her B.Sc. Degree in Chemical and Biological Engineering from Koç University, Istanbul, in 2009. From September 2009 to August 2011 she worked as teaching and research assistant at Koç University, Istanbul, Turkey. She has worked on “Preparation and Characterization of Silica Aerogel-Polymer Composites” during his M.S. study.